

# The Challenger: When Do New Data Sources Justify Switching Machine Learning Models?

Vassilis Digalakis Jr

Boston University

Christophe Pérignon, Sébastien Saurin, Flore Sentenac

HEC Paris

---

**Abstract.** We study the problem of deciding whether, and when an organization should replace a trained incumbent model with a challenger relying on newly available features. We develop a unified economic and statistical framework that links learning-curve dynamics, data-acquisition and retraining costs, and discounting of future gains. First, we characterize the optimal switching time in stylized settings and derive closed-form expressions that quantify how horizon length, learning-curve curvature, and cost differentials shape the optimal decision. Second, we propose three practical algorithms—a one-shot baseline, a greedy sequential method, and a look-ahead sequential method. Using a real-world credit-scoring dataset with gradually arriving alternative data, we show that (i) optimal switching times vary systematically with cost parameters and learning-curve behavior, and (ii) the look-ahead sequential method outperforms other methods and is able to approach in value an oracle with full foresight. Finally, we establish finite-sample guarantees, including conditions under which the sequential look-ahead method achieve sublinear regret relative to that oracle. Our results provide an operational blueprint for economically sound model transitions as new data sources become available.

**Key words:** model transition; alternative data; credit scoring; AI operationalization; trustworthy AI and machine learning

---

## 1. Introduction

Organizations increasingly rely on predictive models to inform decision-making across various domains. The effectiveness of these predictive tasks hinges on two fundamental elements: the choice and optimization of the *predictive model* and the availability and quality of the *data* used to train this model. In this regard, the rise of alternative data has opened new frontiers in predictive modeling. These novel data sources become available either through technological advancements (e.g., satellite imagery, geolocation data, transaction data, web-traffic metrics, social media data, online reviews, sensor data, environmental and weather data, supply chain and shipping data, patent/IP filings) or regulations granting individuals the right to share their personal data with third parties (e.g., the Consumer Financial Protection Bureau’s open banking rules, the EU’s Payment Services Directive 2, or the EU Data Act for IoT-generated data).

The emergence of new data sources is both an opportunity and a disruption in the lifecycle of a predictive model. This opportunity arises because alternative data can offer novel signals and improve forecasting performance beyond what is achievable with the original features. However, newly available features cannot be immediately integrated into existing models. They must first be incorporated into an augmented model, which requires training, validation, and comparison with

the existing model before deployment. Despite its practical importance, the question of how to effectively incorporate new features into an established forecasting process has been overlooked in the literature, and this study seeks to address this gap.

We formalize this problem by considering an organization that has deployed a forecasting model in production, referred to as the *champion* or *incumbent model*  $f_I$ . The latter was fully trained on an initial set of features. At a given point in time, some new features become available, which may enhance prediction accuracy. In response, the organization develops a new model, called the *challenger model*  $f_C$ , that incorporates an expanded set of features including the new features. However, as the large dataset used to train  $f_I$  lacks these new features, it cannot be used to train  $f_C$ . In turn,  $f_C$  must be trained on a new dataset containing a limited number of samples, which typically hinders its initial performance. Over time, as more data including the additional features are collected, the performance of the challenger model  $f_C$  is expected to improve and may eventually exceed that of the incumbent model  $f_I$ .

Transitioning from a fully trained incumbent model to a newly developed challenger involves several important trade-offs. If  $f_C$  delivers a meaningful improvement over  $f_I$ , adopting it earlier can reduce forecasting errors and generate real operational value. These performance gains, however, must be weighed against several types of costs. Accessing new features may require payments to external data providers or incur internal expenses related to data extraction and processing. Training and validating  $f_C$  also entails feature-engineering efforts, computational expenditures—including cloud infrastructure and electricity—and human labor for model development, debugging, and testing. Once  $f_C$  is deemed superior, additional deployment and switching costs arise from integrating the model into production. Feature-access and training/validation costs may include both fixed components and variable components that scale with the number of samples incorporating the new features, whereas deployment and switching costs are fixed and incurred only once.

The central research question we address is: *When does the emergence of new data sources justify switching from the incumbent model  $f_I$  to the challenger model  $f_C$ ?* We propose and study a multi-stage optimization framework that dynamically guides the decision to either (i) *switch*—deploying  $f_C$  and replacing  $f_I$ ; (ii) *discard*—permanently rejecting  $f_C$  and stopping data collection; or (iii) *continue*—collecting more data and deferring the decision until a later time. Our approach integrates performance estimation (while accounting for uncertainty in performance gains), costs, gains, and decision confidence to enable a structured and cost-effective transition between models.

### 1.1. Contributions and Outline

We make the following contributions to the growing literature on data-driven decision making and model lifecycle management—areas that are particularly consequential in finance. This financial context provides both motivation and validation for our framework, and it is the lens through which we conduct our empirical analysis.

(i) *Modeling*: We introduce a new framework for deciding whether, and when an organization should replace an incumbent model with a challenger trained on an expanded feature set. The framework accounts for (a) how the challenger’s performance improves as more full-feature samples arrive, (b) the costs of acquiring new data, retraining, and switching models, and (c) the timing of these costs and gains. This yields a dynamic and economically grounded notion of when new data justify switching models.

(ii) *Theoretical insights*: We formulate the switching problem as an optimal stopping problem and derive structural results under a stylized, analytically tractable model. These results characterize the optimal switching time, identify the key parameters driving the decision (learning-curve shape, horizon length, discounting, and cost differentials), and clarify how epoch design, i.e., the points in time at which models are trained and evaluated, trades off computational cost against responsiveness, measured as the loss in economic value from not switching at the continuous optimum.

(iii) *Algorithms and guarantees*: Building on the theoretical insights, we develop three practical algorithms: a one-shot baseline, a greedy sequential method, and a look-ahead sequential method that anticipates future improvements in the challenger.

(iv) *Empirical validation*: We conduct a comprehensive case study in the financial domain using a large real-world credit-scoring dataset. The study illustrates how learning curves, utility curves, and cost parameters interact; evaluates the performance of our algorithms across multiple scenarios; and demonstrates the practical relevance of our framework for data-driven decision making in financial institutions. The results demonstrate that look-ahead sequential method performs best, and is able to approach the value obtained by an oracle with full foresight.

(v) *Theoretical guarantees*: We establish conservativeness guarantees and derive regret bounds relative to an oracle with full foresight for our algorithms.

The organization of the paper mirrors these various contributions. Section 2 presents the problem formulation and the modeling framework. Section 3 derives the optimal stopping rule under a stylized analytical setting. Section 4 introduces our algorithms. Section 5 reports empirical results from the credit-scoring case study. Section 6 presents theoretical guarantees for our algorithms. Section 7 provides managerial insights, directions for future research, and concludes.

## 1.2. Related Literature

Our work sits at the intersection of three research streams that have evolved largely in parallel. The first is the literature on model retraining, which studies when predictive models should be updated as new data become available. The second is the learning-curve literature, which characterizes how model performance evolves with additional samples and how such curves can guide data acquisition and training decisions. The third is the literature on alternative data sources, especially in finance, where newly accessible signals arrive gradually and often require careful economic evaluation before integration. Our framework bridges these streams by modeling performance gains, data and retraining costs, and the timing of information arrival within a unified formulation, thereby formalizing the decision of when new data justify switching to a challenger model. Our setting also relates conceptually to sequential decision-making and optimal stopping, as the choice to switch, discard, or continue is made repeatedly under uncertainty. However, the stopping problem we study does not match standard formulations, as gains and costs depend endogenously on sample size rather than exogenous stochastic rewards.

*Model retraining.* This stream studies when a deployed predictive model should be retrained as new data and modeling options become available. The literature on model retraining has developed along two main directions. The first examines how to select among competing models using only partial training data: progressive sampling procedures (John and Langley 1996, Provost et al. 1999) enlarge the training set in stages and stop when additional data no longer increases expected utility, trading off performance gains against data and computational costs. The second studies retraining deployed models when the data distribution evolves, focusing on detecting distribution shifts (Bifet and Gavalda 2007, Pesaranghader and Viktor 2016) and adapting models to mitigate their effects (Schwinn et al. 2022, Kabra and Patel 2024, Bertsimas et al. 2024). Cost-aware retraining rules include staleness-based policies (Mahadevan and Mathioudakis 2024) and return-on-investment frameworks for deciding when updates are worthwhile (Žliobaitė et al. 2015). Our work is complementary but tackles a different problem: rather than determining when to update a fixed model under partial training data or distribution drifts, we study when the arrival of new features and new data justifies switching from an incumbent model to a challenger. We integrate learning-curve dynamics, data-acquisition and retraining costs, and future economic gains into a unified optimization problem that formalizes the transition decision.

*Learning curves.* This stream studies how model performance evolves with sample size and how such learning curves can inform data acquisition and training decisions. Two recent surveys summarize this area: Viering and Loog (2023) document that learning curves frequently exhibit smooth, monotone improvement and are often well-approximated by power laws, while also highlighting irregular behaviors—temporary degradation, plateaus, or non-monotonicity—that complicate prediction and planning. For example, Frey and Fisher (1999) and Last (2007) show that learning curves of decision trees follow a power law, allowing early prediction of error rates as data grow. Closer to our setting, Mohr and van Rijn (2024) review *utility curves*, which combine performance gains with data and computational costs. Such curves peak at the optimal training size and enable the development of data-acquisition policies based on expected utility. Weiss and Tian (2008) and Last (2009) fit explicit functional forms to partial learning curves to project future performance or optimal training sizes, whereas Sabharwal et al. (2016) use local linear approximations to estimate near-optimal learners from limited data. Our setting builds on this foundation but differs in the following way: rather than determining how much data to use to train a given model, we study how learning-curve dynamics interact with economic costs to determine *whether, and when*, an organization should transition from an incumbent to a challenger model as new data accumulate.

*Alternative data in finance.* This line of research studies how newly accessible data sources affect forecasting performance. While the challenge of integrating new alternative data sources into a forecasting model is universal, it has been extensively investigated in financial applications (see Foucault et al. (2025) for a survey). Numerous recent studies show that alternative data significantly improve forecasting ability in credit scoring models used by lenders to screen loan applications and by online merchants offering buy-now-pay-later programs. These data sources include applicants' digital footprints (Berg et al. 2020, Gambacorta et al. 2024), borrowers' pictures (Ravina 2025), textual descriptions of the reasons for the loans (Iyer et al. 2016), open banking data (He et al. 2023, Babina et al. 2025), online merchants' transaction volumes and payment history (Gambacorta et al. 2022), mobile phone data (Oskarsdottir et al. 2019), email usage (Djeundje et al. 2021), and psychometric and cognitive assessments (Bryan et al. 2024). In these studies, the incremental value of alternative data is typically assessed by the improvement in forecasting accuracy (e.g., an increase in AUC) when such data are incorporated into credit scoring models, under the simplifying assumption that both standard and alternative data are fully available for all observations. In contrast,

we adopt what we view as a more operationally relevant perspective: in practice, alternative data are accumulated gradually over time, and observed performance gains are subject to uncertainty.<sup>1</sup>

Besides lending, the value of alternative data has been demonstrated in numerous other financial applications. In asset management, Green et al. (2019) examine employer ratings on Glassdoor and find that firms with the largest quarterly rating improvements outperform those with declines. Similarly, Katona et al. (2025) show that daily satellite imagery of parking-lot usage at U.S. retailers can predict their next-quarter earnings, stock returns, and market liquidity. Furthermore, Bonelli and Foucault (2025) show that the introduction of alternative data on a stock reduces asset managers' stock-picking ability. Bonelli (2025) demonstrates that venture capitalists who process alternative data—including startups' digital footprints such as website traffic, app downloads, and online reviews—can gain valuable insights into the likelihood of a startup's success. Moreover, the volume and diversity of alternative data available to financial analysts also have major effects on the informativeness of their forecasts (Chi et al. 2025, Dessaint et al. 2024, Cao et al. 2024). In their analysis of the finance industry, Foucault et al. (2025) report a steady increase in alternative-data vendors, reflecting both growing demand for such data and intensifying competition among data providers in finance. Overall, this literature highlights a practical need that our framework addresses directly: when new data sources become available gradually and at a cost, organizations require principled methods to determine the economically optimal timing of switching from an incumbent model to one that exploits these new sources.

While the rapid proliferation of machine learning techniques and newly available data sources have transformed the information landscape in finance, the *training costs* of machine learning models are largely overlooked in the finance literature. For instance, in the comprehensive survey of financial machine learning by Kelly and Xiu (2022), the term “training cost” does not appear even once across 159 pages (this also applies to other key reference works such as Gu et al. (2020) and Chen et al. (2024)). This lack of attention is particularly striking given the recent and influential line of research, initiated by Kelly et al. (2022, 2024), which emphasizes the virtues of model complexity in finance and advocates for machine learning models with extremely large parameter counts. However, unlike our study, the substantial estimation costs that accompany such complexity are not incorporated into model performance evaluation.

<sup>1</sup> The *expanding feature set* problem we are considering here is more complex than the analog *reducing feature set* problem, which arises when certain features disappear (Bian et al. 2022). The latter can occur when a data source suddenly becomes inaccessible or prohibitively expensive. In such cases, a new model needs to be trained using the original dataset, but excluding the now-unavailable features from the train dataset. There is no comparison between an incumbent and a challenger model in this case, as the former is no longer operational. Indeed, the goal is to identify the best challenger model and deploy it.

## 2. Problem and Model Formulation

In this section, we formalize the decision problem of whether, and when, to replace an incumbent  $f_I$  with a challenger  $f_C$ . We describe the problem setting, how performance and economic gains are measured, the economic structure, and the value expressions that govern switching decisions.

### 2.1. Defining the Problem Setting

We consider a supervised learning setting over a feature space  $\mathcal{X}$  and target space  $\mathcal{Y}$ . The available features are partitioned into two sets: an *initial feature set*  $\mathcal{I}$  and an *expanded feature set*  $\mathcal{C} \supset \mathcal{I}$ , which becomes available only later. Initially, only the features in  $\mathcal{I}$  were observable; we write  $\mathcal{X}_{\mathcal{I}}$  for the projection of  $\mathcal{X}$  onto the features in  $\mathcal{I}$ . An *incumbent* predictive model  $f_I : \mathcal{X}_{\mathcal{I}} \rightarrow \mathcal{Y}$  was trained on a large historical dataset of size  $N_0$ , where each sample contains only the features in  $\mathcal{I}$ . This model belongs to a hypothesis class  $\mathcal{F}_I$  and is assumed to have been trained to (or near) its optimal expected performance under the distribution of  $(\mathcal{X}_{\mathcal{I}}, \mathcal{Y})$ .

At a later point in time, the features in  $\mathcal{C} \setminus \mathcal{I}$  become observable. Their availability enables the training of a new *challenger* model  $f_C : \mathcal{X}_{\mathcal{C}} \rightarrow \mathcal{Y}$ , drawn from a (possibly richer) hypothesis class  $\mathcal{F}_C \supseteq \mathcal{F}_I$ . Because the historical dataset does not contain the new features, the challenger can initially be trained only on a much smaller dataset of size  $n \ll N_0$  for which all features in  $\mathcal{C}$  are observed. As  $n$  grows over time with the collection of new full-feature samples, the challenger's expected performance is uncertain at early stages but may eventually surpass that of the incumbent.

We study a sequential process in which data arrive over discrete time steps  $t \in \mathcal{T} = \{1, \dots, T\} := [T]$ , each representing a natural unit of the process (e.g., a new sample or batch). These time steps are inherent to the problem and determine when new data become available. At each time step  $t$ ,  $n_t$  new samples containing all features in  $\mathcal{C}$  are observed, so that the cumulative number of full-feature samples after  $t$  is  $N_t = \sum_{\tau=1}^t n_{\tau}$ .

The decision maker does not necessarily act at every time step. Instead, decisions are made at a subset of these time points, denoted by decision epochs  $\mathcal{T}_D = \{t_1, t_2, \dots\} \subseteq \mathcal{T}$ . At each decision epoch  $t \in \mathcal{T}_D$ , the decision maker:

- Retrains the challenger on all data collected so far ( $N_t$  samples), producing an updated  $f_C^{(t)}$ .
- Evaluates whether to: (i) *switch* – deploying  $f_C^{(t)}$  and replacing  $f_I$ ; (ii) *discard* – permanently rejecting  $f_C$  and stopping data collection; or (iii) *continue* – collecting more full-feature samples and deferring the decision until a later epoch.

Between decision epochs, data continue to arrive, but the challenger is not retrained or re-evaluated. This separation between time steps and decision epochs captures the practical reality that organizations may acquire data continuously but reassess deployment decisions only at scheduled intervals.

In Section 3, we focus on the theoretical characterization of the optimal stopping rule at the level of individual time steps. That is, we assume that data arrive one (or one batch) at a time, and the decision maker can in principle act after each step. This continuous-monitoring formulation provides full granularity and yields an upper bound on achievable performance. In practice, however, it is rarely optimal or realistic to retrain this frequently; instead, the choice of decision epochs effectively coarsens the time scale and introduces a trade-off between responsiveness and cost. Decision epochs are algorithmic design choices, determined by how frequently the organization elects to revisit the deployment question. Their design can have a significant impact on the performance and cost of different algorithms and will be revisited in Section 4. In the remainder of this section, we characterize the gains, costs, and value expressions that determine the optimal switching policy.

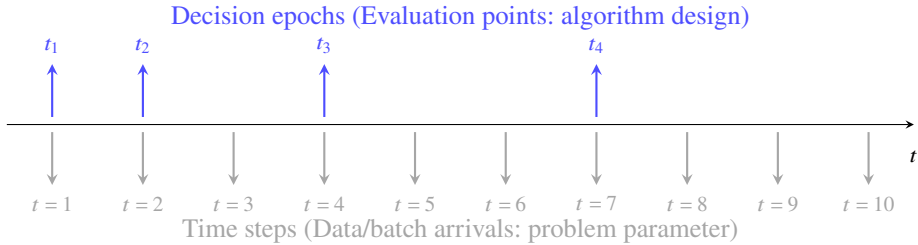


**Figure 1** Time steps vs. decision epochs

*Note.* Time steps (gray, data arrivals) are inherent to the problem and exogenous. Decision epochs (blue, evaluation points), here geometrically spaced, are chosen by the algorithm designer and determine when deployment decisions are revisited.

## 2.2. Measuring Gains

To quantify the benefit of transitioning models, we define how a model's monetary gains are measured. Given any predictive model  $f$ , let  $\ell : \mathcal{Y} \times \mathcal{Y} \rightarrow \mathbb{R}$  be a bounded gain function representing the monetary return  $\ell(f(x), y)$  obtained when  $f$  predicts  $y$  from  $x$ . Then, the expected *economic performance gap* of model  $f_C$  over model  $f_I$  at time step  $t$  is defined as:

$$G(t) := \mathbb{E}[\ell(f_C^{(t_k)}(X_C), Y)] - \mathbb{E}[\ell(f_I(X_I), Y)],$$

where expectations are taken with respect to the data-generating distribution of  $(X, Y)$  and  $X_C$  (resp.  $X_I$ ) is the projection of random variable  $X$  onto the features in  $C$  (resp.  $I$ ). We make two remarks:

- The first expectation evaluates the challenger. Since the challenger is retrained *only* at decision epochs  $t_k \in \mathcal{T}_D$ , the model used at a general time step  $t \in \mathcal{T}$  is the one from the most recent epoch  $k = \max\{k' \in [|\mathcal{T}_D|] : t_{k'} \leq t\}$ :  $f_C^{(t_k)}$ , trained using all  $N_{t_k}$  full-feature samples available at time  $t_k$ .
- The second expectation is the fixed expected performance of the incumbent  $f_I$ , which is trained once on historical data and does not change over time.

Thus  $G(t)$  captures the expected incremental monetary value of switching at time  $t$ , based on the challenger as last trained. In practice,  $G(t)$  is unknown and we rely on an empirical estimate  $\widehat{G}(t)$  computed from the available data. Since  $\widehat{G}(t)$  is estimated from finite data, it is subject to statistical uncertainty; we address this concern in Section 4.

*Examples.* Our formulation accommodates a wide range of practical performance measures through the choice of  $\ell$ . Suppose correct decisions yield monetary gains  $g_1$  (true positives) and  $g_2$  (true negatives), while errors incur costs  $c_1$  (false positives) and  $c_2$  (false negatives). A profit-and-loss function capturing this structure is  $\ell(f(x), y) = g_1 \mathbb{I}\{f(x) = 1, y = 1\} + g_2 \mathbb{I}\{f(x) = 0, y = 0\} - c_1 \mathbb{I}\{f(x) = 1, y = 0\} - c_2 \mathbb{I}\{f(x) = 0, y = 1\}$ , in which case  $G(t)$  measures the expected economic performance gap from improved classification under these weights. In this case,  $G(t) = g_1 \Delta P(\text{TP}) + g_2 \Delta P(\text{TN}) - c_1 \Delta P(\text{FP}) - c_2 \Delta P(\text{FN})$ , where  $\Delta P(\cdot)$  is the challenger–incumbent difference in the corresponding error component. The definition generalizes naturally to performance measures that cannot be expressed as the expectation of loss functions, such as the area-under-the-curve (AUC):  $G(t) = g (\text{AUC}_C(t) - \text{AUC}_I)$ , where we assume that an increase in AUC produces an expected monetary improvement of  $g$  per unit.

### 2.3. Measuring Costs

We organize all costs by *type* (acquisition, training, switching) and by the *time at which they are incurred* (pre-decision, decision-time, or post-decision). Table 1 summarizes the assumed cost structure and functional form of each term.

*Cost types.* We consider three cost types. (i) The first is the *acquisition cost*: each new batch acquired at time step  $t \in \mathcal{T}$  incurs an acquisition cost  $C_{\text{acq}}(t)$ . Those may be the monetary costs associated with sourcing the features, or pre-processing costs. A natural case is, given a constant per-sample cost  $c_{\text{acq}}$ , to consider linear acquisition costs in the batch size, i.e.,  $C_{\text{acq}}(t) = c_{\text{acq}} n_t$ . (ii) The second is the *training cost*: when retraining occurs at a decision epoch  $t \in \mathcal{T}_D$ , a training cost  $C_{\text{train}}(t)$  is incurred. This cost captures two conceptually distinct components: (ii,a) the fixed labor cost associated with setting up or monitoring a training run, and (ii,b) the variable computational cost associated with training. In practice, the relative magnitude of these components determines

how training costs scale with the cumulative sample size  $N_t$ . If computational cost dominates, one typically expects a convex dependence on  $N_t$ , such as  $C_{\text{train}}(t) = c_{\text{train}} N_t^2$ . Conversely, if the main cost is the engineer’s time to launch and supervise the pipeline, training costs may be effectively constant per retraining event, yielding  $C_{\text{train}}(t) = c_{\text{train}}$ . (iii) The third is the *switching cost*: if the challenger replaces the incumbent at decision epoch  $t$ , a one-time switching cost  $c_s$  is incurred.

*Cost timing.* We again distinguish three categories: (i) The first is the *pre-decision cost*, including acquisition and training, incurred before the switching decision and sunk at time  $t$ :  $C_{\text{pre}}(t) = C_{\text{acq}}^{\text{pre}}(t) + C_{\text{train}}(t)$ . (ii) The second is the *decision-time cost*, incurred once at  $t$ :  $c_s$ . (iii) The third is the *post-decision cost*, incurred only after the decision, and that depends on whether the challenger is adopted:  $C_{\text{post}}(t) = C_{\text{acq}}^{\text{post}}(t)$ .

**Table 1 Summary of cost types and timing, and example functional forms.**

Timing	Acquisition	Training	Switching
Pre-decision	$C_{\text{acq}}^{\text{pre}}(t) \stackrel{\text{e.g.}}{=} c_{\text{acq}}^{\text{pre}} n_t$	$C_{\text{train}}(t) \stackrel{\text{e.g.}}{=} c_{\text{train}} \mathbb{I}\{t \in \mathcal{T}_D\}$	
Switching-time			$c_s$
Post-decision	$C_{\text{acq}}^{\text{post}}(t) \stackrel{\text{e.g.}}{=} c_{\text{acq}}^{\text{post}} n_t$		

## 2.4. Defining the Value Functions and Switching Rule

At each decision epoch  $t \in \mathcal{T}_D$ , the decision maker chooses one of three actions: *switch* to the challenger, permanently *discard* it and stop data collection, or *continue* data collection. All cash flows are evaluated at time 0 (before data collection begins) in present value using a per-epoch discount factor  $\beta \in (0, 1]$ . We now compute the value of switching and discarding at epoch  $t$ , derive the incremental value  $\Delta V(t)$ , and, as an extension, we discuss how to incorporate budget constraints.

*Value if switching.* Switching to the challenger at decision epoch  $t \in \mathcal{T}_D$  entails:

- The cumulative pre-decision costs incurred up to  $t$ ,  $\sum_{\tau \leq t} \beta^\tau C_{\text{pre}}(\tau)$  (sunk at  $t$ ).
- A one-time switching cost  $\beta^t c_s$  incurred when switching to the challenger.
- The cumulative post-decision net gain in future time steps,  $\sum_{\tau > t} \beta^\tau [n_\tau \cdot G(t) - C_{\text{post}}(\tau)]$ .

By using  $G(t)$  in the post-decision net gain, we are explicitly assuming that a switch at epoch  $t$  deploys the challenger model trained at that same epoch.<sup>2</sup> Put together, the present value at time 0 of switching to the challenger at  $t$  is:

$$V_{\text{switch}}(t) = \underbrace{- \sum_{\tau \leq t} \beta^\tau C_{\text{pre}}(\tau)}_{\text{pre-decision}} \underbrace{- \beta^t c_s}_{\text{decision-time}} + \underbrace{\sum_{\tau > t} \beta^\tau [n_\tau \cdot G(t) - C_{\text{post}}(\tau)]}_{\text{post-decision}}.$$

<sup>2</sup> For simplicity, we do not consider the option of switching at time  $t$  to a challenger trained earlier at some  $t' < t$ . We revisit this case later and show that, under mild assumptions, such delayed-switch choices are always suboptimal.

*Value if discarding.* Discarding the challenger at decision epoch  $t \in \mathcal{T}_D$  yields no future gains or costs, yielding  $V_{\text{discard}}(t) = -\sum_{\tau \leq t} \beta^\tau C_{\text{pre}}(\tau)$ .

*Stopping rule.* Since the discounted pre-decision costs are common to both branches, the incremental present value of switching is then  $\Delta V(t) := V_{\text{switch}}(t) - V_{\text{discard}}(t) = -\beta^t c_s + \sum_{\tau > t} \beta^\tau [n_\tau \cdot G(t) - C_{\text{post}}(\tau)]$ . Thus, we will consider switching at decision epoch  $t$  only if  $\Delta V(t) > 0$ .

*Budget constraint.* Often, organizations operate under constraints on the resources they can allocate to evaluating challenger models. Under such constraints, a switch can occur only if the available budget covers all pre-decision and decision-time costs incurred up to that point. Concretely, if a total budget  $B$  applies to these costs, then any admissible decision epoch  $t \in \mathcal{T}_D$  must satisfy  $\sum_{\tau \leq t} \beta^\tau C_{\text{pre}}(\tau) + \beta^t c_s \leq B$ . By checking this constraint sequentially for increasing  $t$ , we determine the largest feasible decision epoch  $\bar{T}$  allowed by the budget, which serves as an upper bound on how long the process may continue before switching becomes financially infeasible.

### 3. Optimal Solution Characterization

In this section, we focus on the theoretical characterization of the optimal stopping rule at the granularity of individual time steps. To do so, we assume that all problem parameters, including the trained challengers' expected performances, are known to the decision maker. By analyzing an analytically tractable version of the problem, we derive structural insights that guide the design of the algorithms and empirical implementations developed in later sections.

We cast the problem as an optimal stopping problem: the goal is to determine the optimal time step at which to make one of three decisions—*switch* to the challenger, permanently *discard* it and stop data collection, or *continue* collecting data. A few remarks are in order: (i) “Optimal” is understood in terms of maximizing net profit. (ii) Working at the granularity of individual time steps removes the distinction between decision epochs and time steps ( $\mathcal{T}_D = \mathcal{T}$ ). (iii) The action is irreversible: once the challenger is adopted or discarded, the process stops. (iv) Under this setting, the decision maker trains at most one challenger—the one, if any, it ultimately switches to.

#### 3.1. Deriving the Optimal Stopping Rule for a Stylized Setting

We begin with a stylized setting that admits closed-form stopping rules. We consider two variants of increasing complexity, each showcasing different aspects of the underlying trade-offs. In both settings, we make the following three assumptions:

**ASSUMPTION 1 (Fixed sample flow).** *The batch size per time step is constant:  $n_t = n$  for all  $t$ .*

**ASSUMPTION 2 (Economic performance gap structure).** *The challenger's expected economic performance gap curve follows:  $G(t) = g^* - g_0 N_t^{-\alpha}$ ,  $g^* > 0$ ,  $g_0 > 0$ ,  $\alpha > 0$ .*

**ASSUMPTION 3 (Cost structure).** *The cost functions are:  $C_{\text{acq}}^{\text{pre}}(t) = c_{\text{pre}}^{\text{acq}} n_t$ ,  $C_{\text{train}}(t) = c_{\text{train}}$ ,  $C_{\text{acq}}^{\text{post}}(t) = c_{\text{post}}^{\text{acq}} n_t$ , with  $c_{\text{post}}^{\text{acq}} \geq 0$ ,  $c_{\text{pre}}^{\text{acq}} \geq 0$ ,  $c_s > 0$ , and  $c_{\text{train}} \geq 0$ .*

Assumption 1 is common in the model retraining literature, whereas Assumption 2 is consistent with the theoretical and empirical literature on learning curves (see Section 1.2 and the references therein). Assumption 3, while restrictive, enables the derivation of closed-form solutions, which, in turn, offer insight into how the optimal solution evolves with the problem parameters. Put together, under Assumptions 1-3, the effective per-sample gains, pre-, and post-decision costs are, respectively,  $g^* - g_0 N_t^{-\alpha}$ ,  $c_{\text{pre}}^{\text{acq}} + \frac{c_{\text{train}}}{n} =: c_{\text{pre}}$ ,  $c_{\text{post}}^{\text{acq}} =: c_{\text{post}}$ .

*Setting I: Finite horizon, no discounting, simplified gains and costs.* To expose the core tradeoff between learning (improving  $G(t)$ ) and remaining opportunity ( $T - t$ ), we momentarily consider a further simplified setting, described below:

**ASSUMPTION 4.** *In addition to Assumptions 1–3, (i) the horizon is finite ( $T < \infty$ ); (ii) there is no discounting ( $\beta = 1$ ); (iii) the pre- and post-decision per-sample acquisition costs are equal ( $c_{\text{pre}}^{\text{acq}} = c_{\text{post}}^{\text{acq}} =: c$ ) and the training cost is negligible ( $c_{\text{train}} = 0$ ).*

Assumptions 1–4 taken together constitute Setting I. Under Setting I,  $V_{\text{switch}}(t) = -T n c - c_s + (T - t) n G(t) = -T n c - c_s + (T - t) n \left(g^* - \frac{g_0}{(nt)^\alpha}\right)$  and  $\arg \max_t V_{\text{switch}}(t) = \arg \max_{t \in \mathcal{T}} (T - t) G(t)$ . Then, the continuous first-order condition yields  $\frac{d}{dt} [(T - t) G(t)] = 0 \Leftrightarrow (T - t) \frac{d}{dt} G(t) = G(t) \Leftrightarrow \frac{(T-t)}{t} \alpha g_0 \frac{1}{(nt)^\alpha} = g^* - g_0 \frac{1}{(nt)^\alpha} \Leftrightarrow \left[1 + \frac{\alpha(T-t)}{t}\right] \frac{g_0}{(nt)^\alpha} = g^*$ . For large horizon  $T$ , this implies  $g^* \approx \frac{\alpha g_0 T}{n^\alpha t^{\alpha+1}}$ , which, in turn, implies the following proposition:

**PROPOSITION 1 (Optimal stopping rule in Setting I).** *Under Assumption 4, the (continuous) optimizer verifies  $t^* \sim_{T \rightarrow \infty} \left[ \left( \frac{g_0}{n^\alpha} \right) \frac{\alpha T}{g^*} \right]^{\frac{1}{1+\alpha}}$ .<sup>3</sup> The decision epoch maximizing  $V_{\text{switch}}(t)$  is  $t_{\text{int}}^* \in \{ \lfloor t^* \rfloor, \lceil t^* \rceil \}$  and we switch if and only if  $V_{\text{switch}}(t_{\text{int}}^*) \geq 0$ .*

Proposition 1 reveals that the optimal stopping point  $t^*$  is only determined by the learning curve, the horizon length, and the batch size. Specifically,  $t^*$  grows with  $T$  and  $g_0$  (more time or larger initial gap  $\Rightarrow$  wait longer) and shrinks with  $n$  and  $g^*$  (faster data flow or higher asymptotic gap  $\Rightarrow$  decide earlier). It also highlights the importance of the *shape of the learning curve* through the dependency on  $\alpha$  in the exponent. The costs  $c$  and  $c_s$  do not affect the *stopping time* in this setting (they are  $t$ -constant), but they determine whether switching is worthwhile via the final inequality.

<sup>3</sup> Here, the notation  $t^* \sim_{T \rightarrow \infty} h(T)$  means that  $\lim_{T \rightarrow \infty} t^*/h(T) = 1$ .

*Setting II.* We now turn to a more general and realistic setting. Specifically, here, we consider an infinite deployment horizon with discounting and we relax our assumptions on the cost structure. We replace Assumption 4 with the following assumption:

**ASSUMPTION 5 (Setting II).** *In addition to Assumptions 1–3, we assume that: (i) the horizon is infinite ( $T \rightarrow \infty$ ); (ii) the per-epoch discount factor is  $0 < \beta < 1$ .*

Under Assumption 5, we have  $V_{\text{switch}}(t) = -\sum_{\tau \leq t} \beta^\tau n c_{\text{pre}} - \beta^t c_s + \sum_{\tau > t} \beta^\tau \left[ nG(t) - nc_{\text{post}} \right] = -\frac{nc_{\text{pre}}}{1-\beta} + \frac{\beta^{t+1}}{1-\beta} n \left[ G(t) - \left( c_{\text{post}} - c_{\text{pre}} + \frac{c_s(1-\beta)}{\beta n} \right) \right]$ , where the quantity  $c_{\text{diff}} := \left( c_{\text{post}} - c_{\text{pre}} + \frac{c_s(1-\beta)}{\beta n} \right)$  is the effective per-sample cost of switching: the post–pre per-sample cost difference plus the discounted per-sample equivalent of the one-time switch cost. It is the hurdle that  $G(t)$  must exceed.

Similar with Setting I, we start with an asymptotic analysis of the optimal stopping time for  $\beta$  close to one, which corresponds to the regime where large horizons matter. We again compute the first-order condition  $\frac{d}{dt} V_{\text{switch}}(t) = \frac{n\beta^{t+1}}{1-\beta} \left( \ln(\beta) \left( g^* - \frac{g_0}{(nt)^\alpha} - c_{\text{diff}} \right) + \frac{\alpha g_0}{n^\alpha t^{\alpha+1}} \right)$ , which, in turn, implies the following proposition on the optimal switching time when there is little discounting:

**PROPOSITION 2 (Optimal stopping rule in Setting II).** *Under Assumption 5, the (continuous) optimizer satisfies  $t^* \sim_{\beta \rightarrow 1} \left[ \left( \frac{g_0}{n} \right)^\alpha \frac{\alpha}{g^* - c_{\text{diff}}} \frac{1}{1-\beta} \right]^{\frac{1}{1+\alpha}}$ .*

Note that, if we extend Assumption 5 by adding Part (iii) of Assumption 4, i.e.,  $c_{\text{pre}} = c_{\text{post}}$ , then we get  $c_{\text{diff}} = \frac{c_s(1-\beta)}{\beta n}$ , which goes to zero as  $\beta$  approaches one. Therefore, we recover exactly the expression of Proposition 1, with  $T$  replaced with  $1/(1-\beta)$ . This is coherent with a known fact from the literature on Markov Decision Processes (MDPs): discounted MDPs with a discount factor of  $\beta$  and finite horizon MDPs with  $T = \frac{1}{1-\beta}$  are good approximations to each other.

We now analyze in more detail the optimal solution in the non-asymptotic regime. We define  $K := n^\alpha \left( \frac{g^*}{g_0} - \frac{c_{\text{diff}}}{g_0} \right)$ , which aggregates the normalized asymptotic economic performance gap ( $g^*/g_0$ ) and the net economic gain (per-sample pre–post cost difference minus discounted switching cost, scaled by  $g_0$ ), amplified by the sample-flow factor  $n^\alpha$ .  $K$  is the central quantity in the general-case results, governing whether switching is profitable and, if so, determining the timing of the optimal switch. Then, we have the following theorem:

**THEOREM 1 (Optimal stopping rule in Setting II).** *Let Assumption 5 hold, then:*

1. **Feasibility:** *If  $K \leq 0$  (equivalently,  $g^* \leq c_{\text{diff}}$ ), then switching cannot be optimal.*
2. **Existence & uniqueness:** *If  $K > 0$ , the function  $t \mapsto V_{\text{switch}}(t)$  admits a unique maximizer  $t^* \in \mathcal{T}$  that corresponds to the unique candidate switching epoch and satisfies  $t^* > t_0 := ((\alpha+1)K)^{-1/\alpha}$ .*

3. **Stopping rule:** The smallest  $t \in \mathcal{T}$  satisfying  $G(t) - \beta G(t+1) - (1-\beta)c_{\text{diff}} \geq 0$  equals  $t^*$ . Moreover, switching is globally optimal if and only if  $V_{\text{switch}}(t^*) \geq V_{\text{discard}}(0)$ .

We defer the proof to the Electronic Companion (EC.1). Theorem 1 has three practical implications:

- **Feasibility:** Switching can be optimal only when  $K > 0$ . Equivalently, the long-run gain  $g^*$  must exceed the effective cost differential  $c_{\text{diff}} = c_{\text{post}} - c_{\text{pre}} + \frac{c_s(1-\beta)}{\beta n}$ . If  $K \leq 0$ , then we never switch.
- **Existence & uniqueness:** When  $K > 0$ , there is a unique *candidate* switching epoch. Conditional on switching, faster flow  $n$ , larger  $g^*$  or  $(c_{\text{pre}} - c_{\text{post}})$ , or smaller  $c_s$  raise  $K$ , leading to earlier stopping. Larger  $g_0$  shrinks  $K$ , pushing toward later stopping as the challenger has more to learn.
- **Stopping rule:** Assuming  $G(t)$  is known (which in practice is rarely the case), this provides a condition to identify the candidate switching epoch. Intuitively, we stop at the earliest  $t$  when the marginal, per-epoch discounted net benefit of adopting the challenger (performance improvement plus any pre–post cost advantage) exceeds the effective discount-adjusted, per-batch switching cost.

### 3.2. Defining the Oracle Solution for the General Setting

We consider an *oracle* with perfect knowledge of the true gaps  $\{G(t)\}_{t \in \mathcal{T}}$ . Let  $V_{\text{switch}}(t)$  be the present value defined in Section 2.4, with training at time step  $t$  only. The oracle compares this value with the value of discarding immediately (keeping the incumbent and not collecting any data). If  $\max_{t \in \mathcal{T}} V_{\text{switch}}(t) \leq 0$ , the oracle discards at  $t = 0$ ; otherwise, it switches at  $t^* \in \arg \max_{t \in \mathcal{T}} V_{\text{switch}}(t)$ . Thus, the oracle’s problem reduces to a single-variable optimization over  $t$  together with a final profitability check against discarding immediately, so the resulting value is always nonnegative.

This oracle is optimal in most realistic settings. Under full foresight, two structural properties typically hold: (i) training only one challenger is optimal—since  $t^*$  is known, training any model other than the one deployed at  $t^*$  adds pre-decision cost without increasing value; and (ii) delaying deployment after training is suboptimal under mild conditions, e.g., when pre-deployment costs exceed post-deployment costs or when per-sample post-deployment costs are constant.<sup>4</sup> Accordingly, this oracle serves as a benchmark against which we evaluate our algorithms.

## 4. Algorithm Design

In this section, we turn to the design of practical stopping rules for the general setting in which the true performance gains of the challenger are unknown and must be estimated from data. At each decision epoch, the decision maker observes only an empirical estimate and must decide whether to

<sup>4</sup> Delaying can be optimal in pathological (practically irrelevant) cases, e.g., if post-deployment costs drop sharply at some timestep.

switch, discard, or continue. An effective stopping rule must therefore balance statistical uncertainty against the value of timely adoption.

We present three algorithms, in increasing order of sophistication. The first uses a single, non-adaptive evaluation and ignores statistical uncertainty. The second introduces sequential evaluation and confidence bounds to account for estimation error. The third uses local trends in the estimated learning curve to anticipate future improvements. Together, these algorithms show how incorporating additional information and structure leads to better-timed and more reliable switching decisions. Moreover, as we now design practical algorithms, we re-introduce the distinction between time steps  $\mathcal{T}$  and decision epochs  $\mathcal{T}_D$ —the time steps at which the algorithm evaluates a decision ( $\mathcal{T}_D \subseteq \mathcal{T}$ ). We index decision epochs  $t \in \mathcal{T}_D$  by  $k \in [|\mathcal{T}_D|]$  and write  $t_k$  for the actual time step at which epoch  $k$  occurs, so that the  $k$ th evaluation uses the  $N_{t_k}$  full-feature samples collected up to time  $t_k$ .

#### 4.1. One-Shot Evaluation (OSE) Algorithm

As a starting point, we consider a simple, non-adaptive algorithm that evaluates the challenger only once, at a fixed decision epoch. This algorithm ignores statistical uncertainty and commits to a decision based on a single empirical estimate of the challenger’s performance. Because the optimal switching time depends on unknown problem parameters, such a one-shot decision rule will typically miss the optimal moment to switch. We therefore use it primarily as a baseline for assessing more adaptive strategies.

---

#### Algorithm 1 One-Shot Evaluation (OSE)

---

- 1: **Input:** evaluation epoch  $t_k \in \mathcal{T}_D$ , split ratio  $\rho$
- 2: Collect  $N_{t_k}$  samples and split into training and validation set of sizes  $(1 - \rho)N_{t_k}$  and  $\rho N_{t_k}$
- 3: Train challenger  $f_C^{(t_k)}$  on training set
- 4: Compute empirical gap  $\widehat{G}(t_k)$  via (1) on validation set and  $\widehat{\Delta V}(t_k)$  via (2)
- 5: **if**  $\widehat{\Delta V}(t_k) > 0$  **then** switch; **else** discard

---

We provide the full algorithm in Algorithm 1. At a pre-determined epoch  $t_k \in \mathcal{T}_D$ , the  $N_{t_k}$  samples collected to date are randomly split into a training set of size  $(1 - \rho)N_{t_k}$  and a validation set  $\mathcal{V}_t$  of size  $\rho N_{t_k}$ . The challenger  $f_C^{(t_k)}$  is trained on the  $(1 - \rho)N_{t_k}$  training samples. Its per-sample performance gap is then estimated on the validation set as:

$$\widehat{G}(t_k) := \frac{1}{\rho N_{t_k}} \sum_{i \in \mathcal{V}_{t_k}} (\ell(f_C^{(t_k)}(x_i), y_i) - \ell(f_I(x_i), y_i)), \quad (1)$$

where  $(x_i, y_i)$  denotes the  $i$ th sample in the validation set  $\mathcal{V}_t$ . Using this estimate, the decision maker computes the corresponding empirical value of switching as:

$$\widehat{\Delta V}(t_k) = -\beta^{t_k} c_s + \sum_{\tau > t_k} \beta^\tau [n_\tau \widehat{G}(t_k) - C_{\text{post}}(\tau)], \quad (2)$$

which mirrors the value function in Section 2.4 but replaces unknown quantities with empirical estimates. The algorithm switches if  $\widehat{\Delta V}(t_k) > 0$ .

#### 4.2. Greedy Sequential Evaluation (GSE) Algorithm

We now build on the OSE algorithm by introducing a *sequential* evaluation procedure that incorporates *statistical uncertainty* into the switching decision. To do so, at each decision epoch, we compute conservative lower and upper bounds (LB, UB) on the estimated value of switching, using confidence intervals that shrink as more data accumulate. We switch to (or discard) the challenger when there is sufficient statistical evidence that the value of switching is positive (or negative).

---

#### Algorithm 2 Greedy Sequential Evaluation (GSE)

---

- 1: **Input:** decision epochs  $\mathcal{T}_D$ , split ratio  $\rho$ , confidence parameter  $\gamma$
- 2: **for**  $k = 1, \dots, |\mathcal{T}_D|$  **do**
- 3:     Train challenger  $f_C^{(t_k)}$  on the training set
- 4:     Compute  $\widehat{V}_{\text{switch}}^{\text{LB}}(t_k)$  via (3) and  $\widehat{V}_{\text{switch}}^{\text{UB}}(t_k)$  via (4)
- 5:     **if**  $\widehat{V}_{\text{switch}}^{\text{LB}}(t_k) > 0$  **then** switch and stop
- 6:     **if**  $\widehat{V}_{\text{switch}}^{\text{UB}}(t_k) < 0$  **then**
- 7:         Compute  $\widehat{\Delta V}^{\text{LB}}(t_k)$  via (5)
- 8:         **if**  $\widehat{\Delta V}^{\text{LB}}(t_k) > 0$  **then** switch and stop; **else** discard and stop

---

We provide the full algorithm in Algorithm 2. At each decision epoch  $t_k \in \mathcal{T}_D$ , the algorithm proceeds exactly as before: the  $N_{t_k}$  full-feature samples are split into a training set of size  $(1 - \rho)N_{t_k}$  and a validation set of size  $\rho N_{t_k}$ , the challenger  $f_C^{(t_k)}$  is retrained on the training set, and its per-sample performance gap is estimated on the validation set as  $\widehat{G}(t_k)$  via (1). To account for estimation uncertainty, we define a confidence width  $\delta_k := \gamma \sqrt{\frac{1}{\rho N_{t_k}}}$ , where  $\gamma > 0$  controls the level of conservatism. This width decreases as  $N_{t_k}$  grows, so confidence grows as more samples accumulate. We construct the following lower and upper bounds on the *estimated* value of switching:

$$\widehat{V}_{\text{switch}}^{\text{LB}}(t_k) = -\sum_{\tau \leq t_k} \beta^\tau C_{\text{pre}}(\tau) - \beta^{t_k} c_s + \sum_{\tau > t_k} \beta^\tau [n_\tau (\widehat{G}(t_k) - \delta_k) - C_{\text{post}}(\tau)], \quad (3)$$

$$\widehat{V}_{\text{switch}}^{\text{UB}}(t_k) = - \sum_{\tau \leq t_k} \beta^\tau C_{\text{pre}}(\tau) - \beta^{t_k} c_s + \sum_{\tau > t_k} \beta^\tau [n_\tau(\widehat{G}(t_k) + \delta_k) - C_{\text{post}}(\tau)]. \quad (4)$$

If  $\widehat{V}_{\text{switch}}^{\text{LB}}(t_k) > 0$ , the decision maker switches immediately. If  $\widehat{V}_{\text{switch}}^{\text{UB}}(t_k) < 0$ , the estimated value of switching is negative even under optimistic gaps, so the decision maker stops training. Although it is now estimated that the returned value will be negative, there may still be some value to switching to the challenger. Indeed, since all acquisition and training costs up to  $t_k$  are sunk, we still need to compare the challenger to discarding. We compute the conservative incremental value of switching:

$$\widehat{\Delta V}^{\text{LB}}(t_k) = -\beta^{t_k} c_s + \sum_{\tau > t_k} \beta^\tau [n_\tau(\widehat{G}(t_k) - \delta_k) - C_{\text{post}}(\tau)]. \quad (5)$$

If  $\widehat{\Delta V}^{\text{LB}}(t_k) > 0$ , the algorithm switches to the challenger; otherwise it discards. If neither condition holds, i.e.  $\widehat{V}_{\text{switch}}^{\text{LB}}(t_k) < 0$  and  $\widehat{V}_{\text{switch}}^{\text{UB}}(t_k) > 0$ , the available data are insufficient to make a statistically confident decision, and the algorithm proceeds to the next decision epoch.

### 4.3. Look-ahead Sequential Evaluation (LSE) Algorithm

The previous algorithms evaluate the challenger based solely on its current estimated performance, possibly adjusted for statistical uncertainty, but they do not explicitly reason about how the challenger may continue to improve as additional data arrive. We now introduce a *sequential* evaluation algorithm that attempts to *anticipate* such future improvements by extrapolating trends in estimated gaps. Specifically, the algorithm fits a local linear approximation to the empirical learning curve and uses its slope to construct an optimistic projection of how much further performance could increase, thereby assessing whether waiting for more data may offer a better opportunity to switch.

---

#### Algorithm 3 Look-ahead Sequential Evaluation with/without Confidence Adjustment (LSE/LSEc)

---

- 1: **Input:** epochs  $\mathcal{T}_D$ , split ratio  $\rho$ , confidence parameter  $\gamma$ , smoothing parameter  $w$
- 2: Train challengers  $f_C^{(t_1)}, \dots, f_C^{(t_{w-1})}$ ; compute  $\widehat{G}(t_1), \dots, \widehat{G}(t_{w-1})$
- 3: **for**  $k = w, \dots, |\mathcal{T}_D| - 1$  **do**
- 4:     Train challenger  $f_C^{(t_k)}$ ; compute  $\widehat{G}(t_k)$
- 5:     Estimate slope  $\hat{s}_k$  from  $\widehat{G}(t_{k-w+1}), \dots, \widehat{G}(t_k)$  with confidence  $\gamma$
- 6:     Compute projected values  $\widehat{V}_{\text{switch}}^{\text{UB}}(t_{k'})$  for  $k' > k$  via (6) and current value  $\widehat{V}_{\text{switch}}(t_k)$  via (7)
- 7:     **if**  $\max(\widehat{V}_{\text{switch}}(t_k), -\sum_{\tau \leq t_k} C_{\text{pre}}(\tau)) \geq \max_{k' > k} \widehat{V}_{\text{switch}}^{\text{UB}}(t_{k'})$  **then**
- 8:         **if**  $\widehat{\Delta V}(t_k) > 0$  **then** switch and stop; **else** discard and stop
- 9: **if**  $k = |\mathcal{T}_D|$  **then** train  $f_C^{(t_k)}$ ; compute  $\widehat{G}(t_k), \widehat{\Delta V}(t_k)$ ; **if**  $\widehat{\Delta V}(t_k) > 0$  **then** switch **else** discard

---

We provide the full algorithm in Algorithm 3. At each decision epoch  $t_k \in \mathcal{T}_D$ , we observe  $N_{t_k}$  full-feature samples and compute the empirical per-sample gap  $\widehat{G}(t_k)$ , as in the previous algorithms. The slope-based algorithm then proceeds in three steps: (i) estimate a local slope of the empirical learning curve using recent evaluations, (ii) use this slope to construct optimistic projections of future gaps, and (iii) compare the current estimated value of switching with these projections to determine whether waiting is potentially beneficial. We now detail each component.

*Slope estimation.* The algorithm maintains a local estimate  $\hat{s}_k$  of the slope of the empirical learning curve at epoch  $k$ . Intuitively, the slope estimate  $\hat{s}_k$  can be thought of as the incremental improvement in the challenger's gap per additional sample, as captured by a simple finite difference such as  $\frac{\widehat{G}(t_k) - \widehat{G}(t_{k-1})}{(1-\rho) \cdot (N_{t_k} - N_{t_{k-1}})}$ . In practice, direct finite differences are noisy, and we consider the following robustification procedures, each resulting in a different variant of Algorithm 3:

(i) *Smoothing*: Instead of relying only on the most recent estimate of the gaps, we smooth the finite difference by looking at the last  $w \geq 2$  points. We first apply a monotonicity correction: if the gaps decrease across  $t_{k-w+1}, \dots, t_k$ , the values are replaced by their average. We then perform a least-squares linear regression of these corrected gaps on the sample counts  $N_{t_{k-w+1}}, \dots, N_{t_k}$ , and take the fitted slope as  $\hat{s}_k$ . In practice, we find that a window size of  $w = 3$  is sufficient: learning rates typically decrease quickly, so using four or more points tends to oversmooth the curve and underestimate the local slope. We refer to this variant as LSE.

(ii) *Confidence-adjustment*: We adjust the finite difference using a confidence term. Let  $\delta_k := \gamma / \sqrt{\rho N_{t_k}}$  be the confidence adjustment. If the most recent improvement is negative, i.e.,  $\widehat{G}(t_k) - \widehat{G}(t_{k-1}) < 0$ , we set  $\hat{s}_k = \frac{2\delta_k}{(1-\rho) \cdot (N_{t_k} - N_{t_{k-1}})}$ . Otherwise, we use the uncertainty-adjusted finite difference  $\hat{s}_k = \frac{(\widehat{G}(t_k) + \delta_k) - (\widehat{G}(t_{k-1}) - \delta_k)}{(1-\rho) \cdot (N_{t_k} - N_{t_{k-1}})}$ . In practice, we find that the confidence adjustment counterbalances the noise that motivates a  $w \geq 3$  window, so  $w = 2$  is sufficient. We refer to this variant as LSEc.

In both cases,  $\hat{s}_k$  is a nonnegative, optimism-adjusted estimate of the local slope. For clarity, we compare the effect of the confidence adjustment and the window size in two cases. *Case (i):* When  $w = 2$ , the LSE slope without confidence adjustment is  $\hat{s}_k^{\text{LSE}} = \max \left\{ 0, \frac{\widehat{G}(t_k) - \widehat{G}(t_{k-1})}{(1-\rho) \cdot (N_{t_k} - N_{t_{k-1}})} \right\}$ , whereas the confidence-adjusted LSEc slope becomes  $\hat{s}_k^{\text{LSEc}} = \max \left\{ \frac{2\delta_k}{(1-\rho) \cdot (N_{t_k} - N_{t_{k-1}})}, \frac{(\widehat{G}(t_k) + \delta_k) - (\widehat{G}(t_{k-1}) - \delta_k)}{(1-\rho) \cdot (N_{t_k} - N_{t_{k-1}})} \right\}$ . Since  $\delta_k > 0$ , the numerator of  $\hat{s}_k^{\text{LSEc}}$  is always at least as large as that of  $\hat{s}_k^{\text{LSE}}$ , so  $\hat{s}_k^{\text{LSEc}} \geq \hat{s}_k^{\text{LSE}}$  for all  $k$ . Thus, confidence adjustment strictly increases optimism and tends to delay stopping. *Case (ii):* When  $w = 3$ , LSE instead fits a regression slope over  $\widehat{G}(t_{k-2}), \widehat{G}(t_{k-1}), \widehat{G}(t_k)$ . In contrast, LSEc still relies on the two-point, confidence-adjusted difference. In our empirical trajectories, gaps often accelerate so that  $\widehat{G}(t_{k-1}) - \widehat{G}(t_{k-2}) \gg \widehat{G}(t_k) - \widehat{G}(t_{k-1})$ , and the confidence term  $\delta_k$  is relatively

small. As a result, with  $w = 3$  for LSE and  $w = 2$  for LSEc, the non-confidence-adjusted LSE can in practice produce larger slopes and stop later than LSEc, even though for  $w = 2$  the confidence adjustment is pointwise more optimistic.

*Projected gaps and value of switching.* Given a slope estimate, the projected upper bound on the challenger's gap at a future epoch  $k' \geq k$  is  $\widehat{G}^{\text{UB}}(t_{k'}) := \widehat{G}(t_k) + (1 - \rho) \cdot (N_{t_{k'}} - N_{t_k}) \widehat{s}_k$ . The projected upper bound on future performance is then obtained by linearly extrapolating using  $\widehat{s}_k$ . Given the projected gap, the projected net value of switching at a future epoch  $k' > k$  is:

$$\widehat{V}_{\text{switch}}^{\text{UB}}(t_{k'}) = - \sum_{\tau \leq t_{k'}} \beta^\tau C_{\text{pre}}(\tau) - \beta^{t_{k'}} c_s + \sum_{\tau > t_{k'}} \beta^\tau [n_\tau \widehat{G}^{\text{UB}}(t_{k'}) - C_{\text{post}}(\tau)]. \quad (6)$$

The current estimated value of switching at epoch  $k$  is:

$$\widehat{V}_{\text{switch}}(t_k) = - \sum_{\tau \leq t_k} \beta^\tau C_{\text{pre}}(\tau) - \beta^{t_k} c_s + \sum_{\tau > t_k} \beta^\tau [n_\tau \widehat{G}(t_k) - C_{\text{post}}(\tau)]. \quad (7)$$

*Decision logic.* The algorithm compares the current value to the best optimistic projection:  $\max_{k' > k} \widehat{V}_{\text{switch}}^{\text{UB}}(t_{k'})$ . If  $\widehat{V}_{\text{switch}}(t_k) \geq \max_{k' > k} \widehat{V}_{\text{switch}}^{\text{UB}}(t_{k'})$ , the algorithm stops. To choose between switching and discarding, we compute:

$$\widehat{\Delta V}(t_k) = -\beta^{t_k} c_s + \sum_{\tau > t_k} \beta^\tau [n_\tau \widehat{G}(t_k) - C_{\text{post}}(\tau)]. \quad (8)$$

If  $\widehat{\Delta V}(t_k) > 0$ , we switch; otherwise we discard.

#### 4.4. Designing Decision Epochs

While  $\mathcal{T}_D$  may be chosen arbitrarily, the design of these epochs has a direct impact on cost and responsiveness (statistical accuracy). We examine two standard designs, corresponding to the arithmetic (John and Langley 1996) and geometric (Provost et al. 1999) progressive sampling schedules studied in the sequential learning literature. To keep our analysis clean, we maintain Assumption 1 (fixed sample flow). The two designs are: (i) *Uniform (arithmetic) schedule*: Epochs are equally spaced as  $t_k = t_{k-1} + \Lambda = \Lambda k$ , with  $t_1 = \Lambda$  and  $\Lambda \in \mathbb{N}$  fixed. Then,  $N_{t_k} = n t_k = n \Lambda k$ . (ii) *Geometric schedule*: Epoch spacing grows multiplicatively as  $t_k = t_{k-1} \lambda = \Lambda \lambda^{k-1}$ , with  $t_1 = \Lambda$  and a geometric ratio  $\lambda > 1$ . Then,  $N_{t_k} = n t_k = n \Lambda \lambda^{k-1}$ . We also maintain Assumption 2 (learning curve shape), but consider a general training cost model:

**ASSUMPTION 6 (Training cost).** Assume  $C_{\text{train}}(t) = c_{\text{train}} N_t^q$ , with  $q \geq 0$ .

Intuitively,  $q = 0$  corresponds to a fixed overhead per retrain (as in Section 3), while  $q > 0$  captures polynomial training costs. Since data-acquisition and switching costs are incurred regardless of the epoch schedule, the cost differences induced by epoch design arise solely from the training costs.

Let  $t^*$  denote the optimal stopping time derived in Section 3. For any epoch schedule  $\{t_k\}$ , we consider all epochs  $t_k \leq t^*$  and evaluate the schedule along two dimensions: (i) *Training cost*: The cumulative cost of retraining the challenger at epochs up to  $t^*$ . (ii) *Responsiveness*: The value loss incurred by switching at the nearest epoch to  $t^*$  instead of at  $t^*$  itself. Intuitively, higher training costs justify fewer retraining events, and therefore wider spacing between epochs; a steeper learning curve calls for higher responsiveness, and thus narrower spacing between epochs. In the rest of this section, we characterize how uniform and geometric schedules differ in these dimensions.

*Training cost.* We first compare the cumulative cost of retraining the challenger at epochs up to  $t^*$  under each schedule  $\{t_k\}$ , i.e.,  $C_{\text{train}}(\{t_k \leq t^*\}) = \sum_{t_k \leq t^*} c_{\text{train}} N_{t_k}^q$ .

**PROPOSITION 3 (Training cost of uniform vs. geometric schedules).** *Let Assumptions 1 and 6 hold. Fix  $t^* > 0$  and retrain the challenger at all epochs  $t_k \leq t^*$  under a schedule  $\{t_k\}$ . Then:*

- (a) **Polynomial training cost** ( $q > 0$ ). *Under the uniform schedule  $t_k = \Lambda k$ ,  $C_{\text{unif}}(t^*) = \Theta\left(\frac{t^{*(q+1)}}{\Lambda}\right)$ . Under the geometric schedule  $t_k = \Lambda \lambda^{k-1}$ ,  $C_{\text{geom}}(t^*) = \Theta(t^{*q}) = \Theta(C_{\text{train}}(t^*))$ .*
- (b) **Constant training cost** ( $q = 0$ ). *Under the uniform schedule, the number of retrains up to  $t^*$ , denoted  $K_{\text{unif}}(t^*)$ , is  $K_{\text{unif}}(t^*) = \Theta\left(\frac{t^*}{\Lambda}\right)$ . Under the geometric schedule, the number of retrains up to  $t^*$ , denoted  $K_{\text{geom}}(t^*)$ , is  $K_{\text{geom}}(t^*) = \Theta(\log t^*)$ .*

Proposition 3 shows that, under polynomial training costs ( $q > 0$ ), geometric epoch schedules are asymptotically optimal: their cumulative training cost up to  $t^*$  is within a constant factor of training once at  $t^*$ , matching the order of the oracle cost that knows  $t^*$ . This result is not surprising: it agrees with the asymptotic behavior established by Provost et al. (1999) for geometric progressive sampling schedules. In contrast, uniformly spaced epochs can be arbitrarily more expensive, incurring an extra factor proportional to the number of epochs up to  $t^*$ . Under constant training costs, geometric schedules reduce the number of retrains (and thus total training cost) from  $O(t^*/\Lambda)$  to  $O(\log t^*)$ .

*Responsiveness.* We next evaluate how much economic value is lost by restricting switching to the nearest epoch under each schedule  $\{t_k\}$  instead of the continuous-time optimum  $t^*$ . Define the responsiveness loss  $W(\{t_k\}) := V_{\text{switch}}(t^*) - \max_{t_k \leq T} V_{\text{switch}}(t_k)$ . To obtain cleaner expressions, we make some additional assumptions (similar with Setting I in Section 3).

**PROPOSITION 4 (Responsiveness of uniform vs. geometric schedules).** *Let Assumptions 1–2 hold. Assume  $T < \infty$ ,  $\beta = 1$ ,  $c_{\text{pre}}^{\text{acq}} = c_{\text{post}}^{\text{acq}} =: c$ . Then there exist constants  $C_1, C_2 > 0$  such that:*

(a) **Uniform schedule.** If  $t_k = \Lambda k$  and  $t^\dagger$  is the epoch closest to  $t^*$ , then for  $t^*$  large enough that  $t^\dagger$  lies in the interior of  $(0, T)$ ,  $W_{\text{unif}} := V_{\text{switch}}(t^*) - V_{\text{switch}}(t^\dagger) \leq C_1 \frac{\Lambda^2}{t^{*(\alpha+2)}}$ .

(b) **Geometric schedule.** If  $t_k = \Lambda \lambda^{k-1}$  and  $t^\dagger$  is the epoch closest to  $t^*$ , then for  $t^*$  large enough that  $t^*/\lambda$  and  $\lambda t^*$  both lie in  $(0, T)$ ,  $W_{\text{geom}} := V_{\text{switch}}(t^*) - V_{\text{switch}}(t^\dagger) \leq C_2 \frac{(\lambda-1)^2}{t^{*\alpha}}$ .

Proposition 4 complements Proposition 3 by showing that, because the gap curve  $G(t)$  is power-law and flattens over time, the value of the stopping rule is locally insensitive to small timing errors: both uniform and geometric schedules have vanishing responsiveness loss as  $t^*$  grows, and for reasonable geometric ratios (e.g.,  $\lambda \in [1.5, 2]$ ) the loss  $W_{\text{geom}}$  is negligible. Taken together, Propositions 3 and 4 indicate that geometric epoch schedules offer a favorable balance: they retain near-oracle training cost efficiency while maintaining negligible economic loss. With that in mind, our numerical analysis in Section 5 focuses on geometric epoch designs.

## 5. Empirical Validation: Credit Scoring Case Study

In this section, we evaluate the algorithms introduced earlier using a large, real-world credit-scoring dataset with progressively arriving alternative data. We show that optimal switching times vary systematically with cost parameters and learning-curve dynamics, consistent with the predictions in Section 3. We further find that using an appropriate sequential evaluation algorithm can deliver value close to the oracle benchmark and substantially outperform common one-shot baselines.

### 5.1. Data

Our empirical case study uses a comprehensive dataset from Lending Club, a large peer-to-peer lending platform, covering 705,302 loans issued between 2014 and 2017. For each loan, we observe 29 variables, including loan features (e.g., amount, duration) and borrower characteristics (e.g., monthly income, job tenure). The dataset also reports the repayment outcome (full repayment or default), which is our target variable, encoded as 1 for default and 0 for non-default. Throughout the sample period, yearly default rates range from 19.23% to 21.42%, with an average of 20.87%.

A key feature of the dataset is the availability of *alternative data* on loan applicants, such as the loan grade assigned by Lending Club and banking variables (e.g., number of open credit lines, bank cards, installments, mortgages, and revolving accounts). The loan grade can be viewed as a proprietary signal generated by Lending Club to assess borrower default risk, integrating standard credit attributes with nontraditional information, such as the applicant's digital footprint. We use this structure to define the respective feature sets of the champion and the challenger.

Finally, the dataset records the funding date of each loan. This timing information allows us to align the empirical analysis with our theoretical framework and real-world scenarios by (i) specifying a date at which the alternative data become available and (ii) naturally defining the time steps of our process based on loan dates. We provide details on data pre-processing and feature selection for the champion and the challenger in Section EC.2.1 in the Electronic Companion (EC).

## 5.2. Experimental Methodology and Setting

Here, we describe the general experimental methodology, which follows the framework introduced in Section 2.1. The dataset is chronologically ordered, with each observation indexed by a timestep  $t$  corresponding to the number of months since the start of the experiment. To generate statistically diverse trajectories, each experiment samples without replacement half of the dataset.<sup>5</sup>

First, *the incumbent model* is trained on the first  $N_0$  data points, covering 2014–2015, resulting in an effective dataset of size  $N_0 = 189,250$ . It uses an initial feature set  $\mathcal{I}$  of size  $|\mathcal{I}| = 7$ : annual income, job tenure, debt-to-income ratio, FICO score, funding amount, loan duration, and loan purpose. Starting in 2016, alternative data become available (e.g., loan grade, number of open credit lines, bank cards, installments, mortgages, revolving accounts), expanding the feature set to  $\mathcal{C}$  with  $|\mathcal{C}| = 29$ , and training of the challenger begins. Table EC.1 reports the complete list of features and their descriptions for both the incumbent and challenger models.

At each epoch  $k$  (whose design is detailed in the next subsection), we execute three steps:

1. *Data collection*: collect the next  $N_{t_k} - N_{t_{k-1}}$  observations from the temporally ordered dataset.
2. *Model training*: split the  $N_{t_k}$  collected observations evenly into a training set and a holdout set; train the challenger on the training set and empirically estimate the economic performance gap between challenger and champion on the holdout set.
3. *Decision*: the algorithm chooses whether to switch, discard, or continue based on this empirical estimate and all relevant parameters (e.g., costs, sample counts).

Once samples for all epochs are generated and challenger models are trained, we enter a decision-evaluation phase in which we empirically estimate the value of switching at each epoch along the realized sample path. At epoch  $k$ , we estimate the average economic performance gap between the champion and challenger on samples from each timestep  $\tau \geq t_k$ , denoted  $\hat{G}_{\tau,k}$ , and compute:

$$\bar{V}_{\text{switch}}(t_k) = - \sum_{\tau \leq t_k} \beta^\tau C_{\text{pre}}(\tau) - \beta^{t_k} c_s + \sum_{\tau > t_k} \beta^\tau [n_\tau \hat{G}_{\tau,k} - C_{\text{post}}(\tau)]. \quad (9)$$

<sup>5</sup> At each decision epoch  $t$ , rather than appending the incoming batch of  $n_t$  observations, we sample  $n_t$  observations without replacement from the next  $2n_t$  observations in the chronological data stream. Subsequent batches are generated analogously from disjoint blocks of  $2n_t$  observations, ensuring non-overlapping sample paths that respect temporal ordering.

The oracle reported in the experiments bases its decision on  $\bar{V}_{\text{switch}}(t_k)$ . This yields a stronger benchmark than the oracle defined in Section 3.2: the latter selects the optimal epoch *on average* across trajectories, whereas the experimental oracle adapts to the realized sample path. Note that  $C_{\text{pre}}(\tau)$  is not necessarily the same for our deployed algorithms and the oracle: typically (except for the one-shot algorithm), our algorithms incur training costs at each decision epoch before stopping, whereas the oracle incurs training cost only at its switching epoch. We do not reflect this nuance in the notation to avoid overloading it.

We adopt this evaluation methodology for two reasons. First, obtaining reliable average economic-gap estimates would require holding out additional data, which would reduce the data available to generate diverse sample paths. Second, the dataset exhibits mild but non-negligible time variability (see Figure EC.1b); evaluating performance via (9) preserves this variability and demonstrates that our approach remains robust under small distributional shifts.

### 5.3. Scenario Selection

Our experimental setting depends on three groups of parameters: those governing (i) the epoch design, (ii) the learning curve, and, (iii) the economic structure. We focus on two core scenarios that induce qualitatively distinct behavior concerning the optimal switching point: an *early-switch* scenario (E.1) and a *late-switch* scenario (E.2). We report additional parameter settings and scenarios (e.g., cases in which discarding is optimal), and robustness checks in the EC (Section EC.2).

**Core scenarios.** Scenarios (E.1) and (E.2) share parts of their parameters, as described below:

- **Sample sizes and splits.** The incumbent is trained on  $N_0 = 189,250$  observations. Over the sequential process, the challenger has access to  $N_{t_e} = 163,400$  observations (the subscript  $t_e$  denotes the end of the process). At each decision epoch, we split data evenly into training and testing sets.

- **Timing and epoch design.** We treat the data as a time-ordered stream and implement a geometric schedule in which batch sizes grow by a factor of 2 across 8 decision epochs. We set the first decision-epoch sample size to 500, so the cumulative samples available by epoch are 500, 1,500, 3,500, 7,500, 15,500, 31,500, 63,500, and 127,500. Hence, by construction, our two core scenarios consist of eight decision epochs. The subsequent 35,900 observations are reserved as future data, reflecting the fact that our last decision epoch is not the end of the operational horizon: the decision maker anticipates receiving additional data thereafter and earning potential profits.

- **Economic structure.** In all experiments, we measure the economic performance gap as the difference in AUC between the challenger and the incumbent, which is well suited to our imbalanced classification setting (average default rate 20.87%). We write the per-sample economic gap as

$(\text{AUC}_{\text{challenger}} - \text{AUC}_{\text{incumbent}})$ , so that all costs are expressed in units of “per-sample gain from a unit increase in AUC.” For example,  $c_{\text{acq}} = 0.0025$  means that the acquisition cost per sample is 0.25% of the per-sample gain from a one-point AUC improvement. Since scaling gaps and costs is equivalent up to a rescaling of the value function, this normalization is without loss of generality. In both experiment families (E.1) and (E.2), we hold the discount factor and baseline costs fixed at  $\beta = 0.95$ ,  $c_{\text{acq}} = 0.0025$ , and  $c_s = 0$ , varying only the training-related costs across scenarios.

As we further explain next, the two scenarios differ only in the learning environment (induced by the model class) and the economic structure (induced by different training-cost level). In E.1 (*early switch*), the challenger model is logistic regression (LR) and the per-sample training cost is  $c_{\text{train}} = 0.075$ . In E.2 (*late switch*), the challenger model is LightGBM and the per-sample training cost is  $c_{\text{train}} = 0.005$ . In the remainder of this section, we discuss the implications of these choices.

*Robustness checks.* Section EC.2.5 in the EC examines complementary settings that vary (i) the *economic structure*—no costs, higher acquisition costs, and a positive switching cost, each evaluated for both LR and LightGBM—and (ii) *robustness dimensions*—smaller batches, larger batches with higher acquisition costs, a “timeless” design that removes time ordering (hence investigating the effect of distribution shift), and a smaller total challenger sample size.

*Learning curves.* Since the shape of the learning curve is central to our problem (Section 2), we consider two models commonly used in the finance literature to generate qualitatively different learning-curve patterns. We use LR, which remains the standard in credit scoring (Lessmann et al. 2015), and LightGBM (Ke et al. 2017), a gradient-boosting framework known for its fast training speed and scalability to large datasets.<sup>6</sup> Figure 2 displays the corresponding learning curves. Two results stand out: (i) the performance of LR reaches its plateau much more quickly than that of LightGBM; (ii) the performance of LR at the last epoch is close to the performance of LightGBM.

*Economic structure.* To simplify parameter selection and better illustrate the findings of Section 2, we assume a fixed per-sample gain; a constant per-sample acquisition cost, identical before and after the decision; training costs linear in the batch size; and no switching costs. Rather than selecting specific values of  $c_{\text{acq}}$ ,  $c_{\text{train}}$ , and  $\beta$  arbitrarily, we explore a grid of values and identify two sets that generate an early and a late optimal switching time. As we explain, the two settings differ only in their respective training costs. We believe those choices do not limit the illustrative value of our experiments, and revisit them in the Electronic Companion.

<sup>6</sup> The hyperparameters of the LightGBM model are selected using cross-validation.

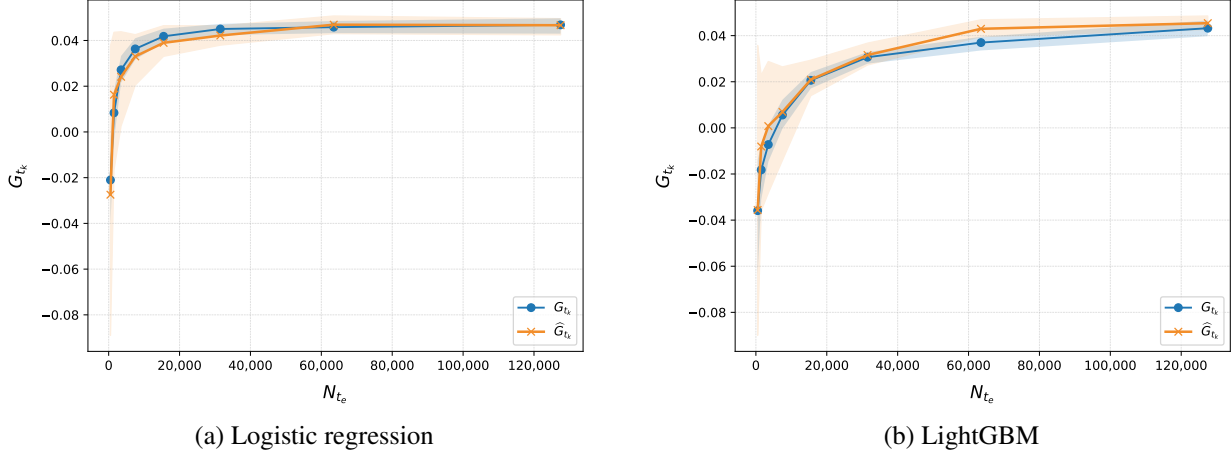


**Figure 2 Learning curves**

*Note.* This figure displays the learning curve of LR and LightGBM. The learning curve is defined as the expected economic performance gap  $G(t_k)$ , expressed as a function of  $N_{t_e}$  the sample size available at each decision epoch  $t_k \in \mathcal{T}_D$ . The orange line reports the empirical estimate using the holdout set at time  $t_k$ , while the blue line reports estimates based on the future data available after  $t_k$ . Each curve represents the average over the 30 generated sample paths (see Section 5.2). The orange and blue intervals represent 90% confidence intervals.

Figure 3 displays the oracle’s optimal switching time and performance across six values of the per-sample acquisition cost, six values of the per-sample training cost, and two discount-factor values, for both the LR and the LightGBM models. We evaluate algorithm performance using the notion of *empirical value* of an algorithm, denoted  $\bar{V}_{\text{ALG}}(T)$ . Let denote  $\tilde{t} \in \mathcal{T}_D$  the epoch at which the algorithm decides to switch or discard. If the algorithm switches at epoch  $k$ , then  $\tilde{t} = t_k$  and  $\bar{V}_{\text{ALG}}(T) = \bar{V}_{\text{switch}}(\tilde{t})$ . Otherwise, if it discards the challenger at epoch  $k$ , then  $\tilde{t} = t_k$  and  $\bar{V}_{\text{ALG}}(T) = -\sum_{\tau \leq \tilde{t}} \beta^\tau C_{\text{pre}}(\tau)$ .<sup>7</sup> Consistent with what we explored in Section 2, our results show that independently of the learning curve or model considered: (i) the acquisition cost does not influence the optimal stopping point, (ii) higher training costs and (iii) lower discount factors lead to earlier switching, and (iv) sufficiently high training and acquisition costs make discarding the challenger optimal. We obtain E.1 and E.2 by selecting an early and a late switching point in Figure 3.<sup>8</sup>

#### 5.4. Algorithm Hyperparameter Selection

The algorithms’ hyperparameters materially affect their stopping behavior and performance. *OSE* depends on the evaluation epoch; we consider three benchmarks: the first epoch, the fourth epoch,

<sup>7</sup> This definition also covers the oracle: if it discards, it does so before starting the sequential process, yielding zero performance.

<sup>8</sup> Over our parameter grid, the earliest average switching point occurs around the fourth epoch using LR with  $c_{\text{train}} = 0.075$  and  $\beta = 0.95$ , independently of  $c_{\text{acq}}$ . Using LightGBM, the latest average switching point occurs around the sixth epoch for multiple parameter combinations. We therefore fix  $\beta = 0.95$  and  $c_{\text{acq}} = 0.0025$ , set  $c_{\text{train}} = 0.075$  (early) and 0.005 (late), and show in Figure EC.3 that results are qualitatively unchanged under alternative specifications.

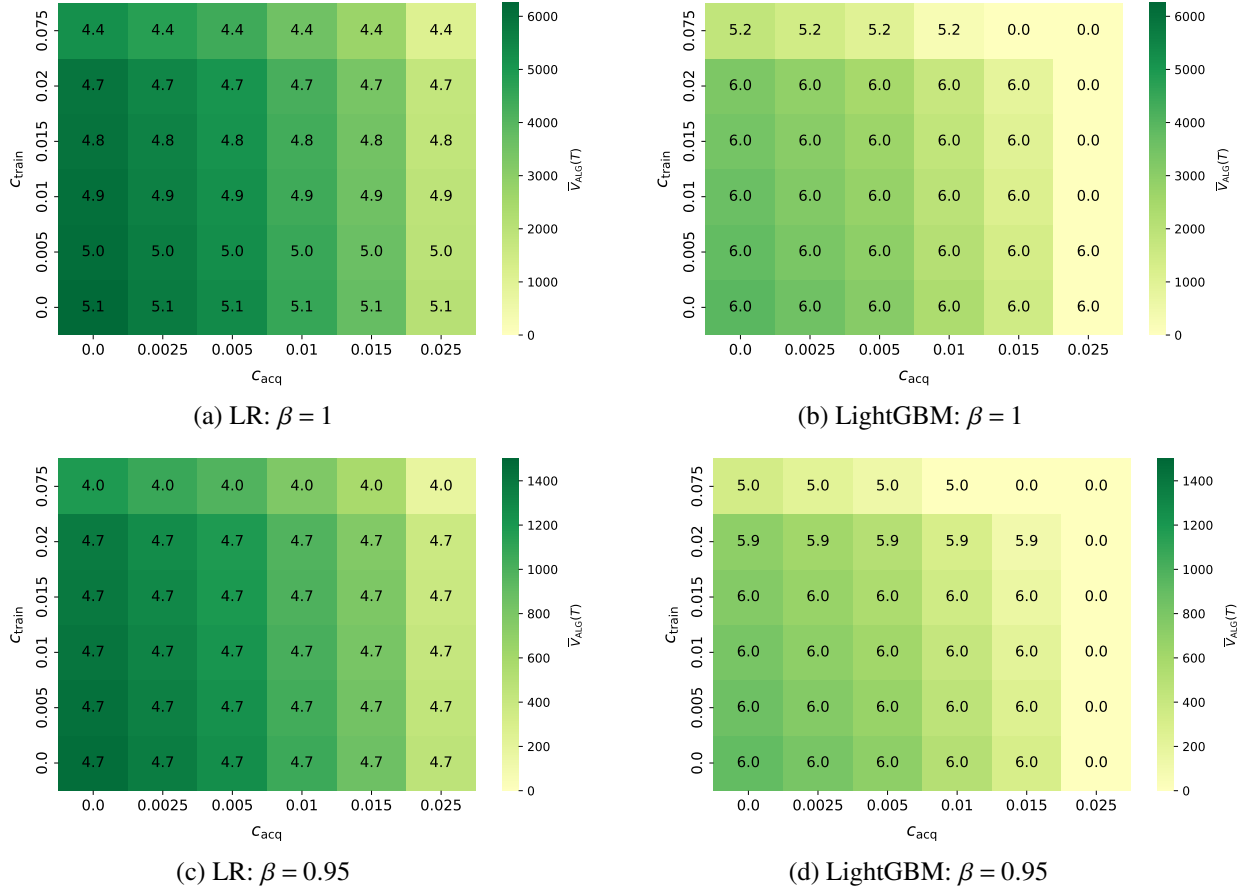


**Figure 3 Oracle's performance and optimal stopping time**

*Note.* Illustration of the oracle's average value and stopping point across 30 sample paths over a grid of per-sample acquisition costs  $c_{acq}$ , training costs  $c_{train}$ , and discount factors  $\beta$ , with  $c_s = 0$ , using LR (first column) and LightGBM (second column). Cell shading indicates average performance, while the value inside each cell reports the stopping point.

and the final epoch. The first and final epochs correspond to purchasing only the first batch or the entire dataset at once, respectively. We include the fourth epoch because it yields the best OSE performance in the first core scenario (E.1). GSE depends on the confidence parameter  $\gamma$ : larger  $\gamma$  implies a more conservative rule and thus later stopping. We study sensitivity to  $\gamma$  in the EC (Section EC.2.4) by evaluating performance over the same parameter grid used to select the core scenarios, for both LR and LightGBM, across a prespecified set of  $\gamma$  values. Performance is highly sensitive to  $\gamma$ , and no single value performs best across experiments. We therefore set  $\gamma \approx 1.92$ , which delivers the highest performance in E.1 in our sensitivity analysis.<sup>9</sup> LSEc also uses a confidence parameter  $\gamma$ . Larger  $\gamma$  yields a more optimistic assessment of future gaps and thus later stopping. In contrast to GSE, LSEc is markedly more robust to the choice of  $\gamma$ : Section EC.2.4

<sup>9</sup> The confidence parameter used in the code is defined as a significance level (e.g., 1% or 5%), which differs from the definition adopted in the paper. The two definitions are equivalent via a one-to-one transformation. Applying this transformation yields the (rounded) values reported in the paper.

shows that  $\gamma = 0.1$  achieves performance consistently close to the best among the values we consider and is relatively insensitive to small perturbations around this value.

### 5.5. Results in the Core Scenarios

We now analyze results for the two core scenarios. Figure 4 summarizes algorithm performance across the 30 sample paths, with the corresponding utility curves in Figures 5 and EC.2. These utility curves report the switching value at each epoch  $t_k$ . We distinguish between the oracle's switching value (blue),  $\bar{V}_{\text{switch}}(t_k)$ , and the algorithm's empirically estimated switching value (orange),  $\hat{V}_{\text{switch}}(t_k)$ . The blue curve plots the oracle's switching value,  $\bar{V}_{\text{switch}}(t_k)$ , computed using future data and assuming training occurs only at the candidate epoch (so no value is lost to excess training). The orange curve plots the empirically estimated switching value available to the algorithms,  $\hat{V}_{\text{switch}}(t_k)$ , constructed along the realized path using the holdout set. Consequently, the two curves differ for two reasons: algorithms (i) estimate performance gaps from the holdout set rather than future data and (ii) typically incur cumulative training costs prior to stopping. Next, we summarize the main takeaways from Figures 4 and 5.

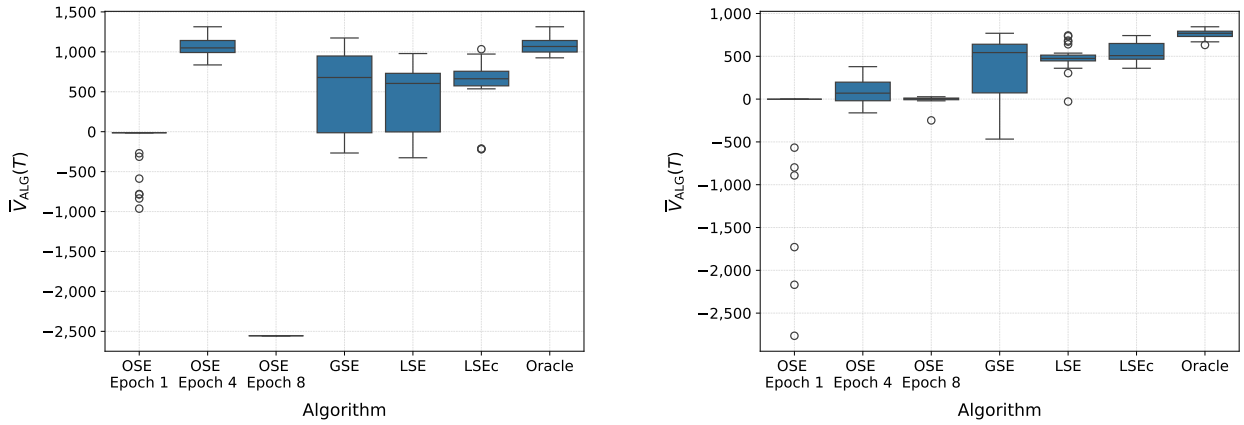


**Figure 4**    **E.1: Early switch & E.2: Late switch**

*Note.* This figure displays the performance of our algorithms across the 30 sample paths for the early- and late-switch scenarios.

**Performance of OSE.** First, setting the evaluation epoch to the fourth epoch yields strong performance for OSE in E.1, but performance deteriorates markedly in E.2. This is expected: the oracle stops at the fourth epoch in E.1 but at the sixth epoch in E.2, so fixing OSE to evaluate at epoch four forces it to act too early in the latter scenario. More broadly, purchasing only the initial batch or the entire dataset upfront is unprofitable in both scenarios. Together, these findings show that OSE is highly sensitive to the evaluation epoch and that no single fixed epoch performs well when the optimal stopping point varies across settings.

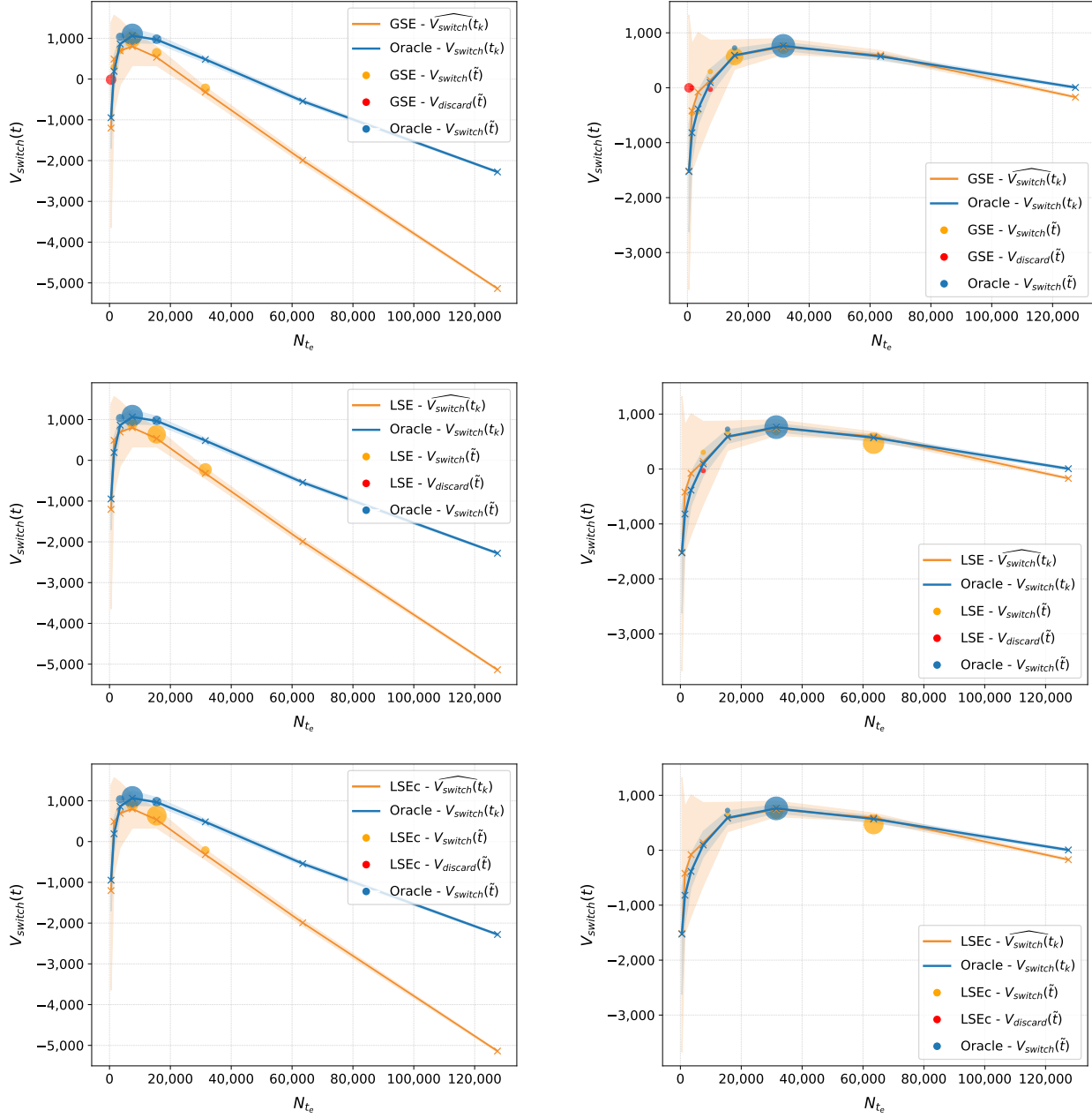


**Figure 5 E.1: Early switch & E.2: Late switch**

*Note.* The figure shows the utility (switching value) and decisions of the algorithms and the oracle across 30 sample paths for the early- and late-switch scenarios. Solid lines report average switching values at each  $t_k$ , with shaded areas indicating 90% confidence intervals. Blue and orange dots denote oracle and algorithm performance at the switching epoch  $\tilde{t}$ , respectively, while red dots indicate discard decisions. Dot sizes are proportional to the frequency of the corresponding decision across sample paths. Dot heights represent the average of the switching or discarding value at the corresponding epoch. Each panel corresponds to a different algorithm.

*Performance of GSE.* Second, GSE is highly volatile across the 30 sample paths in both E.1 and E.2. A first source of volatility is premature discarding: GSE occasionally fails to switch and instead discards the challenger at early stages, as indicated by the red dots in the utility-curve

plots. In the first three epochs, the estimated switching values  $\hat{V}_{\text{switch}}(t)$  (orange curves), on which the algorithm bases its decisions, are highly noisy and frequently negative. Because GSE is not forward-looking and relies on the current estimate, sufficiently conservative confidence settings can make it conclude that the challenger underperforms the incumbent, leading to early discard. A second source of volatility arises even when GSE does not discard: it often remains uncertain about whether switching dominates continuing, and early-epoch noise then causes switching at different epochs across sample paths, further increasing dispersion in realized values.

*Performance of LSE.* Third, LSE behaves differently across the two scenarios. In E.1, its performance is also volatile, but for a different reason than GSE's. Because LSE is forward-looking, it forms expectations about future gaps based on the evolution of past value estimates. This optimism can cause LSE to switch later than is optimal; when the switching value declines sharply after its peak, switching one or two epochs too late produces a substantial opportunity loss, explaining the volatility in E.1. In E.2, by contrast, LSE typically stops only one epoch after the peak; since values decline only mildly thereafter, realized performance remains tightly concentrated and close to the oracle's. Thus, the difference in LSE performance is primarily driven by utility-curve shape: the much higher training cost in E.1 causes switching values to fall steeply after their peak, amplifying the penalty for even slight delays.

*Performance of LSEc.* Fourth, LSEc stands out as the most stable, delivering performance that remains consistently close to the oracle across sample paths in both E.1 and E.2. Although closely related to LSE, LSEc estimates its slope using only the most recent gap and incorporates a confidence adjustment, whereas in our empirical analysis LSE uses a window of  $w = 3$  and thus relies on the two preceding epochs. As discussed in Section 4.3, these design choices affect how optimistic each algorithm is when extrapolating future gaps: using three points can amplify optimism when gaps increase sharply, while confidence adjustment reinforces optimism when recent estimates are noisy. This pattern aligns with the observed behavior. In E.1, the learning curve exhibits steep early improvements (Figure 2), so LSE's three-point slope becomes inflated and it tends to switch later than LSEc. In E.2, the learning curve is less steep and early estimates are noisier, making confidence-adjusted LSEc slightly more optimistic; e.g., LSEc defers switching until epochs five, six, or seven, while LSE occasionally switches or even discards at epoch four.

*Model choice.* Fifth, higher model complexity does not automatically translate into higher profitability. In particular, LR in E.1 achieves higher value than LightGBM in E.2 for most algorithms,

including the oracle, and this pattern holds throughout our empirical analysis. The reason is straightforward: LR’s learning curve is consistently steeper and lies above LightGBM’s at all decision epochs (Figure 2). As a result, for a given economic structure, LR dominates in economic value.

## 6. Theoretical Guarantees

In this section, we theoretically analyze the performance of the algorithms introduced in Section 4. Our goal is not to derive the tightest possible bounds, but rather to explain empirical patterns and clarify the role of tuning parameters in shaping stopping and switching decisions. This theory complements the empirical evidence in Section 5: e.g., the empirical results show that LSEc is typically closest to the oracle across environments, and we therefore use the theoretical analysis to explain this robustness and to formalize how performance depends on the key parameters of the problem. We evaluate each procedure through its *value*, defined as the cumulative economic objective collected over the course of the model-selection process, and compare this value to that of an oracle with full knowledge of the challenger’s learning curve.

### 6.1. Setting and Value Definition

We first specify the stylized setting in which our guarantees hold and then define the value of an algorithm. We define payoffs and value at the level of time steps  $t \in \mathcal{T}$ , while the algorithms’ stopping times are expressed in terms of decision epochs  $t_k \in \mathcal{T}_D$ . When we write  $t_{\text{ALG}}$  or  $t_k$ , we always interpret these as elements of  $\mathcal{T}$ ; the distinction is only whether the algorithm is allowed to act at that time. To obtain clean guarantees, we work in a simplified environment that mirrors Setting I from Section 3, but without imposing a specific functional form on the learning curve.

**ASSUMPTION 7 (Setting III).** *Let Assumptions 1, 3, and 4 hold. In addition, we assume that:* (i) *the horizon is finite ( $T < \infty$ ); (ii) there is no discounting ( $\beta = 1$ ); (iii)  $\ell$  takes values in  $\{-1, 1\}$ .*

Under Assumption 7, the batch size is constant ( $n_t = n, \forall t$ ), costs follow the structure of Section 2.3, the horizon is finite and non-discounted, and per-sample monetary gains are uniformly bounded.

For any algorithm  $\text{ALG}$  and time step  $t \in \mathcal{T}$ , let  $\pi_{\text{ALG}}(t)$  denote the value collected at time  $t$ . Its definition reflects the state of the algorithm at that time:  $\pi_{\text{ALG}}(t) = 0$  if  $\text{ALG}$  discarded at some  $t' < t$ ;  $\pi_{\text{ALG}}(t) = -C_{\text{pre}}(t) - c_s$  if  $\text{ALG}$  switches at  $t$ ;  $\pi_{\text{ALG}}(t) = n_t G(t') - C_{\text{post}}(t)$  if  $\text{ALG}$  switched at some  $t' < t$ ; and  $\pi_{\text{ALG}}(t) = -C_{\text{pre}}(t)$  if it has neither switched nor discarded. The (non-discounted) finite-horizon value of the algorithm over horizon  $T$  is then  $V_{\text{ALG}}(T) = \sum_{t=1}^T \pi_{\text{ALG}}(t)$ . In what follows, we use this setup to answer two complementary questions. First, what is the effect of introducing explicit confidence bounds into a sequential evaluation scheme? We analyze GSE and show how its

use of confidence intervals shapes stopping behavior and yields a finite-horizon value lower bound. Second, what is the effect of adding a look-ahead component on top of such sequential evaluation? We study LSE and show how extrapolating local learning-curve trends leads to asymptotic regret guarantees relative to the oracle.

## 6.2. Controlling the Value of the GSE Algorithm

We first establish conditions under which the GSE algorithm enjoys a lower bound on its value. Recall from Section 4 that GSE maintains conservative lower and upper bounds  $\widehat{V}_{\text{switch}}^{\text{LB}}(t_k)$  and  $\widehat{V}_{\text{switch}}^{\text{UB}}(t_k)$  on the value of switching at each decision epoch  $t_k \in \mathcal{T}_D$ , and that it expands the training sample only while the current data leave open the possibility that switching could be valuable. When the upper confidence bound becomes negative, it stops and commits to either switching or discarding. For sufficiently large  $\gamma$ , this mechanism leads to a provable lower bound on  $V_{\text{GSE}}(T)$ .

For the analysis, we work with a slightly modified version of GSE. This modification is almost never triggered in practice, but it simplifies the proof. It affects only the case in which the stopping condition  $\widehat{V}_{\text{switch}}^{\text{UB}}(t_k) < 0$  is met. In that event, instead of evaluating only the challenger trained at epoch  $k$ , we also consider the challenger from epoch  $k-1$ . We define  $\widehat{\Delta V}^{\text{LB}}(t_k) = \max_{k' \in \{k, k-1\}} \left\{ -c_s + (T - t_k) n \left[ (\widehat{G}(t_{k'}) - \delta_{t_{k'}}) - c \right] \right\}$ , and, if  $\widehat{\Delta V}^{\text{LB}}(t_k) > 0$ , the algorithm switches to the challenger with the larger lower bound. Let  $\mathcal{E}$  be the event that, for all epochs  $t_k \in \mathcal{T}_D$ ,  $\widehat{V}_{\text{switch}}^{\text{LB}}(t_k)$  and  $\widehat{V}_{\text{switch}}^{\text{UB}}(t_k)$  are valid bounds on  $V_{\text{switch}}(t_k)$ .

**PROPOSITION 5.** *Let Assumption 7 (Setting III) hold. If event  $\mathcal{E}$  holds and the (modified) GSE algorithm stops at epoch  $t_k \in \mathcal{T}_D$ , then*

$$V_{\text{GSE}}(T) > -\gamma \frac{(T - t_k) n}{\sqrt{\rho N_{t_{k-1}}}} - (t_k - t_{k-1}) n.$$

Moreover, for any  $\gamma \geq \sqrt{2 \log(|\mathcal{T}_D|/\epsilon)}$ , event  $\mathcal{E}$  holds with probability at least  $1 - \epsilon$ .

Proposition 5 shows that the confidence parameter  $\gamma$  directly controls a worst-case performance guarantee for GSE. The larger  $\gamma$  is, the more conservative the confidence bands become, and the looser (more negative) the numerical lower bound. At the same time,  $\gamma$  must exceed the threshold  $\sqrt{2 \log(|\mathcal{T}_D|/\epsilon)}$  for the probabilistic guarantee on  $\mathcal{E}$  to hold. This trade-off between statistical coverage and tightness mirrors the empirical behavior reported in Section 5.4: higher  $\gamma$  protects against overly optimistic decisions but tends to delay stopping and accumulate more pre-decision cost. Overall, the algorithm is highly sensitive to this parameter, and no single value of  $\gamma$  performs well across scenarios.

### 6.3. Controlling the Regret of the LSEc Algorithm

The oracle's optimal solution is, in most cases, unattainable: computing it would require knowledge of both the challenger's optimal performance and the precise shape of the learning curve. Nonetheless, it provides a natural benchmark against which to evaluate any algorithm.

We define the oracle's value  $V_{\text{ORACLE}}(T)$  as in Section 3, i.e., as the maximum value it can achieve by choosing the optimal switching time (or by discarding). The *regret* of an algorithm  $\text{ALG}$  over horizon  $T$  is defined as  $R_{\text{ALG}}(T) = \mathbb{E}[V_{\text{ORACLE}}(T) - V_{\text{ALG}}(T)]$ , where the expectation is taken over both algorithmic and sampling randomness.

**THEOREM 2.** *Consider any algorithm  $\text{ALG}$ , and denote by  $t_{\text{ALG}}$  the decision epoch (hence time step) at which the algorithm decides to either discard or switch to the challenger. Suppose that the hypothesis class  $\mathcal{F}_C$  of the challenger has finite VC-dimension  $d$ , and that training is performed through ERM. Also suppose that there exist constants  $w_1, w_2, w_3, w_4 > 0$  such that, for all sufficiently large  $T$ , the following conditions hold with probability at least  $1 - w_1/T$ :*

- (C1) *The decision epoch  $t_{\text{ALG}}$  satisfies  $w_2 T^{2/3} < t_{\text{ALG}} < w_3 T^{2/3}$ .*
- (C2)  *$\text{ALG}$  uses a consistent switching rule: if  $\Delta V(t_{\text{ALG}}) + w_4 T^{2/3} \sqrt{\log T} < 0$ , then  $\text{ALG}$  discards, and if  $\Delta V(t_{\text{ALG}}) - w_4 T^{2/3} \sqrt{\log T} > 0$ , then  $\text{ALG}$  switches.*

*Then,  $R_{\text{ALG}}(T) = O(T^{2/3} \sqrt{\log T})$ .*

Theorem 2 establishes that, under Setting III, any algorithm satisfying two structural conditions achieves sublinear regret in  $T$ . Condition (C2) is not intended as a directly implementable switching rule: the quantity  $\Delta V(t_{\text{ALG}})$  is not observable and must, in practice, be estimated from data. Rather, (C2) formalizes a sufficient condition under which the regret guarantee holds: the algorithm must behave as if it had an estimate of  $\Delta V(t_{\text{ALG}})$  that concentrates around the truth at rate  $T^{-1/3} \sqrt{\log T}$ . OSE and LSE satisfy these structural conditions for suitable choices of their tuning parameters:

**COROLLARY 1.** *There exist constants  $w_2, w_3$ , and  $w_4$  (defined in the Electronic Companion) such that the OSE algorithm, when implemented with a decision epoch  $t_k = T^{2/3}$ , satisfies conditions (C1) and (C2) of Theorem 2 with probability at least  $1 - 1/T$ .*

**PROPOSITION 6.** *There exist constants  $w_2, w_3$ , and  $w_4$  (defined in the Electronic Companion) such that the LSEc algorithm, implemented with a geometric epoch schedule  $t_k = \Lambda \lambda^{k-1}$  with ratio  $\lambda > 1$ , satisfies conditions (C1) and (C2) of Theorem 2 with probability at least  $1 - 2/T$ .*

#### 6.4. Discussion of the Theoretical Guarantees

The LSE algorithm implicitly assumes that the challenger’s learning curve is, on average, increasing and concave (up to noise): it extrapolates local slopes to construct optimistic projections of future gains. One may therefore wonder how robust the procedure remains when this structure does not hold, and whether theoretically grounded upper bounds on future gains—such as those derived from Rademacher complexity or VC-dimension—would be better suited for constructing projections.

In practice, two limitations make such theory-driven bounds ill-suited for our setting. First, standard generalization bounds are typically far too loose to provide meaningful guidance at the scale of individual epochs. Second, as Theorem 2 and Proposition 6 illustrate, the heuristic projections used by LSE need not be valid statistical upper bounds pointwise in order to guarantee good long-run performance: it is sufficient that they remain optimistic enough on average. This level of optimism ensures that the algorithm’s asymptotic performance matches that of the oracle up to a sublinear regret term in  $T$ , while allowing the procedure to adapt more flexibly to the non-asymptotic regime than formal learning-theoretic bounds typically permit.

On the other hand, LSE sacrifices some of the conservativeness enjoyed by GSE. In particular, an analogue of Proposition 5 does not hold for LSE: for moderate epochs, before concentration from statistical learning theory becomes effective, we do not have a tight control on the estimated slope of the learning curve. However, this limitation is not specific to LSE. Whenever generalization bounds become tight enough to control the slope, they also imply that the gains themselves are well-concentrated, at which point the lower-bound guarantees of GSE already apply. In this sense, GSE and LSE occupy complementary roles: GSE offers finite-sample conservativeness controlled by  $\gamma$ , whereas LSE provides a more aggressive, forward-looking policy that remains asymptotically near-optimal relative to the oracle.

### 7. Conclusion

We develop a unified economic and statistical framework for deciding when an organization should replace an incumbent predictive model with a challenger that relies on newly available features. The framework links learning-curve dynamics, data-acquisition and retraining costs, and discounting of future gains to characterize optimal switching policies. Building on a stylized optimal-stopping analysis, we propose practical stopping rules, establish finite-sample and regret guarantees, and validate the framework using a large credit-scoring dataset with gradually arriving alternative data.

*Managerial implications.* Our results show that the value of new data and more complex models depends jointly on *how fast* the challenger improves and *how costly* it is to keep evaluating it, rather than on final predictive performance alone. First, the optimal switching time responds systematically to learning-curve shape, acquisition and training costs, and discount factors: “switch as soon as the challenger looks better” is generally suboptimal, while always waiting for more data may destroy value through unnecessary costs and foregone gains. Second, the comparison of OSE, GSE, and LSE illustrates concrete governance choices. Simple one-shot evaluations are cheap but brittle; confidence-based sequential policies (GSE) offer conservative protection against costly mistakes; and look-ahead policies (LSE) can recover a large fraction of the oracle value with limited additional complexity. For practitioners, this suggests that model-lifecycle management should explicitly specify (i) how often challenger models are re-evaluated, (ii) how much statistical confidence is required before switching or discarding, and (iii) how much “optimism” about future improvements is acceptable, given cost and risk tolerances.

*Future research.* This work opens several avenues for extension. One direction is to allow for multiple competing challengers, portfolio deployment of models, or environments in which the incumbent’s performance also evolves over time. Another is to incorporate richer forms of uncertainty, including model misspecification and distributional shift, and to study how robust or ambiguity-averse decision makers should adapt their switching rules. Finally, although our empirical analysis centers on finance, the proposed framework generalizes to other domains, including health-care. Consider a hospital deploying a machine learning model for disease diagnosis: the incumbent model relies on demographic and laboratory data, whereas the challenger model augments these with genetic markers and real-time monitoring information. While the expanded feature set may enhance diagnostic accuracy, it also entails additional expenditures related to genetic testing, data integration, and infrastructure investment.

## References

Babina T, Bahaj S, Buchak G, De Marco F, Foulis A, Gornall W, Mazzola F, Yu T (2025) Customer data access and fintech entry: Early evidence from open banking. *Journal of Financial Economics*, forthcoming.

Berg T, Burg V, Gombović A, Puri M (2020) On the rise of fintechs: Credit scoring using digital footprints. *Review of Financial Studies* 33(7):2845–2897.

Bertsimas D, Digalakis Jr V, Ma Y, Paschalidis P (2024) Towards stable machine learning model retraining via slowly varying sequences. *arXiv preprint* 2403.19871.

Bian B, Ma X, Tang H (2022) The supply and demand for data privacy: Evidence from mobile apps. *SSRN preprint* 3987541.

Bifet A, Gavalda R (2007) Learning from time-changing data with adaptive windowing. *Proceedings of the 2007 SIAM international conference on data mining*, 443–448 (SIAM).

Bonelli M (2025) Data-driven investors. *Review of Financial Studies* forthcoming.

Bonelli M, Foucault T (2025) Does big data devalue traditional expertise? Evidence from active funds. *SSRN preprint* 4527672.

Bryan G, Karlan D, Osman A (2024) Big loans to small businesses: Predicting winners and losers in an entrepreneurial lending experiment. *American Economic Review* 114(9):2825–60.

Cao S, Jiang W, Wang J, Yang B (2024) From man vs. machine to man + machine: The art and AI of stock analyses. *Journal of Financial Economics* 160:103910.

Chen L, Pelger M, Zhu J (2024) Deep learning in asset pricing. *Management Science* 70(2):714–750.

Chi F, Hwang BH, Zheng Y (2025) The use and usefulness of big data in finance: Evidence from financial analysts. *Management Science* 71(6):4599–4621.

Dessaint O, Foucault T, Fresard L (2024) Does alternative data improve financial forecasting? The horizon effect. *Journal of Finance* 79(3):2237–2287.

Djeundje VB, Crook J, Calabrese R, Hamid M (2021) Enhancing credit scoring with alternative data. *Expert Systems with Applications* 163:113766.

Foucault T, Gambacorta L, Jiang W, Vives X (2025) Artificial intelligence in finance. Report, Centre for Economic Policy Research (CEPR).

Frey LJ, Fisher DH (1999) Modeling decision tree performance with the power law. Heckerman D, Whittaker J, eds., *Proceedings of the Seventh International Workshop on Artificial Intelligence and Statistics*, volume R2 of *Proceedings of Machine Learning Research* (PMLR).

Gambacorta L, Huang Y, Li Z, Qiu H, Chen S (2022) Data versus collateral. *Review of Finance* 27(2):369–398.

Gambacorta L, Huang Y, Qiu H, Wang J (2024) How do machine learning and non-traditional data affect credit scoring? New evidence from a chinese fintech firm. *Journal of Financial Stability* 73:101284.

Green TC, Huang R, Wen Q, Zhou D (2019) Crowdsourced employer reviews and stock returns. *Journal of Financial Economics* 134(1):236–251.

Gu S, Kelly B, Xiu D (2020) Empirical asset pricing via machine learning. *Review of Financial Studies* 33(5):2223–2273.

He Z, Huang J, Zhou J (2023) Open banking: Credit market competition when borrowers own the data. *Journal of Financial Economics* 147(2):449–474.

Iyer R, Khwaja AI, Luttmer EFP, Shue K (2016) Screening peers softly: Inferring the quality of small borrowers. *Management Science* 62(6):1554–1577.

John GH, Langley P (1996) Static versus dynamic sampling for data mining. *KDD-96 Proceedings*, volume 96, 367–370.

Kabra A, Patel KK (2024) The limitations of model retraining in the face of performativity. *arXiv preprint 2408.08499*.

Ke G, Meng Q, Finley T, Wang T, Chen W, Ma W, Ye Q, Liu TY (2017) LightGBM: A highly efficient gradient boosting decision tree. *Advances in Neural Information Processing Systems* 30.

Kelly B, Malamud S, Zhou K (2022) The virtue of complexity everywhere. *SSRN preprint 4166368*.

Kelly B, Malamud S, Zhou K (2024) The virtue of complexity in return prediction. *Journal of Finance* 79(1):459–503.

Kelly B, Xiu D (2022) Financial machine learning. *Foundations and Trends in Finance* 13(3-4):205–363.

Last M (2007) Predicting and optimizing classifier utility with the power law. *Seventh IEEE International Conference on Data Mining Workshops (ICDMW 2007)*, 219–224.

Last M (2009) Improving data mining utility with projective sampling. *Proceedings of the 15th ACM SIGKDD International Conference on Knowledge Discovery and Data Mining*, 487–496, KDD '09.

Lessmann S, Baesens B, Seow HV, Thomas LC (2015) Benchmarking State-of-the-Art Classification Algorithms for Credit Scoring: An Update of Research. *European Journal of Operational Research* 247(1):124–136.

Mahadevan A, Mathioudakis M (2024) Cost-aware retraining for machine learning. *Knowledge-Based Systems* 293:111610.

Mohr F, van Rijn JN (2024) Learning curves for decision making in supervised machine learning: a survey. *Machine Learning* 113(11–12):8371–8425.

Mohri M, Rostamizadeh A, Talwalkar A (2012) *Foundations of machine learning* (MIT Press).

Oskarsdottir M, Bravo C, Sarraute C, Vanthienen J, Baesens B (2019) The value of big data for credit scoring: Enhancing financial inclusion using mobile phone data and social network analytics. *Applied Soft Computing* 74:26–39.

Pesaranghader A, Viktor HL (2016) Fast hoeffding drift detection method for evolving data streams. *Joint European conference on machine learning and knowledge discovery in databases*, 96–111 (Springer).

Provost F, Jensen D, Oates T (1999) Efficient progressive sampling. *Proceedings of the Fifth ACM SIGKDD International Conference on Knowledge Discovery and Data Mining*, 23–32, KDD '99 (New York, NY, USA: Association for Computing Machinery).

Ravina E (2025) Love & loans: The effect of beauty and personal characteristics in credit markets. *Management Science*, forthcoming.

Sabharwal A, Samulowitz H, Tesauro G (2016) Selecting near-optimal learners via incremental data allocation. *Proceedings of the Thirtieth AAAI Conference on Artificial Intelligence*, 2007–2015, AAAI'16.

Schwinn L, Bungert L, Nguyen A, Raab R, Pulsmeyer F, Precup D, Eskofier B, Zanca D (2022) Improving robustness against real-world and worst-case distribution shifts through decision region quantification. *International Conference on Machine Learning*, 19434–19449 (PMLR).

Viering T, Loog M (2023) The shape of learning curves: A review. *IEEE Trans. Pattern Anal. Mach. Intell.* 45(6):7799–7819.

Weiss GM, Tian Y (2008) Maximizing classifier utility when there are data acquisition and modeling costs. *Data Min. Knowl. Discov.* 17(2):253–282.

Žliobaitė I, Budka M, Stahl F (2015) Towards cost-sensitive adaptation: When is it worth updating your predictive model? *Neurocomputing* 150:240–249.

## EC.1. Technical Proofs

This section provides technical proofs and auxiliary lemmas for the analytical results and theoretical guarantees presented in the main paper.

### EC.1.1. Proofs for Section 3

*Proof of Theorem 1.* We first compute the derivative of the economic gap  $G(t)$  and the value function  $V_{\text{switch}}(t)$ . For real  $t \geq 0$ , the gap is  $G(t) = g^* - g_0 n^{-\alpha} t^{-\alpha}$  and its derivative is  $\frac{d}{dt}G(t) = \alpha g_0 n^{-\alpha} t^{-(\alpha+1)}$ . For the value function, we have

$$\begin{aligned} \frac{d}{dt}V_{\text{switch}}(t) &= \frac{d}{dt} \left[ -\beta^t c_s + \frac{\beta^{t+1}}{1-\beta} n(G(t) - c_{\text{post}} + c_{\text{pre}}) - \frac{nc_{\text{pre}}}{1-\beta} \right] \\ &= -(\ln \beta) \beta^t c_s + \frac{n}{1-\beta} \left[ (\ln \beta) \beta^{t+1} (G(t) - c_{\text{post}} + c_{\text{pre}}) + \beta^{t+1} \frac{d}{dt}G(t) \right] \\ &= \beta^t \ln \beta \left[ -c_s + \frac{n\beta}{1-\beta} \left( -c_{\text{post}} + c_{\text{pre}} + g^* - g_0 n^{-\alpha} t^{-\alpha} + \frac{1}{\ln \beta} \alpha g_0 n^{-\alpha} t^{-(\alpha+1)} \right) \right]. \end{aligned}$$

Equating the  $t$ -dependent part to zero yields the FOC

$$\begin{aligned} -c_s + \frac{n\beta}{1-\beta} \left( -c_{\text{post}} + c_{\text{pre}} + g^* - g_0 n^{-\alpha} t^{-\alpha} + \frac{\alpha g_0 n^{-\alpha}}{\ln \beta} t^{-(\alpha+1)} \right) &= 0 \\ \iff \left( \frac{g^* + (c_{\text{pre}} - c_{\text{post}}) - \frac{1-\beta}{n\beta} c_s}{g_0 n^{-\alpha}} \right) t^{\alpha+1} - t + \frac{\alpha}{\ln \beta} &= 0. \end{aligned}$$

Letting

$$K := n^\alpha \left( \frac{g^*}{g_0} - \frac{c_{\text{diff}}}{g_0} \right),$$

where  $c_{\text{diff}} := \left( c_{\text{post}} - c_{\text{pre}} + \frac{c_s(1-\beta)}{\beta n} \right)$ , the FOC reduces to

$$f(t) := K t^{\alpha+1} - t + \frac{\alpha}{\ln \beta} = 0, \quad \text{with } \alpha > 0, 0 < \beta < 1, \ln \beta < 0.$$

Then,

$$f'(t) = (\alpha+1)K t^\alpha - 1, \quad f''(t) = \alpha(\alpha+1)K t^{\alpha-1}.$$

**Feasibility.** If  $K \leq 0$ , then  $f'(t) \leq -1 < 0$  for all  $t > 0$ , so  $f$  is strictly decreasing with  $f(0^+) = \frac{\alpha}{\ln \beta} < 0$  and  $f(t) \rightarrow -\infty$  as  $t \rightarrow \infty$ . Hence no positive root exists. In particular, this proves necessity: if a positive root exists, then  $K > 0$ .

**Existence & uniqueness.** If  $K > 0$ , then  $f''(t) > 0$  for all  $t > 0$ ; thus  $f$  is strictly convex and has a single critical point

$$t_0 = ((\alpha+1)K)^{-1/\alpha} \quad \text{given by } f'(t_0) = 0.$$

Moreover,  $f(0^+) = \frac{\alpha}{\ln \beta} < 0$  and  $f(t) \rightarrow +\infty$  as  $t \rightarrow \infty$ . Therefore  $f$  crosses zero exactly once on  $(0, \infty)$ ; the unique root  $t^* > 0$  satisfies  $t^* > t_0$ .

**Stopping rule.** Compute the one-step difference  $V_{\text{switch}}(t+1) - V_{\text{switch}}(t)$ . Note that the term  $-\frac{nc_{\text{pre}}}{1-\beta}$  is constant in  $t$  (and hence does not affect the maximizer) and rearrange to obtain:

$$G(t) - \beta G(t+1) + (1-\beta)(c_{\text{pre}} - c_{\text{post}}) \geq \frac{(1-\beta)^2}{\beta} \frac{c_s}{n}. \quad (\text{EC.1})$$

Because  $G(t)$  is increasing and concave in  $t$  (for  $\alpha > 0$ ), the quantity  $G(t) - \beta G(t+1)$  is strictly increasing in  $t$  (for  $0 < \beta < 1$ ). Hence the left-hand side of (EC.1) is strictly increasing in  $t$ , so  $V_{\text{switch}}(t+1) - V_{\text{switch}}(t)$  is strictly decreasing in  $t$ . It follows that  $V_{\text{switch}}(t)$  is unimodal and the maximizer is unique. Therefore, the smallest  $t$  satisfying (EC.1) is the unique maximizer.

**Global optimality vs discarding.** Theorem 1 characterizes the maximizer of  $V_{\text{switch}}(t)$  over  $t$ . Since discarding at epoch  $t$  yields  $V_{\text{discard}}(t)$ , the globally optimal action at time 0 is to switch at  $t^*$  if and only if  $V_{\text{switch}}(t^*) \geq V_{\text{discard}}(0)$  (and otherwise discard immediately).  $\square$

### EC.1.2. Proofs for Section 4

*Proof of Proposition 3.* Under Assumption 1, we have  $N_t = nt$  for all  $t$ . Under Assumption 6,  $C_{\text{train}}(t) = c_{\text{train}}N_t^q = c_{\text{train}}(nt)^q$ .

(a) *Polynomial training cost ( $q > 0$ ). Uniform schedule.* Let  $t_k = \Lambda k$  with  $\Lambda > 0$  fixed. Let  $K$  be the largest integer such that  $t_K \leq t^*$ , i.e.,  $K = \lfloor t^*/\Lambda \rfloor$ . The total training cost is

$$C_{\text{unif}}(t^*) = \sum_{k=1}^K C_{\text{train}}(t_k) = \sum_{k=1}^K c_{\text{train}}(nk\Lambda)^q = c_{\text{train}}n^q\Lambda^q \sum_{k=1}^K k^q.$$

Using the standard bounds

$$\int_0^K x^q dx \leq \sum_{k=1}^K k^q \leq \int_1^{K+1} x^q dx,$$

we have

$$\frac{K^{q+1}}{q+1} \leq \sum_{k=1}^K k^q \leq \frac{(K+1)^{q+1}-1}{q+1}.$$

Hence  $\sum_{k=1}^K k^q = \Theta(K^{q+1})$  as  $K \rightarrow \infty$ . Since  $K \sim t^*/\Lambda$  for large  $t^*$ , we obtain

$$C_{\text{unif}}(t^*) = \Theta\left(c_{\text{train}}n^q\Lambda^q K^{q+1}\right) = \Theta\left(c_{\text{train}}n^q \frac{t^{*(q+1)}}{\Lambda}\right),$$

which yields  $C_{\text{unif}}(t^*) = \Theta(t^{*(q+1)}/\Lambda)$ .

*Geometric schedule.* Let  $t_k = \Lambda\lambda^{k-1}$  with  $\Lambda > 0$  and  $\lambda > 1$ . Let  $b$  be the largest integer such that  $t_b \leq t^* < t_{b+1}$ . Then

$$C_{\text{geom}}(t^*) = \sum_{k=1}^b C_{\text{train}}(t_k) = \sum_{k=1}^b c_{\text{train}}(nt_k)^q = c_{\text{train}}n^q \sum_{k=1}^b (\Lambda\lambda^{k-1})^q = c_{\text{train}}n^q \Lambda^q \sum_{k=0}^{b-1} \lambda^{qk}.$$

The geometric sum satisfies

$$\sum_{k=0}^{b-1} \lambda^{qk} = \frac{\lambda^{qb} - 1}{\lambda^q - 1}.$$

Since  $t_b = \Lambda\lambda^{b-1} \leq t^* < t_{b+1} = \Lambda\lambda^b$ , we have

$$\lambda^{b-1} = \frac{t_b}{\Lambda} \leq \frac{t^*}{\Lambda} < \lambda^b \quad \Rightarrow \quad \lambda^b \leq \lambda \frac{t^*}{\Lambda} \quad \Rightarrow \quad \lambda^{qb} \leq \lambda^q \left(\frac{t^*}{\Lambda}\right)^q.$$

Using this in the upper bound,

$$C_{\text{geom}}(t^*) \leq c_{\text{train}}n^q \Lambda^q \frac{\lambda^{qb}}{\lambda^q - 1} \leq c_{\text{train}}n^q \Lambda^q \frac{\lambda^q}{\lambda^q - 1} \left(\frac{t^*}{\Lambda}\right)^q = c_{\text{train}}n^q \frac{\lambda^q}{\lambda^q - 1} t^{*q}.$$

For a lower bound, note that  $t_b \geq t^*/\lambda$  (since  $t_{b+1} = \Lambda\lambda^b > t^*$ ). Then

$$C_{\text{geom}}(t^*) \geq C_{\text{train}}(t_b) = c_{\text{train}}(nt_b)^q \geq c_{\text{train}}n^q \left(\frac{t^*}{\lambda}\right)^q = c_{\text{train}}n^q \lambda^{-q} t^{*q}.$$

Thus

$$c_{\text{train}}n^q \lambda^{-q} t^{*q} \leq C_{\text{geom}}(t^*) \leq c_{\text{train}}n^q \frac{\lambda^q}{\lambda^q - 1} t^{*q},$$

so  $C_{\text{geom}}(t^*) = \Theta(c_{\text{train}}n^q t^{*q}) = \Theta(C_{\text{train}}(t^*))$ , as claimed.

(b) *Constant per-retrain cost* ( $q = 0$ ). If  $q = 0$ , then  $C_{\text{train}}(t) \equiv c_{\text{train}}$  for all  $t$ , so the total training cost up to  $t^*$  is  $c_{\text{train}}$  times the number of epochs with  $t_k \leq t^*$ .

*Uniform schedule.* For  $t_k = k\Lambda$ , the largest  $k$  with  $t_k \leq t^*$  is  $K = \lfloor t^*/\Lambda \rfloor$ , so

$$K_{\text{unif}}(t^*) = K = \Theta\left(\frac{t^*}{\Lambda}\right).$$

*Geometric schedule.* For  $t_k = \Lambda\lambda^{k-1}$ , let  $K$  be the largest integer with  $t_K \leq t^*$ . Then

$$\Lambda\lambda^{K-1} \leq t^* < \Lambda\lambda^K.$$

Dividing by  $\Lambda$  and taking  $\log_\lambda$ ,

$$K - 1 \leq \log_\lambda\left(\frac{t^*}{\Lambda}\right) < K,$$

so

$$K_{\text{geom}}(t^*) = K = \Theta\left(\log_\lambda\frac{t^*}{\Lambda}\right) = \Theta(\log t^*).$$

This completes the proof.  $\square$

*Proof of Proposition 4.* Under Assumption 1, we have  $N_t = nt$  for all  $t$ , and under Assumption 2,  $G(t) = g^* - g_0(nt)^{-\alpha}$ , with  $g^* > 0$ ,  $g_0 > 0$ ,  $\alpha > 0$ . We further assume that: (i) the horizon is finite ( $T < \infty$ ); (ii) there is no discounting ( $\beta = 1$ ); (iii) the pre- and post-decision per-sample acquisition costs are equal ( $c_{\text{pre}}^{\text{acq}} = c_{\text{post}}^{\text{acq}} =: c$ ). Then, up to  $t$ -independent constants, the value of switching at time  $t$  is

$$V_{\text{switch}}(t) = (T - t) n G(t),$$

and  $t^*$  denotes the unique continuous maximizer of  $V_{\text{switch}}(t)$  in  $(0, T)$ .

*Step 1: Second derivative and curvature bound.* First we compute  $G'(t)$  and  $G''(t)$ :

$$G'(t) = -g_0 \frac{d}{dt} (n^{-\alpha} t^{-\alpha}) = -g_0 n^{-\alpha} (-\alpha t^{-(\alpha+1)}) = g_0 \alpha n^{-\alpha} t^{-(\alpha+1)},$$

and

$$G''(t) = \frac{d}{dt} [g_0 \alpha n^{-\alpha} t^{-(\alpha+1)}] = g_0 \alpha n^{-\alpha} [-(\alpha+1)t^{-(\alpha+2)}] = -\alpha(\alpha+1)g_0 n^{-\alpha} t^{-(\alpha+2)}.$$

Now we differentiate  $V_{\text{switch}}(t) = (T - t)nG(t)$ :

$$V'_{\text{switch}}(t) = n[(T - t)G'(t) - G(t)],$$

and

$$V''_{\text{switch}}(t) = n[(T - t)G''(t) - 2G'(t)].$$

We substitute  $G'$  and  $G''$ :

$$(T - t)G''(t) = (T - t) [ -\alpha(\alpha+1)g_0 n^{-\alpha} t^{-(\alpha+2)} ],$$

$$-2G'(t) = -2g_0 \alpha n^{-\alpha} t^{-(\alpha+1)}.$$

Thus

$$\begin{aligned} V''_{\text{switch}}(t) &= n \left[ (T - t) ( -\alpha(\alpha+1)g_0 n^{-\alpha} t^{-(\alpha+2)} ) - 2g_0 \alpha n^{-\alpha} t^{-(\alpha+1)} \right] \\ &= g_0 \alpha n^{1-\alpha} t^{-(\alpha+2)} \left[ (\alpha-1)t - (\alpha+1)T \right]. \end{aligned}$$

Since  $T \geq t$  and  $\alpha > 0$ , the bracket is negative and  $V_{\text{switch}}$  is concave near  $t^*$ . Moreover, for  $t$  in any compact subinterval of  $(0, T)$  there exists a constant  $C > 0$  (depending only on  $(g^*, g_0, \alpha, n, T)$ ) such that

$$|V''_{\text{switch}}(t)| \leq C t^{-(\alpha+2)}. \quad (\text{EC.2})$$

*Step 2: Local quadratic bound around  $t^*$ .* By Taylor's theorem, for any  $t$  in a neighborhood of  $t^*$  there exists  $\xi$  between  $t$  and  $t^*$  such that

$$V_{\text{switch}}(t) = V_{\text{switch}}(t^*) + V'_{\text{switch}}(t^*)(t - t^*) + \frac{1}{2}V''_{\text{switch}}(\xi)(t - t^*)^2.$$

Since  $t^*$  is the (unique) maximizer,  $V'_{\text{switch}}(t^*) = 0$  and  $V_{\text{switch}}(t) \leq V_{\text{switch}}(t^*)$ , so

$$0 \leq V_{\text{switch}}(t^*) - V_{\text{switch}}(t) = -\frac{1}{2}V''_{\text{switch}}(\xi)(t - t^*)^2 \leq \frac{1}{2}|V''_{\text{switch}}(\xi)|(t - t^*)^2.$$

For  $t$  sufficiently close to  $t^*$ ,  $\xi$  lies in a neighborhood where (EC.2) applies with  $t$  replaced by  $t^*$  (up to a constant factor), yielding

$$V_{\text{switch}}(t^*) - V_{\text{switch}}(t) \leq \frac{C}{2}t^{*(\alpha+2)}(t - t^*)^2. \quad (\text{EC.3})$$

*Step 3: Uniform schedule bound.* For the uniform schedule  $t_k = k\Lambda$ , let  $t^\dagger$  be the epoch closest to  $t^*$ . Then  $|t^\dagger - t^*| \leq \Lambda$ . For  $t^*$  large enough that  $t^\dagger$  lies in the interior of  $(0, T)$  and (EC.3) applies, we obtain

$$W_{\text{unif}} = V_{\text{switch}}(t^*) - V_{\text{switch}}(t^\dagger) \leq \frac{C}{2}t^{*(\alpha+2)}\Lambda^2 := C_1 \frac{\Lambda^2}{t^{*(\alpha+2)}}.$$

*Step 4: Geometric schedule bound.* For the geometric schedule  $t_k = \Lambda\lambda^{k-1}$  with  $\lambda > 1$ , let  $k$  be such that  $t_k \leq t^* < t_{k+1}$ . Then  $t_{k+1} = \lambda t_k$  and  $t^* \in [t_k, t_{k+1})$ . Choose  $t^\dagger \in \{t_k, t_{k+1}\}$  as the closer epoch. Then

$$|t^\dagger - t^*| \leq \frac{t_{k+1} - t_k}{2} = \frac{(\lambda - 1)t_k}{2} \leq \frac{(\lambda - 1)}{2}t^*,$$

since  $t_k \leq t^*$ . For  $t^*$  large enough that the interval  $[t^*/\lambda, \lambda t^*]$  lies inside  $(0, T)$  and (EC.3) applies for all  $t$  in this range, we can again use (EC.3) with  $t = t^\dagger$ :

$$W_{\text{geom}} = V_{\text{switch}}(t^*) - V_{\text{switch}}(t^\dagger) \leq \frac{C}{2}t^{*(\alpha+2)}|t^\dagger - t^*|^2 \leq \frac{C}{2}t^{*(\alpha+2)}\left(\frac{\lambda - 1}{2}\right)^2 t^{*2}.$$

Thus

$$W_{\text{geom}} \leq \frac{C}{8}(\lambda - 1)^2 t^{*2} := C_2 \frac{(\lambda - 1)^2}{t^{*\alpha}}.$$

This completes the proof.  $\square$

### EC.1.3. Proofs for Section 6

*Proof of Proposition 5.* We start by proving the first part of the proposition. Consider a run for which event  $\mathcal{E}$  holds and the GSE algorithm stops at epoch  $k$ . We distinguish two cases.

- *Case (i):* The stop happens following condition  $\widehat{V}_{\text{switch}}^{\text{LB}}(t_k) > 0$ .
- *Case (ii):* The stop happens following condition  $\widehat{V}_{\text{switch}}^{\text{UB}}(t_k) < 0$ .

Let us first consider Case (i). Under event  $\mathcal{E}$ , the following holds:

$$V_{\text{GSE}}(T) = V_{\text{switch}}(t_k) \geq \widehat{V}_{\text{switch}}^{\text{LB}}(t_k) > 0.$$

As the lower bound in the proposition is negative, it is directly implied in this case.

We now turn to Case (ii). We show that:

$$V_{\text{GSE}}(T) \geq -cnt_k - c_s + n(T - t_k) \left[ (\widehat{G}_{k-1} - \delta_{k-1}) - c \right] \quad (\text{EC.4})$$

To do so, we further decompose Case (ii) into two subcases: (ii,a) the algorithm discards the challenger; (ii,b) the algorithm switches to the challenger of epoch  $\tilde{k} \in \{k-1, k\}$ .

Case (ii,a) happens only if  $\widehat{\Delta V}^{\text{LB}}(t_k) < 0$ , which implies:

$$-c_s + n(T - t_k) \left[ (\widehat{G}_{k-1} - \delta_{k-1}) - c \right] < 0.$$

Moreover, when discarding at epoch  $k$ ,  $V_{\text{GSE}}(T) = -cnt_k$ . Putting those two facts together implies that equation EC.4 holds in case (ii,a).

In case (ii,b), our modified algorithm switches to the challenger of epoch  $\tilde{k}$ , with  $\tilde{k} = \arg \max_{k' \in \{k, k-1\}} \widehat{G}(t_{k'}) - \delta_{k'}$ , and :

$$V_{\text{GSE}}(T) = -cnt_k - c_s + n(T - t_k) [G(\tilde{k}) - c].$$

Under event  $\mathcal{E}$ , we get:

$$\begin{aligned} V_{\text{GSE}}(T) &\geq -cnt_k - c_s + n(T - t_k) [\widehat{G}(\tilde{k}) - \delta_{\tilde{k}} - c], \\ &\geq -cnt_k - c_s + n(T - t_k) [\widehat{G}(t_{k-1}) - \delta_{k-1} - c]. \end{aligned}$$

Hence, equation EC.4 also holds in case (ii,b).

Having established equation EC.4, we rearrange the terms and obtain:

$$\begin{aligned}
V_{\text{GSE}}(T) &\geq -cnt_k - c_s + n(T - t_k) \left[ (\widehat{G}_{k-1} - \delta_{k-1}) - c \right] \\
&\geq \underbrace{-cnt_{k-1} - c_s + n(T - t_{k-1}) \left[ (\widehat{G}_{k-1} + \delta_{k-1}) - c \right]}_{= \widehat{V}_{\text{switch}}^{\text{UB}}(k-1)} \\
&\quad - 2n(T - t_{k-1})\delta_{k-1} - n(t_k - t_{k-1}) \underbrace{(\widehat{G}_{k-1} - \delta_{k-1})}_{\leq 1} \\
&\geq \widehat{V}_{\text{switch}}^{\text{UB}}(k-1) - 2\delta_{k-1}(T - t_{k-1})n - (t_k - t_{k-1})n
\end{aligned} \tag{EC.5}$$

The algorithm goes to epoch  $k$  only if following conditions are satisfied at epoch  $k-1$ :

$$V_{\text{switch}}^{\text{UB}}(k-1) > 0.$$

This implies the first term in the right hand side of equation EC.5 is positive. Replacing  $\delta_{k-1}$  by its definition then yields the bound of the proposition.

It remains to show the second statement of the proposition. By Hoeffding's inequality and a union bound, with probability at least  $1 - \epsilon$ , for all  $k \in \mathcal{T}_D$ :

$$|\widehat{G}(k) - G(k)| \leq \delta_k. \tag{EC.6}$$

By definition of the upper and lower bounds, this implies that with probability at least  $1 - \epsilon$ ,  $\widehat{V}_{\text{switch}}^{\text{LB}}(t_k)$  and  $\widehat{V}_{\text{switch}}^{\text{UB}}(t_k)$  are valid lower and upper bounds on  $V_{\text{switch}}(t_k)$  for all epochs.  $\square$

*Proof of Theorem 2.* Define  $g^* := \max_{t \geq 0} G(t)$ . The following bound on the value of the oracle holds:

$$V_{\text{ORACLE}}(T) \leq \max ([g^* - cn] T - c_s, 0). \tag{EC.7}$$

We show that under the conditions of the theorem, sublinear regret with respect to the upper bound of that inequality is achievable. Let us start by introducing the event that the generalization error of the challenger is well behaved. Set

$$\delta'_{N_t} := 2\sqrt{\frac{2d \log(e(1-\rho)N_t/d)}{(1-\rho)N_t}} + \sqrt{\frac{2 \log(2T^2)}{(1-\rho)N_t}}.$$

By Corollary 3.19 from Mohri et al. (2012), applied once to the optimal challenger and to the challenger of each type step  $t$ , combined with a union bound, the following Lemma holds:

**LEMMA EC.1.** *With probability at least  $1 - (1 - w_1)/T$ :*

$$(C1) \text{ and } (C2) \text{ hold and } g^* - G(t) \leq \delta'_{N_t}, \text{ for all } t \leq T. \quad (\text{event } \mathcal{A})$$

Decomposing the regret along event  $\mathcal{A}$ , we obtain:

$$R_{\text{alg}}(T) = \underbrace{\mathbb{E}[(V_{\text{ORACLE}}(T) - V_{\text{ALG}}(T))\mathbb{I}\{\mathcal{A}\}]}_{(i)} + \underbrace{\mathbb{E}[(V_{\text{ORACLE}}(T) - V_{\text{ALG}}(T))\mathbb{I}\{\overline{\mathcal{A}}\}]}_{(ii)}.$$

We start by upper bounding (ii). Since the loss takes value in  $\{-1; 1\}$ ,  $g^* \leq 2$ , hence, by equation EC.7,  $V_{\text{ORACLE}}(T) \leq 2T$ . On the other hand, the algorithm can at worse pay all the costs without getting any benefit, which implies  $V_{\text{ALG}}(T) \geq -c_s - cnT$ . Combining those two facts:

$$\begin{aligned} (ii) &\leq (2 + cn + \frac{c_s}{T})T\mathbb{P}(\overline{\mathcal{A}}), \\ &\leq (1 + w_1)(2 + cn + \frac{c_s}{T}), \end{aligned} \quad (\text{EC.8})$$

where the second line holds by Lemma EC.1.

We now work on upper bounding (i). Consider any  $t \geq w_2 T^{2/3}$ . Under event  $\mathcal{A}$ , we have:

$$g^* \leq G(t) + \delta'_{w_2 T^{2/3}}.$$

This implies:

$$\begin{aligned} V_{\text{switch}}(t) &\geq -cnT - c_s + n(T - t) \left( g^* - 2\sqrt{\frac{2d \log(e(1 - \rho)w_2 n T^{2/3}/d)}{(1 - \rho)w_2 n T^{2/3}}} - \sqrt{\frac{2 \log(2T^2)}{(1 - \rho)w_2 n T^{2/3}}} \right), \\ &\geq [g^* - cn]T - c_s - ntg^* - nT^{2/3} \left( 2\sqrt{\frac{2d \log(e(1 - \rho)w_2 n T^{2/3}/d)}{(1 - \rho)w_2 n}} - \sqrt{\frac{2 \log(2T^2)}{(1 - \rho)w_2 n}} \right). \end{aligned}$$

Therefore, for any  $t \in [w_2 T^{2/3}; w_3 T^{2/3}]$ , there exists a constant  $w_5$ , such that for any large enough  $T$ , we have:

$$V_{\text{switch}}(t) \geq [g^* - cn]T - c_S - w_5 T^{2/3} \sqrt{\log(T)}.$$

This, combined with condition (C1) implies:

$$V_{\text{switch}}(t_{\text{ALG}}) \geq [g^* - cn]T - c_S - w_5 T^{2/3} \sqrt{\log(T)}.$$

Condition (C1) also implies:

$$V_{\text{discard}}(t_{\text{ALG}}) \geq -w_2 nc T^{2/3}.$$

By condition (C2),

$$V_{\text{ALG}}(T) \geq \max(V_{\text{switch}}(t_{\text{ALG}}); V_{\text{discard}}(t_{\text{ALG}})) - w_4 T^{2/3} \sqrt{\log(T)}$$

Putting those last inequalities together yields:

$$\begin{aligned} V_{\text{ALG}}(T) &\geq \max([g^* - cn]T - c_S - w_5 T^{2/3} \sqrt{\log(T)}; -w_2 nc T^{2/3}) - w_4 T^{2/3} \sqrt{\log(T)} \\ &\geq \max([g^* - cn]T - c_S; 0) - (w_2 nc + w_4 + w_5) T^{2/3} \sqrt{\log(T)}. \end{aligned}$$

The first term on the right hand side matches the right hand side of equation EC.7, which gives a bound on (i). Combining with equation EC.8 yields the theorem.  $\square$

*Proof of Corollary 1.* By design, the OSE algorithm with  $t_k = T^{2/3}$  verifies (C1) with  $w_2 = w_3 = 1$ . Let us show it also verifies (C2) with high enough probability.

The OSE algorithm switches if and only if

$$\widehat{\Delta V(T^{2/3})} \geq 0.$$

Therefore (C2) is valid as soon as:

$$|\widehat{\Delta V(T^{2/3})} - \Delta V(T^{2/3})| \leq w_4 T^{2/3} \sqrt{\log(T)}.$$

The following holds:

$$|\widehat{\Delta V(T^{2/3})} - \Delta V(T^{2/3})| \leq Tn|G(T^{2/3}) - \widehat{G}(T^{2/3})|.$$

We have:

$$\begin{aligned} \mathbb{P}\left(Tn|G(T^{2/3}) - \widehat{G}(T^{2/3})| \geq T^{2/3} \sqrt{\frac{2n \log(T)}{\rho}}\right) &= \mathbb{P}\left(|G(T^{2/3}) - \widehat{G}(T^{2/3})| \geq \sqrt{\frac{2 \log(T)}{\rho n T^{2/3}}}\right) \\ &\leq 2 \exp\left(-\frac{\rho n T^{2/3}}{2} \times \frac{2 \log(T)}{\rho n T^{2/3}}\right) \\ &\leq \frac{2}{T}, \end{aligned} \quad (\text{EC.9})$$

where the second line holds by Hoeffding's inequality. This implies that the OSE algorithm verifies (C2) with  $w_1 = 2$  and  $w_4 = \sqrt{2n}/\rho$ .  $\square$

*Proof of Proposition 6.* Here, we study the LSEc algorithm, implemented with  $\gamma > 0$  and geometric epoch rate  $\lambda > 1$ .

We start by showing that the stopping time of the algorithm  $t_{\text{LSEc}}$  is lower bounded (first part of condition (C1)). By design, at each epoch  $k \geq 3$ , the algorithm keeps going to epoch  $k + 1$  if and only if

$$\widehat{V}_{\text{switch}}(t_k) \leq \max_{k' > k} \widehat{V}_{\text{switch}}^{\text{UB}}(t_{k'}), \quad (\text{EC.10})$$

and

$$-nct_k \leq \max_{k' > k} \widehat{V}_{\text{switch}}^{\text{UB}}(t_{k'}). \quad (\text{EC.11})$$

The following lemma, whose proof we defer, states that for small  $k$ , these two conditions are satisfied:

**LEMMA EC.2 (Lower bound condition (C1)).** *For any large, enough  $T$ ,*

$$t_k \leq \left( \frac{\gamma n T}{4\gamma(4c+1)(\lambda n)^{3/2}(\lambda-1)} \right)^{2/3} \implies \text{Conditions EC.10 and EC.11.}$$

As the LSEc algorithm keeps going whenever Conditions EC.10 and EC.11 are satisfied together, this in turn implies the lower bound of condition (C1):

$$t_{\text{LSEc}} \geq \left( \frac{\gamma n T}{4\gamma(4c+1)(\lambda n)^{3/2}(\lambda-1)} \right)^{2/3}. \quad (\text{EC.12})$$

We now show that the second part of condition (C1), the upper bound on  $t_{\text{LSEc}}$ , holds with high probability. We first combine Lemma EC.1 and Equation EC.6 instantiated with  $\epsilon = 1/T$  and obtain:

**LEMMA EC.3.** *With probability at least  $1 - 2/T$ :*

$$|G(t_k) - \widehat{G(t_k)}| \leq \sqrt{\frac{2 \log(T^2)}{\rho N_{t_k}}} \quad (\text{event } C)$$

and

$$|g^* - \widehat{G(t_k)}| \leq \delta''_{N_{t_k}}, \text{ for all } t_k \leq T, \quad (\text{event } \mathcal{A}')$$

where

$$\delta''_{N_{t_k}} = 2\sqrt{\frac{2d \log(eT/d)}{N_{t_k}}} + \sqrt{2 \frac{\log(2T^2)}{N_{t_k}}} + \sqrt{\frac{2 \log(T^2)}{\rho N_{t_k}}}.$$

The following lemma, whose proof we defer, states that, under event  $\mathcal{A}'$ , for any large enough  $k$ , one of Conditions EC.10 and EC.11 is not satisfied.

**LEMMA EC.4 (Upper bound condition (C1)).** *Suppose that event  $\mathcal{A}'$  holds. Then, there exists a constant  $\gamma'$ , such that for any large enough  $T$ :*

- if  $g^* > 0$ , then

$$t_k \geq \left( 2nT \frac{\gamma' \sqrt{\log(T)}}{g^*} \right)^{2/3} \implies \text{Condition EC.10 does not hold,} \quad (\text{EC.13})$$

- if  $g^* = 0$

$$t_k \geq \left( 4nT \frac{\gamma' \sqrt{\log(T)}}{c} \right)^{2/3} \implies \text{Condition EC.11 is not satisfied.}$$

This lemma directly implies that, under event  $\mathcal{A}'$ , the algorithm satisfies:

$$t_{\text{LSEc}} \leq \lambda \left( 2nT \frac{\gamma' \sqrt{\log(T)}}{g^* + c\mathbb{I}\{g^* = 0\}} \right)^{2/3}.$$

This complements EC.12 and shows that, under event  $\mathcal{A}'$ , the algorithm satisfies condition (C1).

Let us now show it also satisfies condition (C2). The algorithm switches if and only if

$$\widehat{\Delta V(t_{\text{LSEc}})} \geq 0.$$

The following holds:

$$|\widehat{\Delta V(t_{\text{LSEc}})} - \Delta V(t_{\text{LSEc}})| \leq Tn|G(t_{\text{LSEc}}) - \widehat{G(t_{\text{LSEc}})}|.$$

Under event  $C$ ,

$$T|G(t_{\text{LSEc}}) - \widehat{G(t_{\text{LSEc}})}| \leq T \sqrt{\frac{4 \log(T)}{\rho N_{t_{\text{LSEc}}}}}.$$

By equation EC.12, this implies:

$$T|G(t_{\text{LSEc}}) - \widehat{G(t_{\text{LSEc}})}| \leq T^{2/3} \sqrt{\frac{4 (4\gamma(4c+1)(\lambda n)^{3/2}(\lambda-1))^{2/3} \log(T)}{\rho(\gamma n)^{2/3}}},$$

which implies condition (C2).

Lemma EC.3 states that event  $\mathcal{A}$  and  $C$  hold together with probability at least  $1 - 2/T$ , so the result follows.  $\square$

*Proof of Proposition EC.2.* Consider any epoch  $k \geq 3$ . For any  $k' > k$ , we have by design:

$$\begin{aligned} \widehat{V}_{\text{switch}}^{\text{UB}}(t_{k'}) &= -cnT - c_s + \sum_{\tau > t_{k'}} n\widehat{G}^{\text{UB}}(t_{k'}), \\ &= -cnT - c_s + (T - t_{k'})n \left[ \widehat{G}(t_k) + n(t_{k'} - t_k)\widehat{s}_k \right]. \end{aligned} \tag{EC.14}$$

Let us first give sufficient conditions for equation EC.10 to hold. Rearranging the terms of the above equation instantiated for  $k' = k + 1$ , we have:

$$\widehat{V}_{\text{switch}}^{\text{UB}}(t_{k+1}) - \widehat{V}_{\text{switch}}^{\text{UB}}(t_k) = n(T - t_{k+1}) \times n(t_{k+1} - t_k) \hat{s}_k - n(t_{k+1} - t_k) \widehat{G}(t_k).$$

Therefore, the right hand side is positive as soon as  $n(T - t_{k+1}) \hat{s}_k \geq \widehat{G}(t_k)$ , or, since  $\widehat{G}(t_k) \leq 1$ :

$$n(T - t_{k+1}) \hat{s}_k \geq 1. \quad (\text{EC.15})$$

Note that the above is a sufficient condition for Condition EC.10. Consider any epoch  $k \geq 3$  with  $N_{t_k} = \Lambda \lambda^{k-1} n$ . By design of the slope estimation, we have:

$$\begin{aligned} \hat{s}_k &\geq \frac{\gamma}{N_{t_k} - N_{t_{k-1}}} \times \frac{1}{\sqrt{N_{t_{k-1}}}} \\ &= \frac{\gamma}{(\Lambda \lambda^{k-2} n)^{3/2} (\lambda - 1)}. \end{aligned} \quad (\text{EC.16})$$

Take any  $k$  with  $t_{k+1} \leq T/2$ . Condition EC.15 is satisfied as soon as:

$$\frac{\gamma}{(\Lambda \lambda^{k-2} n)^{3/2} (\lambda - 1)} \geq \frac{2}{nT}.$$

Rearranging the terms and injecting the formula  $t_k = \Lambda \lambda^{k-1}$ , this yields the following fact:

$$t_k \leq \min \left( \left( \frac{\gamma n T}{(\lambda n)^{3/2} (\lambda - 1)} \right)^{2/3}; \frac{T}{2\gamma} \right) \implies \text{Condition EC.15} \implies \text{Condition EC.10}.$$

For any large enough  $T$ , the first term in the min is the smallest, therefore, for any large enough  $T$ :

$$t_k \leq \left( \frac{\gamma n T}{(\lambda n)^{3/2} (\lambda - 1)} \right)^{2/3} \implies \text{Condition EC.10}. \quad (\text{EC.17})$$

Let us now give sufficient conditions for equation EC.11 to hold. Take  $k' = \lfloor \frac{\log(T/2\Lambda)}{\log(\gamma)} + 1 \rfloor$ , so that:

$$\frac{T}{2\gamma} \leq t_{k'} \leq \frac{T}{2}. \quad (\text{EC.18})$$

From equation EC.14, we get:

$$\begin{aligned}\widehat{V}_{\text{switch}}^{\text{UB}}(t_{k'}) - cn t_k &= -cn(T - t_k) - c_s + (T - t_{k'})n \left[ \widehat{G}(t_k) + n(t_{k'} - t_k)\hat{s}_k \right], \\ &\geq -cnT - c_s + \frac{T}{2}n \left[ -1 + n \left( \frac{T}{2\gamma} - t_k \right) \hat{s}_k \right].\end{aligned}$$

For any  $T \geq c_s/cn$ , the right hand side above is positive as soon as:

$$n \left( \frac{T}{2\gamma} - t_k \right) \hat{s}_k > 4c + 1.$$

Consider any  $t_k \leq \frac{T}{4\gamma}$ . Combining the above with equation EC.16, we get that a sufficient condition for Condition EC.11 is:

$$\frac{\gamma T n}{4\gamma(\Lambda\lambda^{k-2}n)^{3/2}(\lambda-1)} \geq 4c + 1.$$

Rearranging the terms and injecting  $t_k = \Lambda\lambda^{k-1}$  yields:

$$t_k \leq \min \left( \left( \frac{\gamma n T}{4\gamma(4c+1)(\lambda n)^{3/2}(\lambda-1)} \right)^{2/3}; \frac{T}{4\gamma} \right) \implies \text{Condition EC.11}.$$

Once again for large enough  $T$ , the right hand side of this equation is the smallest. Hence, combining with equation EC.17, we get that for any large enough  $T$ ,

$$t_k \leq \left( \frac{\gamma n T}{4\gamma(4c+1)(\lambda n)^{3/2}(\lambda-1)} \right)^{2/3} \implies \text{Conditions EC.10 and EC.11.}$$

□

*Proof of Lemma EC.4* By the triangle inequality, lemma EC.3 implies:

$$|\widehat{G}(t_k) - \widehat{G}(t_{k-1})| \leq \delta'_{N_{t_k}} + \delta'_{N_{t_{k-1}}}.$$

Hence, the estimate  $\hat{s}_k$  satisfies:

$$\begin{aligned}\hat{s}_k &\leq \frac{2\sqrt{2d\log(eT/d)} + \sqrt{2\log(2T^2)} + \sqrt{\frac{2\log(T^2)}{\rho}} + 2\gamma}{(N_{t_k} - N_{t_{k-1}})\sqrt{N_{t_{k-1}}}} \\ &\leq \frac{\gamma'\sqrt{\log(T)}}{t_k^{3/2}},\end{aligned}\tag{EC.19}$$

with  $\gamma'$  some constant that depends on  $\rho, d, \gamma, \lambda$  and  $\Lambda$ .

We now decompose the proof in two subcases: (i)  $g^* > 0$  and (ii)  $g^* = 0$ .

We deal first with (i),  $g^* > 0$ . Rearranging the terms of the equation EC.14, we have:

$$\begin{aligned} \widehat{V}_{\text{switch}}^{\text{UB}}(t_{k'}) - \widehat{V}_{\text{switch}}^{\text{UB}}(t_k) &= n(T - t_{k'}) \times n(t_{k'} - t_k) \hat{s}_k - n(t_{k'} - t_k) \widehat{G}(k) \\ &\leq nT \times n(t_{k'} - t_k) \hat{s}_k - n(t_{k'} - t_k) \widehat{G}(k). \end{aligned} \quad (\text{EC.20})$$

This is negative as soon as:

$$nT \hat{s}_k \leq \widehat{G}(k).$$

Consider  $T$  large enough so that  $\delta''_{N_{T^{2/3}}} \leq g^*/2$ . By Lemma EC.3, for any such  $T$ , for any  $t_k \geq T^{2/3}$ , we have  $\widehat{G}(k) \geq g^*/2$ . Combining with equation EC.19 implies that, for any  $t_k \geq T^{2/3}$ , equation EC.20 is negative as soon as:

$$nT \frac{\gamma' \sqrt{\log(T)}}{t_k^{3/2}} \leq \frac{g^*}{2}.$$

Rearranging the terms, we obtain:

$$t_k \geq \left( 2nT \frac{\gamma' \sqrt{\log(T)}}{g^*} \right)^{2/3} \implies \text{Condition EC.10 does not hold.} \quad (\text{EC.21})$$

This is the first part of the lemma.

We now turn to the case  $g^* = 0$ . Consider  $T$  large enough so that  $\delta'_{N_{T^{2/3}}} \leq c/4$  and  $T^{2/3} \leq \frac{T}{2}$ . From equation EC.14, for any  $t_k \in [T^{2/3}; \frac{T}{2}]$ , we get that for all  $k' \geq k$ :

$$\begin{aligned} \widehat{V}_{\text{switch}}^{\text{UB}}(t_{k'}) - \text{cnt}_k &= -cn(T - t_k) - c_s + (T - t_{k'})n \left[ \widehat{G}(t_k) + n(t_{k'} - t_k) \hat{s}_k \right] \\ &\leq -cn \frac{T}{2} - c_s + Tn \left[ \frac{c}{4} + nT \hat{s}_k \right] \end{aligned}$$

The right hand side is negative as soon as:

$$nT \hat{s}_k \leq \frac{c}{4}.$$

Combining with equation EC.19, it is implied by:

$$nT \frac{\gamma' \sqrt{\log(T)}}{t_k^{3/2}} \leq \frac{c}{4}$$

Rearranging, we get:

$$\left( 4nT \frac{\gamma' \sqrt{\log(T)}}{c} \right)^{2/3} \leq t_k \implies \text{Condition EC.11 is not satisfied.}$$

This is the second part of the lemma. □

## EC.2. Credit Scoring Case Study: Additional Empirical Results

This section describes data management procedures, reports complementary results to the main analysis, and presents sensitivity analyses and robustness checks.

### EC.2.1. Data management

Our empirical analysis uses a comprehensive dataset from Lending Club, a large peer-to-peer lending platform. The original dataset, obtained from Kaggle, covers the period 2007–2020 and contains 2,925,493 loans with 141 variables.<sup>10</sup>

*Sample selection.* We restrict the sample to loans with a final status of *fully paid* or *charged off*, excluding 1,065,162 loans with other outcomes. We further remove 588,361 loans with unverified income and 44,371 loans involving co-borrowers. An additional 138,071 observations are dropped due to missing values, and 2,237 are excluded as outliers, leaving 1,086,683 observations.

We exclude data from 2018–2020 to avoid the Lending Club crisis period, during which loan applications declined sharply and default rates exhibited substantial instability. Specifically, applications fell by more than 45% per year (45.45% in 2018 and 65.89% in 2019), while default rates fluctuated markedly relative to 2017 (+2.96 percentage points in 2018 and –5.06 percentage points in 2019). We also omit data from 2012–2013, which display unusually low default rates compared with subsequent years (17.7% in 2012 and 16.87% in 2013 versus 19.4% in 2014, the lowest among retained years). Finally, we drop the first four months of 2014 and the last eight months of 2017 due to abnormally low and high default rates, respectively. The resulting dataset contains 705,302 loans issued between May 2014 and April 2017.

<sup>10</sup> The dataset is available at <https://www.kaggle.com/datasets/ethon0426/lending-club-20072020q1>.

Incumbent features	Description
annual_inc	The self-reported annual income provided by the borrower during registration.
dti	A ratio calculated using the borrower's total monthly debt payments on the total debt obligations, excluding mortgage and the requested LC loan, divided by the borrower's self-reported monthly income.
fico_range_high	The upper boundary range the borrower's FICO at loan origination belongs to.
funded_amnt	The total amount committed to that loan at that point in time.
loan_duration	Duration of the loan, 1 for 60 months (5 years) and 0 for 36 months (3 years).
emp_length	Employment length in years. Possible values are between 0 and 10 where 0 means less than one year and 10 means ten or more years.
purpose	A category provided by the borrower for the loan request.
Additional challenger features	Description
avg_cur_bal	Average current balance of all accounts
bc_open_to_buy	Total open to buy on revolving bankcards.
bc_util	Ratio of total current balance to high credit/credit limit for all bankcard accounts.
delinq_2yrs	The number of 30+ days past-due incidences of delinquency in the borrower's credit file for the past 2 years
pub_rec	Number of derogatory public records
pub_rec_bankruptcies	Number of public record bankruptcies
tax_liens	Number of tax liens
inq_last_6mths	The number of inquiries in past 6 months (excluding auto and mortgage inquiries)
mort_acc	Number of mortgage accounts.
revol_bal	Total credit revolving balance
revol_util	Revolving line utilization rate, or the amount of credit the borrower is using relative to all available revolving credit.
open_acc	The number of open credit lines in the borrower's credit file.
num_rev_accts	Number of revolving accounts
num_bc_tl	Number of bankcard accounts
num_il_tl	Number of installment accounts
num_actv_bc_tl	Number of currently active bankcard accounts
mths_since_recent_bc	Months since most recent bankcard account opened.
mo_sin_old_rev_tl_op	Months since oldest revolving account opened
mo_sin_rcnt_rev_tl_op	Months since most recent revolving account opened
mo_sin_rcnt_tl	Months since most recent account opened
grade	LC assigned loan grade
sub_grade	LC assigned loan subgrade

**Table EC.1 Incumbent and challenger features**

*Feature selection.* We begin by excluding variables that (i) contain post-issuance information, (ii) relate to co-borrowers, (iii) have more than 5% missing values, (iv) are highly correlated with variables retained in the dataset, (v) lack a clear definition, or (vi) are unlikely to be informative for predicting loan default. In addition, to facilitate a clear illustration of the algorithms' behavior across different regimes, including scenarios in which switching is optimal, we exclude three variables: interest rate, home ownership status, and employment title. This restriction increases the performance gap between the challenger and the incumbent models and enables a clearer analysis of the resulting switching decisions. The *incumbent model* has therefore access to a feature set  $\mathcal{I}$  of size  $|\mathcal{I}| = 7$ , which consists of annual income, job tenure, debt-to-income ratio, FICO

score, funding amount, loan duration, and loan purpose. In contrast, the *challenger model* benefits from access to all the alternative data. (e.g., loan grade, number of open credit lines, bank cards, installments, mortgages, and revolving accounts), thereby expanding the feature set to  $C$ , with  $|C| = 29$ . Table EC.1 reports the complete list of features and their descriptions for both the incumbent and challenger models. Among all these features, 27 are continuous and 2 are categorical.

*Feature engineering.* Continuous variables are standardized, categorical variables are one-hot encoded, and loan grade and subgrade, which are originally categorical, are transformed into numerical (ordinal) scales.

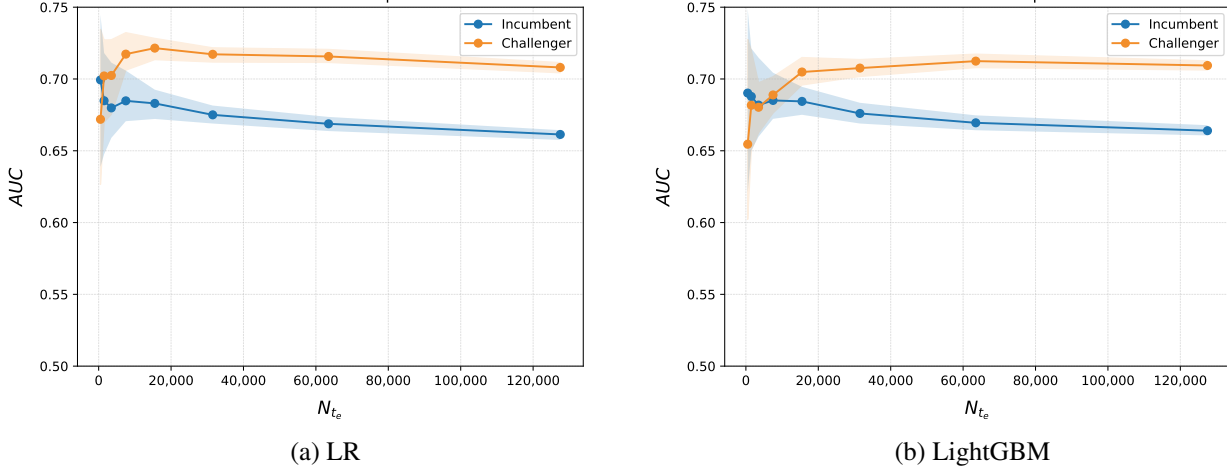
### EC.2.2. Details on Scenario Selection

Parameter	Core scenario		Economic structure			Robustness			
	Early (E.1)	Late (E.2)	No costs (E.3)	High $c_{\text{acq}}$ (E.4)	$c_S > 0$ (E.5)	Small batch (E.6)	Large batch/cost (E.7)	Timeless (E.8)	Small size (E.9)
Batch type	(geometric, 2)	-	-	-	-	(geometric, <b>1.5</b> )	(geometric, <b>2.5</b> )	-	-
Time series	Yes	-	-	-	-	-	-	No	-
$N_0$	189,250	-	-	-	-	-	-	-	-
$N_{I_e}$	163,400	-	-	-	-	-	-	-	81,700
$N_1$	250	-	-	-	-	-	-	-	-
Train-test ratio	1	-	-	-	-	-	-	-	-
Sampling ratio	0.5	-	-	-	-	-	-	-	-
$c_{\text{acq}}$	0.0025	-	<b>0</b>	<b>0.025</b>	-	-	<b>0.025</b>	-	-
$\beta$	0.95	-	-	-	-	-	-	-	-
$C_s$	0	-	-	-	250	-	-	-	-
$c_{\text{train}}$	0.075	0.005	<b>0</b>	0.075/0.005	0.075/0.005	-	0.075/0.005	-	-
$\gamma$ (GSE)	1.92	-	-	-	-	-	-	-	-
$\gamma$ (LSEc)	0.1	-	-	-	-	-	-	-	-
Metric	AUC	-	-	-	-	-	-	-	-
Model	LR	LightGBM	Both	Both	Both	Both	Both	Both	Both
Model re-estimation	-	No	No	No	No	Yes	Yes	Yes	Yes

**Table EC.2 Parameters of all experiments**

*Note.* The table reports the parameters for all experiments, grouped into core scenarios, economic structure, and robustness. Parameters cover epoch design, costs, algorithms, models, and performance. A dash indicates that the parameter value coincides with experiment E.1. When a cell lists two values separated by a slash, the experiment is run using logistic regression with the first value and LightGBM with the second. Experiments under economic structure and robustness are reported in Appendix EC.2.5.

### EC.2.3. Core scenarios: Extended Numerical Results



*Note.* This figure reports the AUC of the incumbent (blue curve) and challenger (orange curve) models as a function of  $N_{t_e}$ , the sample size available at each decision epoch  $t_k \in \mathcal{T}_D$ , with shaded areas indicating 90% confidence intervals.. The challenger is a logistic regression in panel (a) and a LightGBM in panel (b). At each decision epoch, the challenger is retrained using half of the available sample  $N_{t_e}$ . AUC for both the incumbent and the challenger is computed on the corresponding cumulative test set, consisting of the remaining half of the data from the current epoch through the end of the process. Each curve shows the average AUC across 30 sample paths (see Section 5.2). The decreasing AUC is due to a small distribution shift in the data.

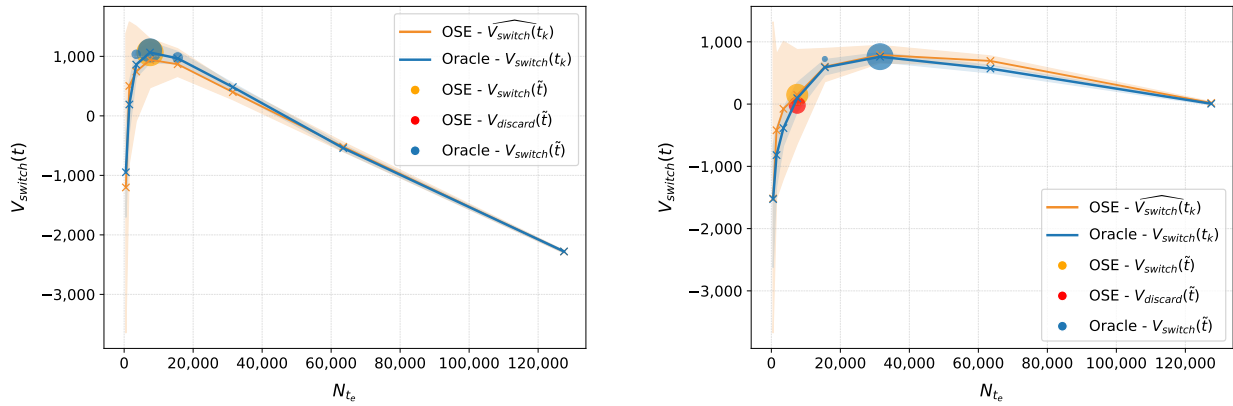


**Figure EC.2 Early switch vs late switch - OSE algorithm**

*Note.* The figure shows the utility (switching value) and decisions of OSE algorithm and the oracle across 30 sample paths for experiments E.1 and E.2. Solid lines report average switching values at each  $t_k$ , with shaded areas indicating 90% confidence intervals. Blue and orange dots denote oracle and algorithm performance at the switching epoch  $\tilde{t}$ , respectively, while red dots indicate discard decisions. Dot sizes are proportional to the frequency of the corresponding decision across sample paths. Dot heights represent the average of the switching or discarding value at the corresponding epoch.

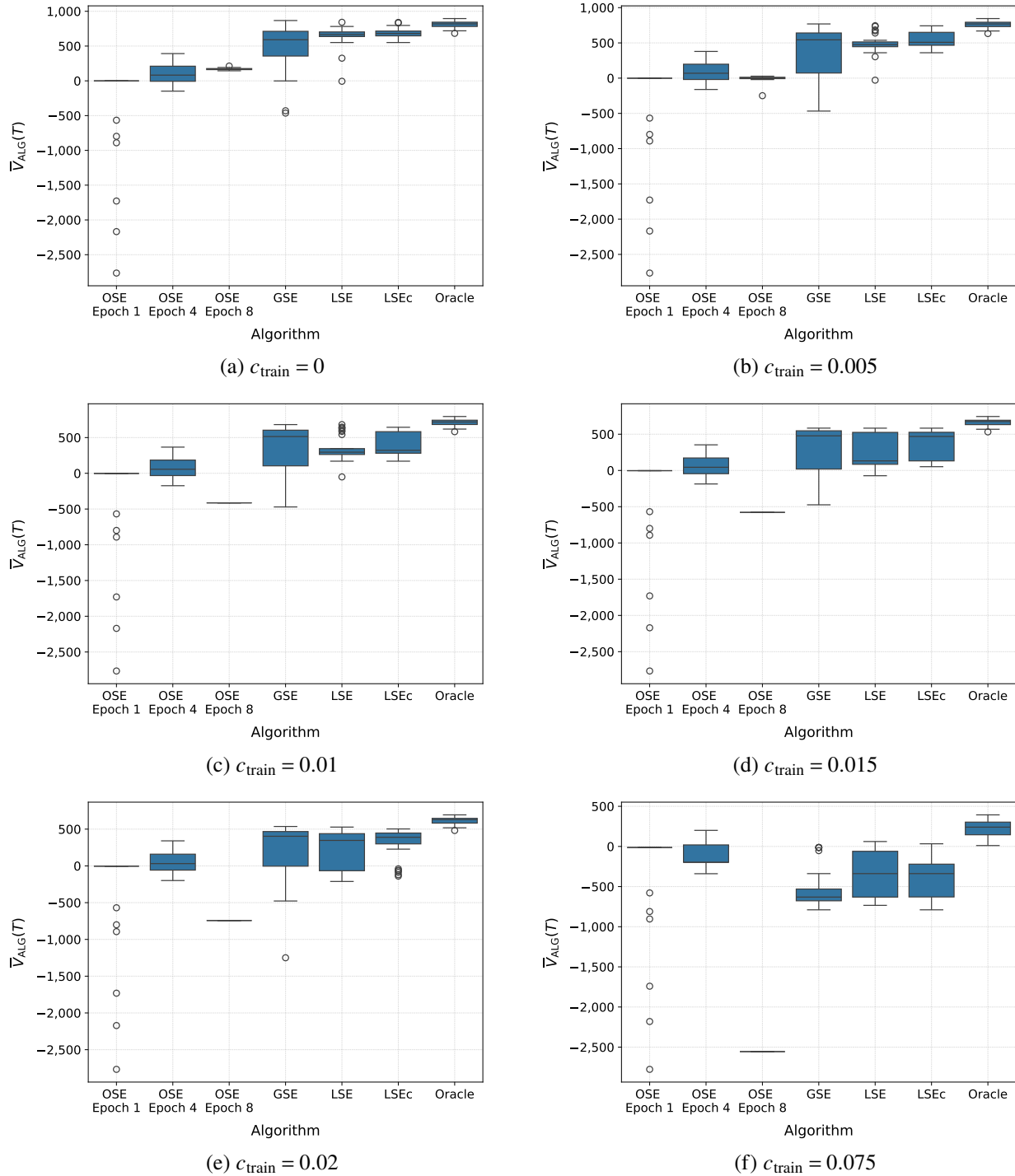


**Figure EC.3 E.2 for different per-sample training costs  $c_{\text{train}}$**

*Note.* This figure displays the performance of our algorithms across the 30 sample paths for experiment E.2, when varying the per-sample training cost  $c_{\text{train}}$ .

#### EC.2.4. Sensitivity Analysis: Effect of Algorithm Hyperparameters

We analyze how the performance of GSE and LSEc algorithms varies with the confidence parameter  $\gamma$ . For GSE, a larger  $\gamma$  corresponds to a more conservative decision rule and therefore leads to later stopping. For LSEc, a larger  $\gamma$  results in a more optimistic assessment of future gaps, which likewise delays stopping.

*Design.* To assess sensitivity to  $\gamma$ , we evaluate algorithm performance across a large set of experiments constructed from the same parameter grid used to define the core scenarios (see Section EC.2.2), for both LR and LightGBM, over a prespecified range  $\Gamma$  of  $\gamma$  values. For each algorithm, we proceed in two steps. First, we consider a wide range of  $\gamma$  values, evaluate performance across experiments, and select a reference value. Second, we examine local sensitivity by varying  $\gamma$  within a tighter neighborhood around the selected value.

In both steps, we summarize the results using heatmaps (see Figure EC.4). Each cell of a heatmap corresponds to a single experiment defined by values of  $c_{\text{acq}}$  and  $c_{\text{train}}$ , with  $c_s = 0$  and  $\beta$  fixed at a default value. The specific value of  $\beta$  is reported in the subtitle of the figure or its description. Within each cell, we compute the sample-path-averaged performance for each  $\gamma \in \Gamma$ , denoted  $\bar{V}_{\text{ALG}}^{\text{SP}}(T; \gamma)$ , and report the maximum percentage performance gain  $P$ , defined as:

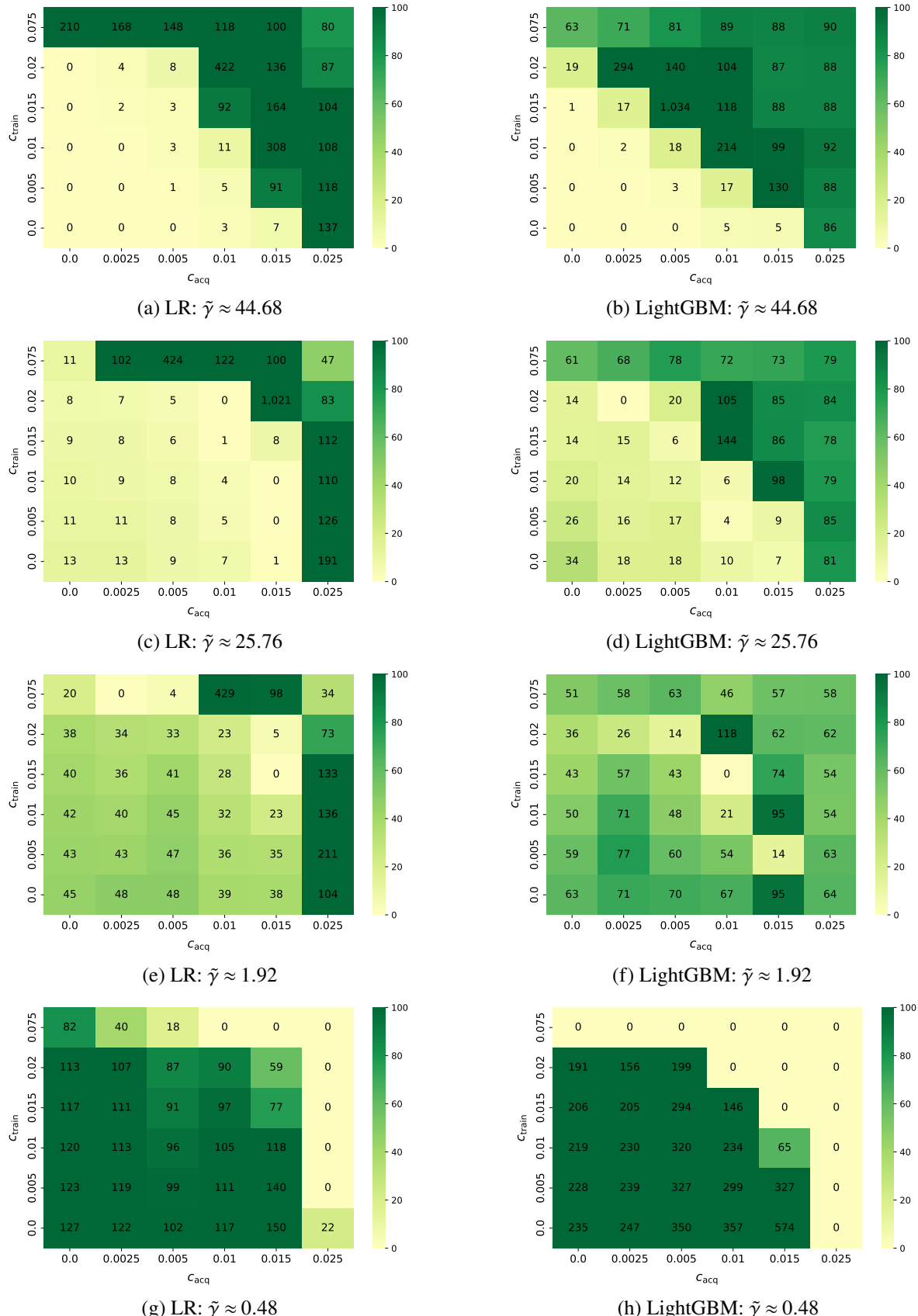
$$P = \max_{\gamma \in \Gamma} \frac{\bar{V}_{\text{ALG}}^{\text{SP}}(T; \gamma) - \bar{V}_{\text{ALG}}^{\text{SP}}(T; \tilde{\gamma})}{\left| \bar{V}_{\text{ALG}}^{\text{SP}}(T; \tilde{\gamma}) \right|} \cdot 100, \quad (\text{EC.22})$$

where  $\tilde{\gamma} \in \Gamma$  denotes a reference value. Thus,  $P$  measures the maximal percentage improvement in sample-path-averaged performance relative to the reference value  $\tilde{\gamma}$ . Since  $\tilde{\gamma} \in \Gamma$  it follows that  $P \geq 0$ .

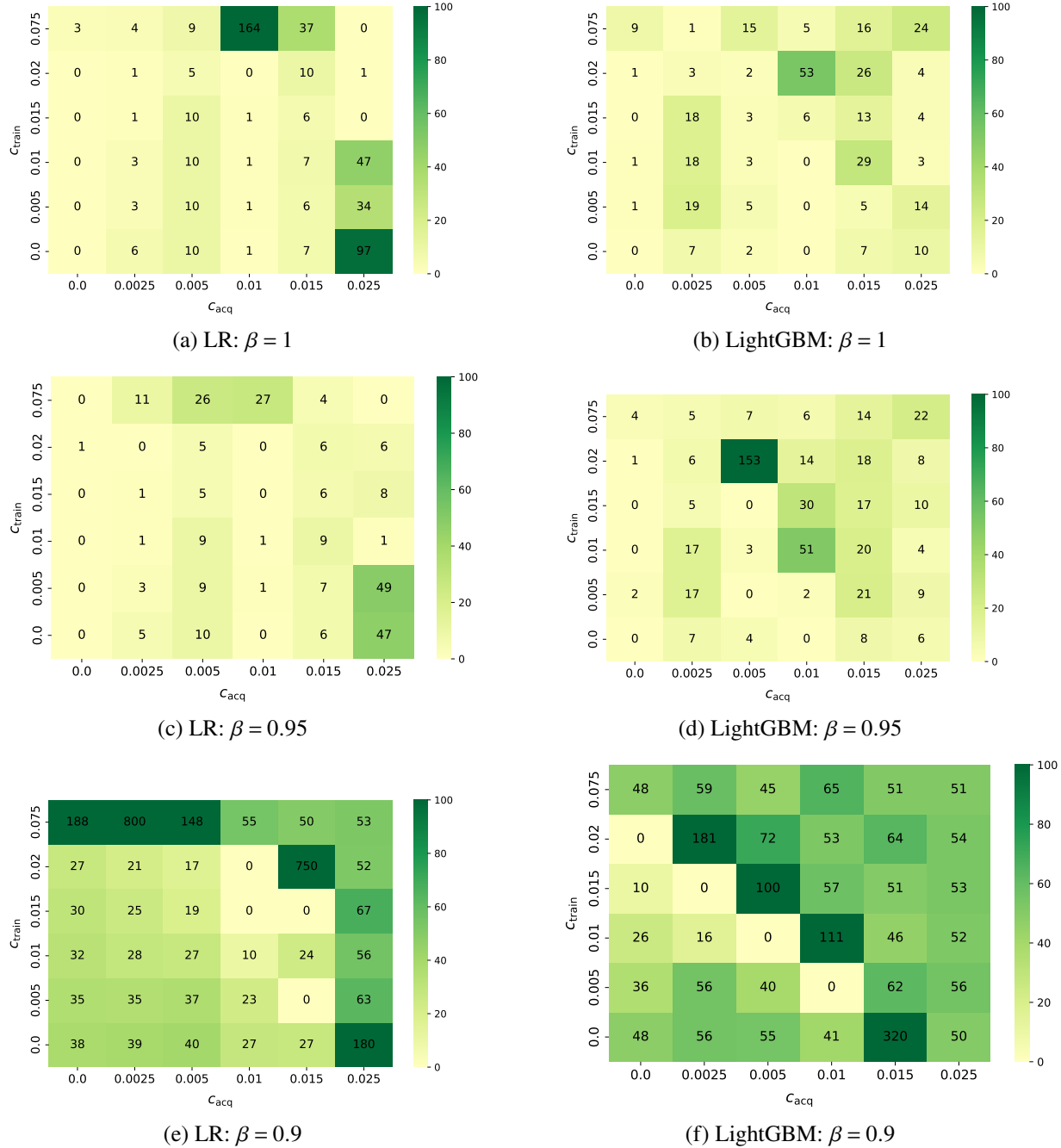
*GSE results.* Overall, we find that GSE performance is highly sensitive to  $\gamma$ , and no single value performs best across experiments. We first consider a wide grid  $\Gamma = \{44.68, 25.76, 19.2, 12.01, 7.69, 5.6, 4.32, 1.92, 0.96, 0.48\}$  and report heatmaps for selected values  $\tilde{\gamma} \in \{44.68, 25.76, 1.92, 0.48\}$ . Results are shown for both LR and LightGBM, with  $c_s = 0$  and  $\beta = 1$ , in Figure EC.4. As shown, there is no single value of  $\gamma$  that consistently delivers the close-to-best sample-path-averaged performance across experiments. As a single value of  $\gamma$  must be selected for the core scenarios, we choose  $\gamma = 1.92$ , which delivers the best performance in experiment E.1 among the values in  $\Gamma$  (see Figure EC.4e, column 2, row 1). We then examine local sensitivity around this reference value by fixing  $\tilde{\gamma} = 1.92$  and considering a tighter grid  $\Gamma = \{2.31, 2.14, 1.99, 1.92, 1.85, 1.73, 1.61\}$ . Heatmaps for  $\beta \in \{1, 0.95, 0.9\}$ , with  $c_s = 0$ , are

reported for both LR and LightGBM in Figure EC.5. Even in the vicinity of  $\gamma = 1.92$ , performance varies substantially, and  $\gamma = 1.92$  is often far from delivering close-to-best sample-path-averaged performance, particularly when  $\beta = 0.9$ .

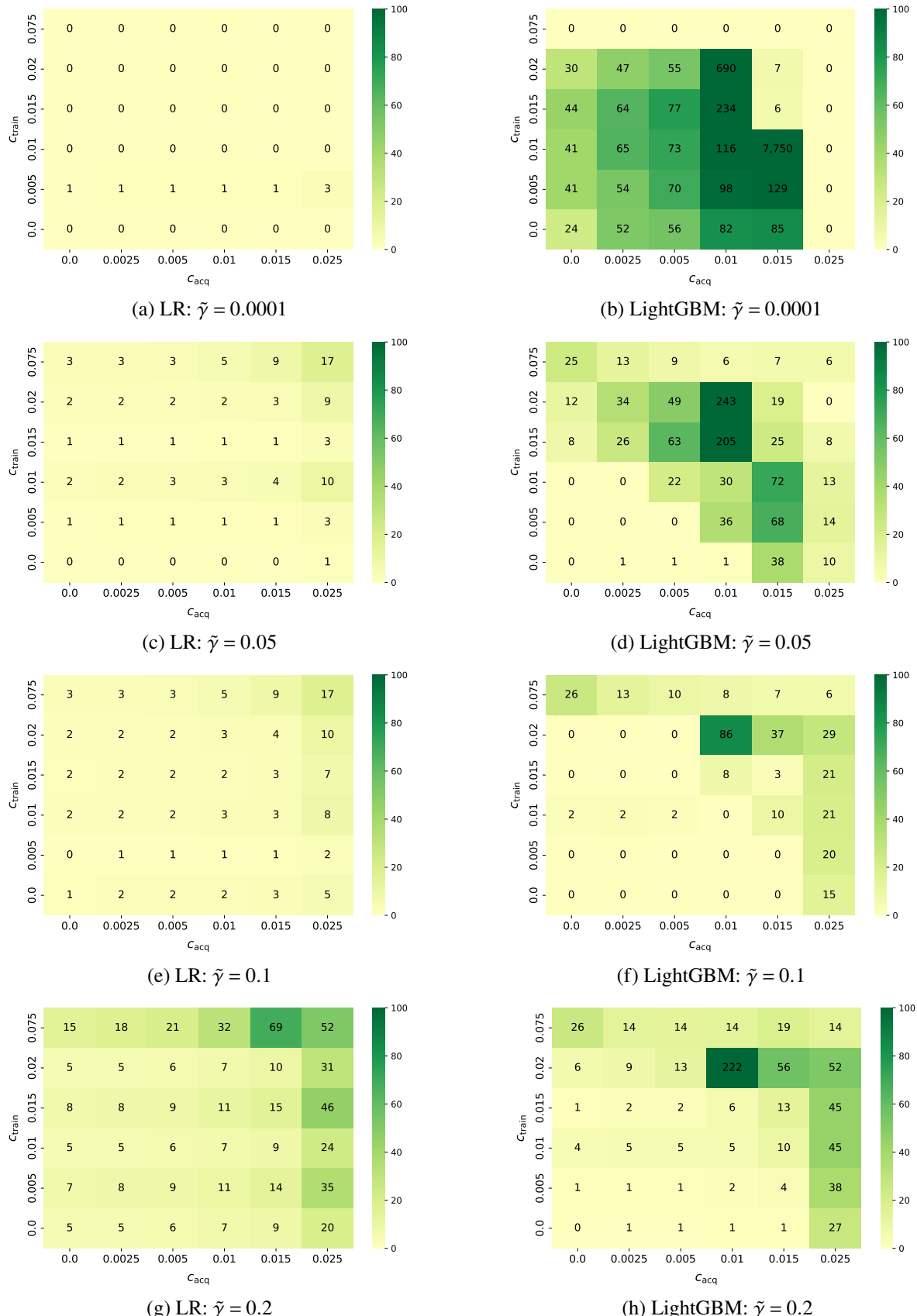
*LSEc results.* In contrast, LSEc is markedly more robust to the choice of  $\gamma$ . Over a wide grid  $\Gamma = \{0.001, 0.01, 0.025, 0.05, 0.075, 0.09, 0.1, 0.125, 0.15, 0.2\}$ , we report heatmaps for selected values  $\tilde{\gamma} \in \{0.001, 0.05, 0.1, 0.2\}$  in Figure EC.6, for both LR and LightGBM, with  $c_s = 0$  and  $\beta = 1$ . As shown,  $\gamma = 0.1$  consistently delivers close-to-best sample-path-averaged performance across experiments, particularly under LR. Accordingly, we set  $\gamma = 0.1$  for the core scenarios and other experiments. Local sensitivity analysis using a tighter grid  $\Gamma = \{0.0875, 0.095, 0.0975, 0.1, 0.1025, 0.105, 0.1125\}$  and  $\beta \in \{1, 0.95, 0.9\}$ , reported in Figure EC.7, shows limited performance variation in the vicinity of  $\gamma = 0.1$ . Overall, LSEc performance is substantially less sensitive to  $\gamma$  than GSE, and  $\gamma = 0.1$  remains close to optimal across experiments.

**Figure EC.4 GSE's sensitivity to  $\gamma$  - Wide range  $\Gamma$** 

*Note.* Illustration of GSE's sensitivity to the confidence parameter  $\gamma$  across 30 sample paths over a grid of per-sample acquisition costs  $c_{\text{acq}}$ , training costs  $c_{\text{train}}$ , with  $c_s = 0$  and  $\beta = 1$ , using LR (first column) and LightGBM (second column). Cell shading indicates maximum percentage performance gain  $P$ , as defined in Equation EC.22, with  $\Gamma = \{44.68, 25.76, 19.2, 12.01, 7.69, 5.6, 4.32, 1.92, 0.96, 0.48\}$ .

**Figure EC.5 GSE's sensitivity to  $\gamma$  - Close range  $\Gamma$** 

*Note.* Illustration of GSE's sensitivity to the confidence parameter  $\gamma$  across 30 sample paths over a grid of per-sample acquisition costs  $c_{\text{acq}}$ , training costs  $c_{\text{train}}$ , and discount factor  $\beta$ , with  $c_s = 0$  and  $\tilde{\gamma} = 1.92$ , using LR (first column) and LightGBM (second column). Cell shading indicates maximum percentage performance gain  $P$ , as defined in Equation EC.22, with  $\Gamma = \{2.31, 2.14, 1.99, 1.92, 1.85, 1.73, 1.61\}$ .

**Figure EC.6 LSEC's sensitivity to  $\gamma$  - Wide range  $\Gamma$** 

*Note.* Illustration of LSEC's sensitivity to the confidence parameter  $\gamma$  across 30 sample paths over a grid of per-sample acquisition costs  $c_{\text{acq}}$ , training costs  $c_{\text{train}}$ , with  $c_s = 0$  and  $\beta = 1$ , using LR (first column) and LightGBM (second column). Cell shading indicates maximum percentage performance gain  $P$ , as defined in Equation EC.22, with  $\Gamma = \{0.001, 0.01, 0.025, 0.05, 0.075, 0.09, 0.1, 0.125, 0.15, 0.2\}$ .

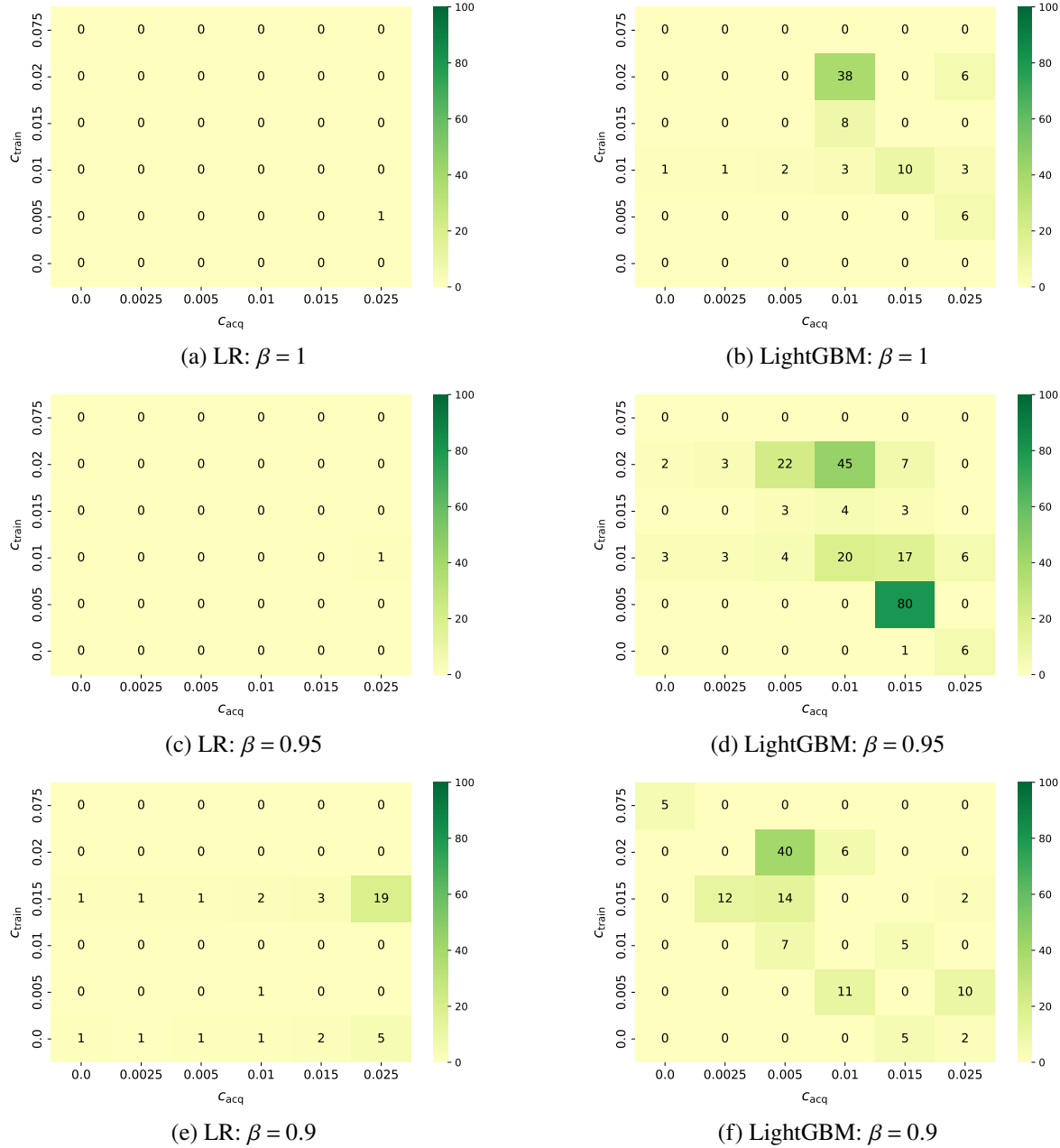


**Figure EC.7 LSEc's sensitivity to  $\gamma$  - Close range  $\Gamma$**

*Note.* Illustration of LSEc's sensitivity to the confidence parameter  $\gamma$  across 30 sample paths over a grid of per-sample acquisition costs  $c_{\text{acq}}$ , training costs  $c_{\text{train}}$ , and discount factor  $\beta$ , with  $c_s = 0$  and  $\tilde{\gamma} = 0.1$ , using LR (first column) and LightGBM (second column). Cell shading indicates maximum percentage performance gain  $P$ , as defined in Equation EC.22, with  $\Gamma = \{0.0875, 0.095, 0.0975, 0.1, 0.1025, 0.105, 0.1125\}$ .

### EC.2.5. Robustness Checks: Numerical Results Beyond the Core Scenarios

The two core scenarios analyzed in Section 5.5 provide a baseline understanding of how the algorithms behave when the optimal stopping time occurs early or late in the sequential process. We now turn to a set of additional experiments with two objectives. First, we study how algorithmic behaviors vary under alternative economic structures. Second, we assess the robustness of our findings to changes in the experimental design, including batch sizes, the role of time ordering, and the total sample size.

*Economic Structure* We next examine how algorithmic behavior changes under three alternative economic structures—(i) no costs, (ii) high acquisition costs, and (iii) positive switching costs—each evaluated for both the logistic regression and the LightGBM. The full specification of these experiments, denoted E.3, E.4, and E.5, is reported in Table EC.2. We display the results of these experiments in Figure EC.8.

Under the no-costs scenario, several results stand out. First, the OSE algorithm becomes profitable when acquiring the entire dataset at once. Although profitable, it remains dominated by the other algorithms, highlighting that, even in the absence of costs, sequential decision rules can deliver higher value than a one-shot strategy buying the entire dataset at once. Second, the GSE algorithm exhibits substantially lower performance’s volatility in both the early- and late-switch scenarios when costs are set to zero. While removing costs does not affect statistical uncertainty, it fundamentally alters the shape of the utility curves. In particular, eliminating acquisition costs shifts the utility curves upward, and eliminating training costs makes them flatter across epochs (see Figure EC.9). As a result, although the GSE algorithm remains sensitive to early-stage noise, the value differences across epochs are smaller, which reduces dispersion in stopping decisions and, consequently, lowers performance volatility. Third, the LSEc algorithm delivers the highest performance, with values that remain very close to the oracle’s. Its performance is notably closer to the oracle in E.3 than in E.1 and E.2, reflecting the fact that setting the training cost to zero removes an important source of divergence between LSEc and the oracle’s behavior.

Under the high-acquisition-cost scenario, we examine whether the algorithms make appropriate switching or discarding decisions in settings where acquisition costs substantially reduce economic value and can even render switching unprofitable. Recall that acquisition costs affect the decision to switch or discard but do not influence the optimal stopping point. We distinguish between two cases, depending on the challenger model. When the challenger is a logistic regression, the oracle’s optimal decision is to switch for all sample paths, albeit with a value close to zero. This case allows us to

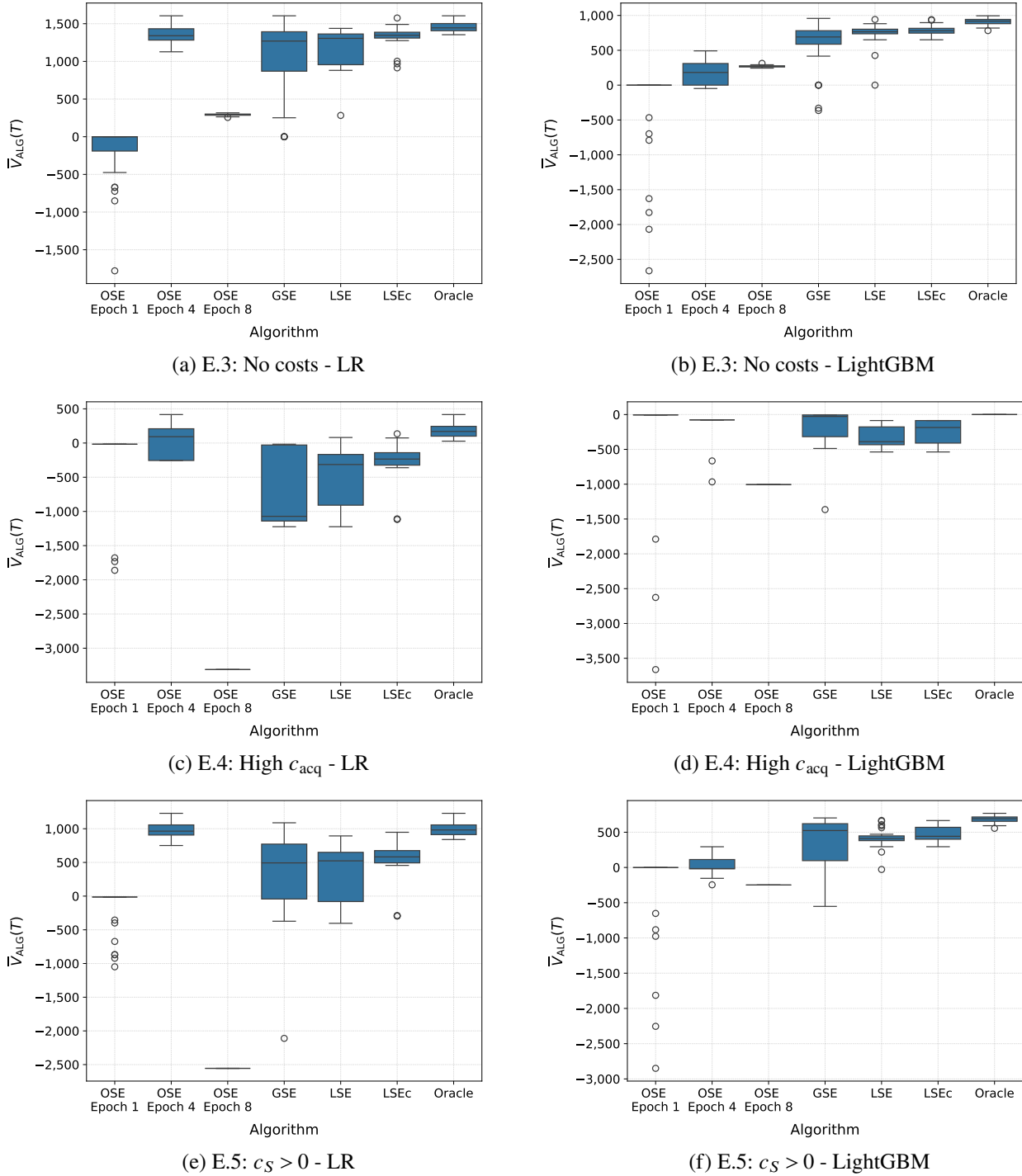
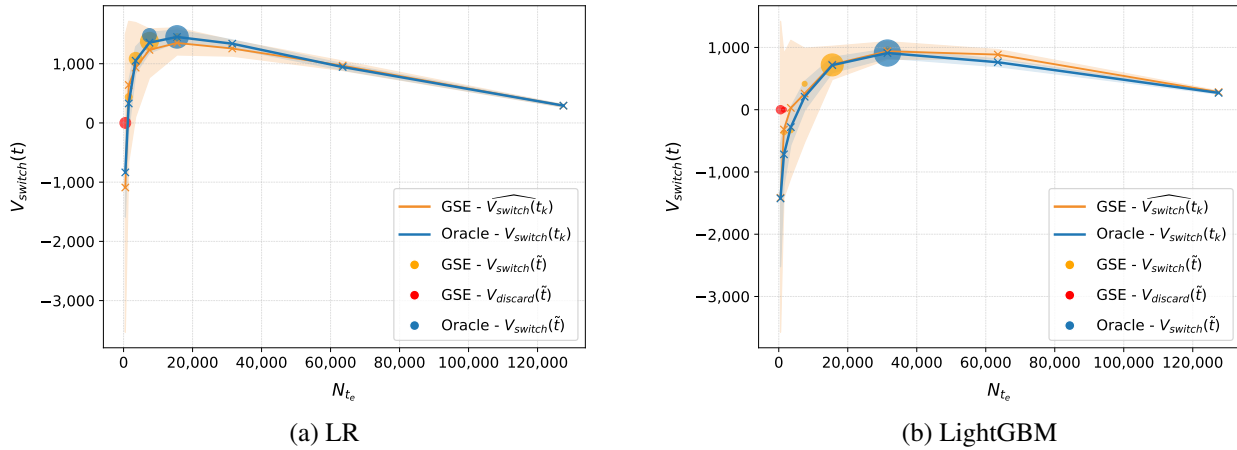


Figure EC.8 Economic structure

*Note.* This figure displays the performance of our algorithms across the 30 sample paths for experiments E.3 to E.5.

assess whether the algorithms can correctly switch despite limited economic upside. In contrast, when the challenger is a LightGBM, the oracle's optimal decision is to discard the challenger for all



**Figure EC.9 Economic structure - E.3: No costs**

*Note.* The figure shows the utility (switching value) and decisions of GSE algorithm and the oracle across 30 sample paths for experiment E.3, using the logistic regression and LightGBM. Solid lines report average switching values at each  $t_k$ , with shaded areas indicating 90% confidence intervals. Blue and orange dots denote oracle and algorithm performance at the switching epoch  $\tilde{t}$ , respectively, while red dots indicate discard decisions. Dot sizes are proportional to the frequency of the corresponding decision across sample paths. Dot heights represent the average of the switching or discarding value at the corresponding epoch. Each panel corresponds to a different algorithm.

sample paths. This case enables us to evaluate whether the algorithms appropriately avoid switching when doing so would be unprofitable. In both cases, the LSEc algorithm switches or discards sufficiently early to avoid substantial losses, particularly relative to the GSE and LSE algorithms, with this advantage being most pronounced when the challenger is a logistic regression.<sup>11</sup>

Under the final scenario, we analyze how introducing a switching cost affects algorithm performance. Recall that, like the acquisition cost, the switching cost does not affect the optimal stopping time but instead influences whether the algorithm chooses to switch or to discard the challenger. Consequently, as long as the switching cost does not change the optimal decision, the value of any algorithm that switches should decrease mechanically by the amount of the switching cost. This is exactly what we observe for all our algorithms. The only exception arises in the logistic regression case, where introducing the switching cost leads the GSE algorithm to discard the challenger in one additional sample path relative to the zero-switching-cost setting.

**Robustness** We finally assess the robustness of our findings by considering four additional experiments by varying batch sizes, discarding the time ordering, and the total sample size. Complete details about these experiments, denoted E.6, E.7, E.8 and E.9, are provided in Table EC.2. Figure

<sup>11</sup> LSEc always switches in the logistic regression case and always discards the challenger in the LightGBM case. Although LSEc switches at a time close to the oracle on average (4.87 versus 4.03), switching yields a lower and negative value for LSEc. This gap arises because even small delays in switching can be costly when gaps decline rapidly and because LSEc incurs cumulative training costs prior to switching, whereas the oracle pays the training cost only at the switching epoch. Given the high training costs in the logistic regression case, the latter effect is likely the dominant driver.

EC.10 and EC.11 display the performance of our algorithms across the 30 sample paths for these additional experiments.

First, we reduce the batch-size growth across epochs from a factor of 2 to 1.5. As shown in Figures EC.10a and EC.11a, this change has little effect on the performance of the oracle, OSE, and LSEc, with LSEc remaining close to oracle performance. In contrast, the impact on GSE and LSE is mixed: GSE performs worse with logistic regression but better with LightGBM, while LSE improves with LightGBM and is largely unaffected with logistic regression. These patterns reflect the impact of reduced batch-size growth, which increases decision frequency but also raises performance variability from repeated model training, leading to greater dispersion in stopping times (Figure EC.12). In particular, for GSE, it leads to earlier and more dispersed stopping with LightGBM and later stopping with logistic regression, improving and worsening performance, respectively. For LSE, smaller batches allow earlier decision-making after the optimal stopping time, improving performance under logistic regression.

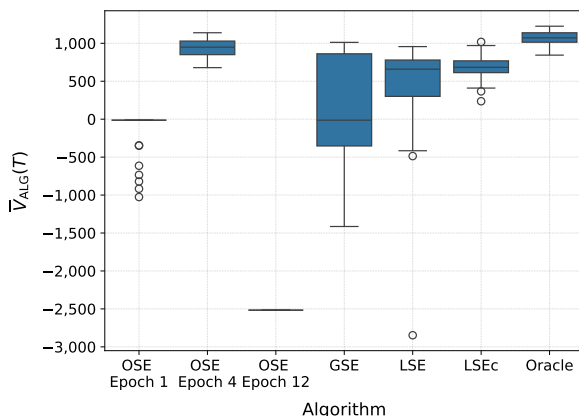
Second, we increase the batch-size growth across epochs from 2 to 2.5 and simultaneously raise the per-sample acquisition cost by a factor of 10. This experiment closely mirrors E.4, differing only in the larger batch-size growth, which allows us to isolate and assess the effect of increased batch size by comparing E.4 and E.7. As shown in Figure EC.10b and EC.11b, this change has a small impact on the oracle. Although LSEc's performance deteriorates, it remains the best-performing algorithm under logistic regression, and its ranking is unchanged under LightGBM.

Third, we repeat experiments E.1 and E.2 after randomly shuffling the data to break the original time ordering, while still conducting the sequential evaluation based on this permuted sequence for 30 different sample paths. Figures EC.10c and EC.11c show the results of experiment E.8 for the logistic regression and the LightGBM, respectively.<sup>12</sup> Overall, the oracle's performance increases and the ranking of the algorithms remains largely unchanged, except that GSE drops to last place when excluding OSE. Importantly, LSEc performs near the oracle under both logistic regression and LightGBM.

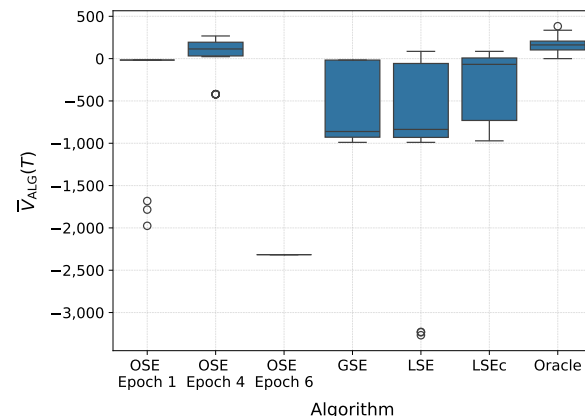
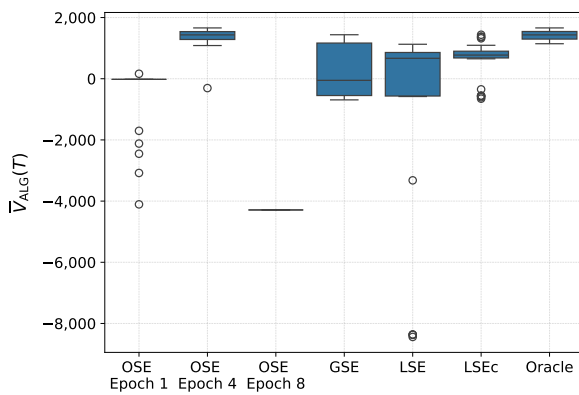
Finally, in the last experiment, denoted E.9, the total sample size available to the change is divided by two. As a consequence, the oracle's performance diminishes, since a smaller total sample size limits the accumulation of per-sample gains from switching. This change has virtually no effect on the LightGBM results. By contrast, with the logistic regression, the GSE algorithm's

<sup>12</sup> Experiment E.8 with logistic regression is the modified version of experiment E.1. Similarly experiment E.8 with LightGBM is the modified version of experiment E.2.

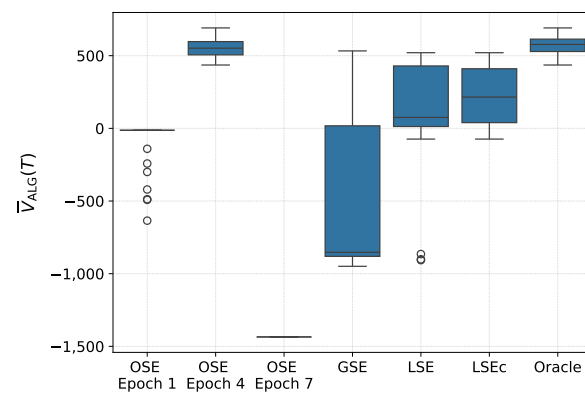
performance deteriorates sharply and becomes largely unprofitable, whereas all other algorithms remain profitable, albeit with increased volatility (see Figure EC.10d). This result highlights a key weakness of the GSE algorithm: when faced with substantial uncertainty about whether switching or discarding is optimal, the algorithm continues acquiring additional data until the relative cost of discarding exceeds that of switching, rather than committing earlier to a decision (see Figure EC.13).



(a) E.6: Small batch

(b) E.7: High  $c_{\text{acq}}$  and large batches

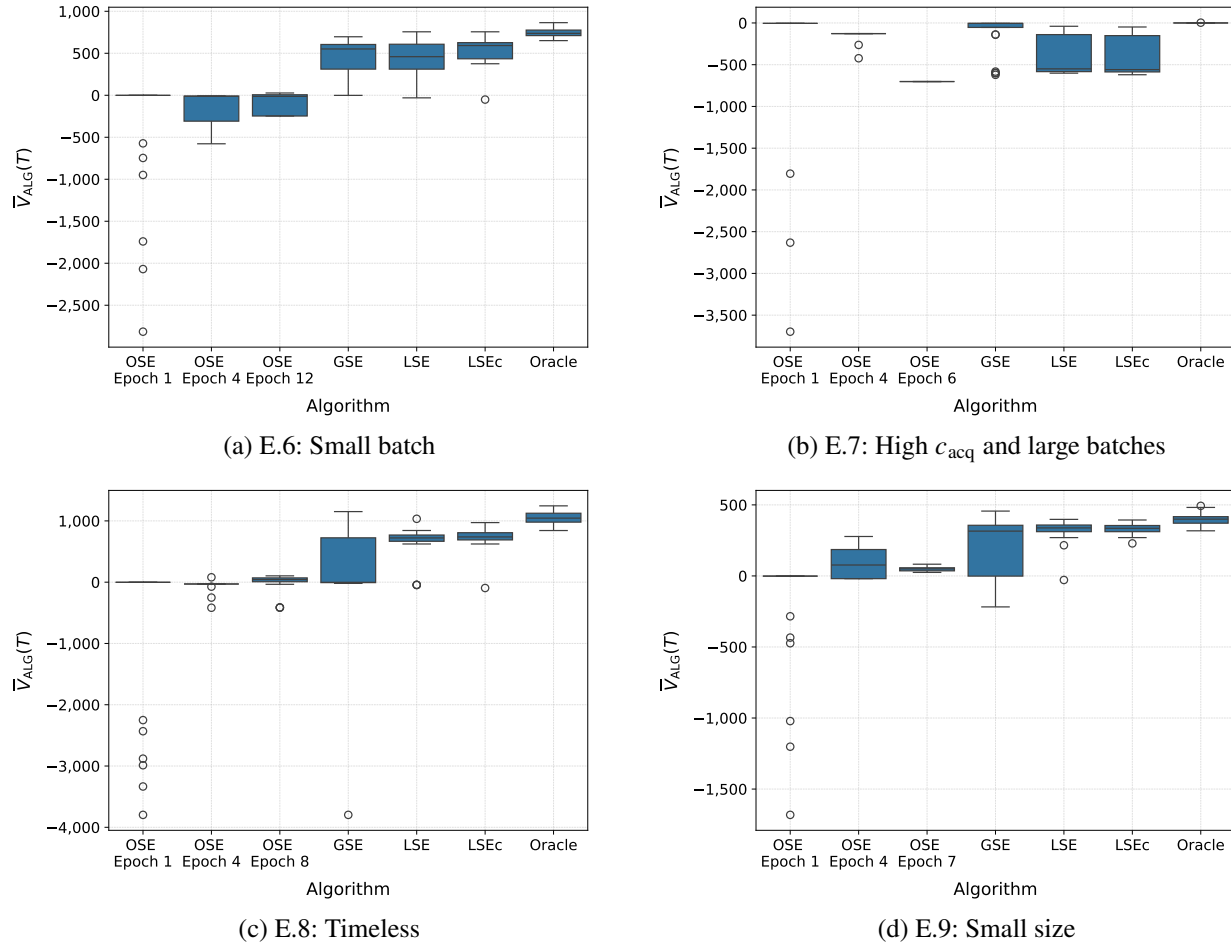
(c) E.8: Timeless



(d) E.9: Small size

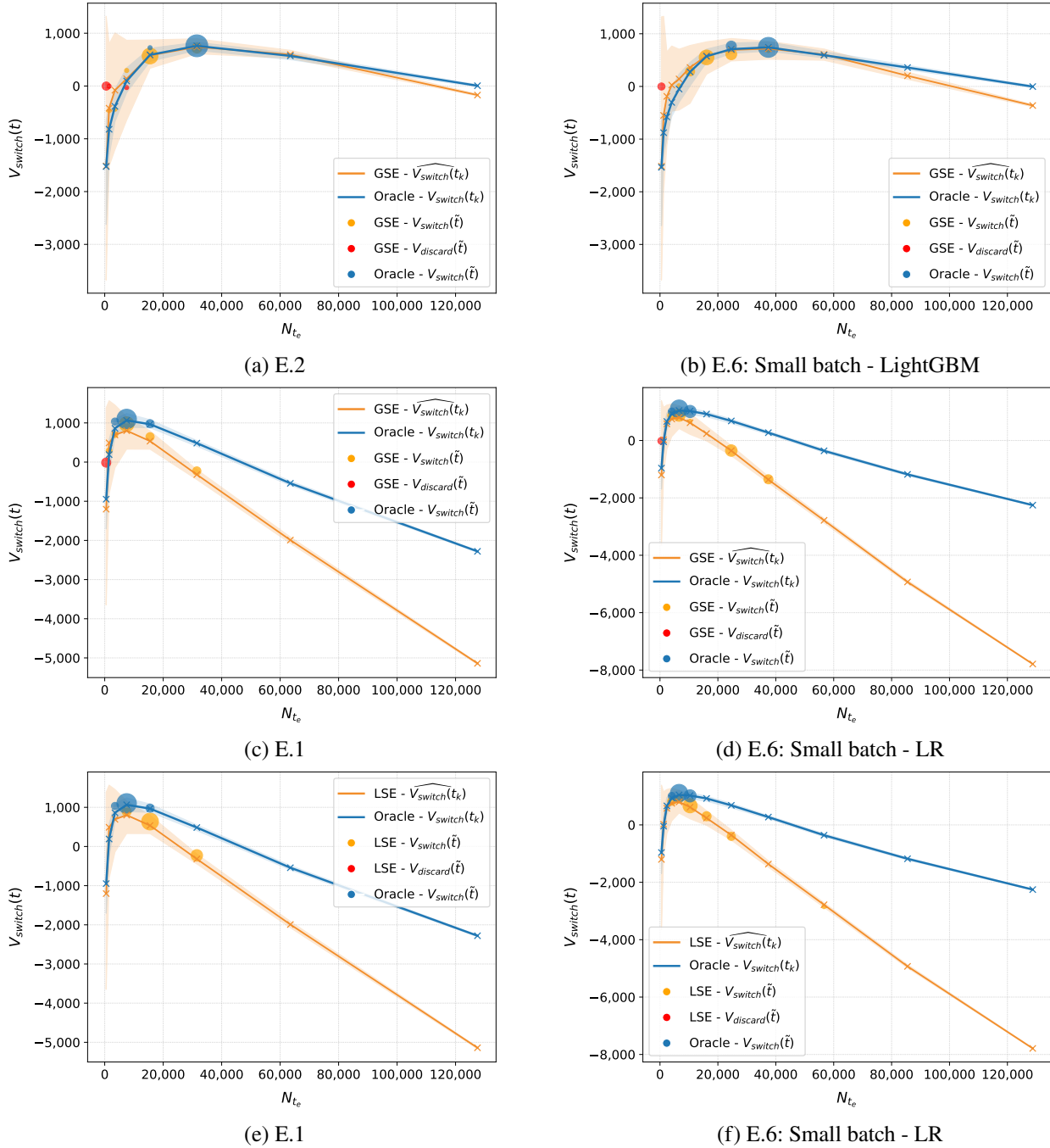
**Figure EC.10 Robustness - Logistic regression**

*Note.* This figure displays the performance of our algorithms across the 30 sample paths for experiments E.6 to E.9, using the logistic regression.



**Figure EC.11 Robustness - LightGBM**

*Note.* This figure displays the performance of our algorithms across the 30 sample paths for experiments E.6 to E.9, using the LightGBM.

**Figure EC.12 Robustness - Small batch**

*Note.* The figure shows the utility (switching value) and decisions of GSE and LSE algorithms and the oracle across 30 sample paths for experiments E.1 and E.6, using the logistic regression and LightGBM. Solid lines report average switching values at each  $t_k$ , with shaded areas indicating 90% confidence intervals. Blue and orange dots denote oracle and algorithm performance at the switching epoch  $\tilde{t}$ , respectively, while red dots indicate discard decisions. Dot sizes are proportional to the frequency of the corresponding decision across sample paths. Dot heights represent the average of the switching or discarding value at the corresponding epoch.

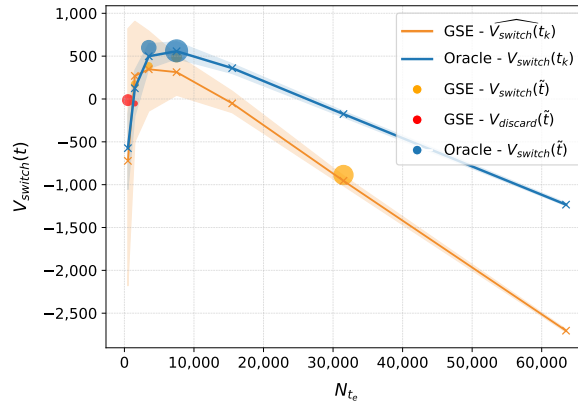


**Figure EC.13 Robustness - Small Size - Logistic regression**

*Note.* The figure shows the utility (switching value) and decisions of GSE algorithm and the oracle across 30 sample paths for experiment E.9, using the logistic regression. Solid lines report average switching values at each  $t_k$ , with shaded areas indicating 90% confidence intervals. Blue and orange dots denote oracle and algorithm performance at the switching epoch  $\tilde{t}$ , respectively, while red dots indicate discard decisions. Dot sizes are proportional to the frequency of the corresponding decision across sample paths. Dot heights represent the average of the switching or discarding value at the corresponding epoch.